Deep frying: from mechanisms to product quality

Kevin N. van Koerten

Thesis committee

Promotor

Prof. Dr R.M. Boom

Professor of Food Process Engineering

Wageningen University

Co-promotor

Dr M.A.I. Schutyser

Associate professor, Laboratory of Food Process Engineering

Wageningen University

Other members

Prof. Dr M.A.J.S. van Boekel, Wageningen University

Prof. Dr G. Trystram, AgroParisTech, Paris

Dr M. de Roode, Sensus, Roosendaal

Dr A.J.B. van Boxtel, Wageningen University

This research was conducted under the auspices of the Graduate School VLAG (Advanced studies in Food Technology, Agrobiotechnology, Nutrition and Health Sciences).

Deep frying: from mechanisms to product quality

Kevin N. van Koerten

Thesis

submitted in fulfilment of the requirements for the degree of doctor

at Wageningen University

by the authority of the Rector Magnificus

Prof. Dr A.P.J. Mol

in the presence of the

Thesis Committee appointed by the Academic Board

to be defended in public

on Monday, 14th March 2016

at 4 p.m. in the Aula.

Kevin N. van Koerten

Deep frying: from mechanisms to product quality

119 pages.

PhD thesis, Wageningen University, Wageningen, NL (2016)

With references, with summaries in Dutch and English

ISBN 978-94-6257-647-6

Table of contents

1. General introduction

1.1.Frying to prepare foods

Frying is a food processing technique that has been around for more than 4000 years. The method involves the use of hot oil as heating medium to prepare food. Since hot oil can reach much higher temperatures than water, the food is prepared much faster. Frying has many variants that apply different amounts of hot oil, handling of the food and cooking times. Stir frying for example uses small amounts of oil, while the product is continuously stirred, keeping the average temperature of the product relatively low. During deep frying, the product is completely immersed in hot oil; the oil is used several times before being discarded.

Deep frying has provided the basis for a global industry. Due to the fast heating by the hot oil, a crispy crust is formed, while the interior can remain moist and mealy. The textural properties, combined with the distinct flavour produced by deep frying have made it one of the main methods of food preparation in the present day. Practically any food can be prepared using deep frying, including, but not limited to vegetables, fruit, bread, fish, and meat (Figure 1.1). Additionally, foods may be coated with a batter to improve and alter the crust formation. Deep frying of potatoes is especially popular in western culture; one can think of the production of potato chips, and batons of potato, commonly called French fries, chips, fries or finger chips. The last category is a very important product, with around 11 million metric tons production per year (Makki and Plummer, 2005).This is one of the major reasons that the focus of this thesis is on the processing of French fries.

Figure 1.1. Examples of fried food. From left to right and top to bottom: French fries (“www.myfries.ca,” 2015)**, spring roll** (“www.minghongfood.com,” 2015)**, krupuk** (“www.pasundan.nl,” 2015)**, Kibbeling** (“www.smulweb.nl,” 2015)**, onion rings** (“www.kudu.com.sa,” 2015)**, doughnut** (“en.wikipedia.org,” 2015)**.**

1.2.Production process French fries

The preparation of French fries revolves around two consecutive frying steps. The first step, called the pre-frying step, cooks the fries, while the second step, called the finish-frying step, creates a crispy crust around the fries. This last step is carried out close to the place of consumption (i.e. at home or at a restaurant). The pre-frying of French fries is a well-established industrial process, often producing several tonnes of French fries per hour. The general scheme for the production of French fries is given in Figure 1.2.

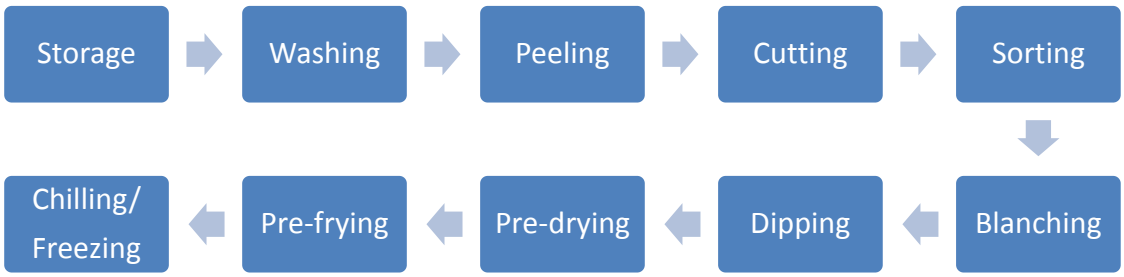

Figure 1.2. Schematic overview of the French fry production process.

Besides the processing steps, the storage of the raw potatoes is a critical factor in the final product quality. Cold storage prolongs the shelf life and prevents sprouting, due to a slowing of the potato metabolism (Duckham et al., 2002). However, storage at lower temperatures also increases the level of reducing sugars, which can lead to excessive browning of the final product (Pravisani and Calvelo, 1986). Before processing, the potatoes are therefore reconditioned at a higher temperature to mitigate this increase in reducing sugars to a certain degree (Somsen et al., 2004).

A washing step is used to remove any foreign materials from the potatoes. Peeling is performed using steam. This involves a short cooking step, in which potatoes are exposed to steam of 14-18 bars for several seconds, which loosens the skin from the potatoes due to the rapid boiling of water underneath the skin. Afterwards, abrasion is applied to remove the loosened skin with minimal product loss (Rossell, 2001; Derk Somsen et al., 2004). The peeled potatoes are then cut into long rectangular strips, by pushing the potatoes through a number of set knives using pressurised water. The high velocity of the water orients the potatoes in the longitudinal direction and pushes them through the knives. This length wise cutting also ensures maximum length of the fries and minimum cutting losses.

The cut strips are then subjected to a sorting step, where too small strips are removed through size separation, and strips with visual defects (e.g. deviating colour or skin remainders) are removed using automated optical sorting (Fazzari et al., 1997). This involves image analysis of the strips on a conveyor belt, and subsequent removal of said defects further down the line.

The first step in the actual food preparation is the blanching of the potato strips, performed to leach out reducing sugars (fructose and glucose), which prevents excessive browning during the frying step. Browning is caused by the Maillard reaction, which involves the reaction between reducing sugars and amino acids and subsequent production of brown coloured melanoidines (Achir et al., 2008). Besides browning, a major function of blanching is the inactivation of enzymes to prevent unwanted metabolic reactions during storage of the final product (e.g. grey discolouration). Enzymes rapidly inactivate at high temperatures in the presence of water. However, the leaching out of sugars takes time, even at elevated temperatures, which does promote the diffusion of reducing sugars (Gekas et al., 1993).

As prolonged blanching at a higher temperature may result in overcooking of the fries, it is usually performed in two steps: one short blanching step at a high temperature for enzyme inactivation; and one long blanching step at a lower temperature to allow further leaching out of the reducing sugars. After blanching, a dipping step is usually performed using a glucose solution, which ensures a desired colour formation in the final product. Sodium pyrophosphate is also used in this dipping step to chelate metal ions and prevent unwanted discolouration (Bunger et al., 2003). Prior to the pre-frying step, surface water is removed from the fries by means of hot air. This allows for a shorter frying time.

Additionally, the oil uptake during the subsequent frying step is reduced by the drying due to some shrinkage and the formation of an initial crust (Krokida et al., 2001). Pre-frying almost completely prepares the fries for consumption, cooking the interior while creating an initial crust. This allows the use of a short finish-frying step close to the place of consumption. Before packaging, the fries need to be cooled to prevent condensation inside the packaging material. An additional freezing step is commonly used to increase shelf life.

1.3.Deep frying: process characteristics

The quality of deep fried products is determined by a few key properties: moisture content, oil content, colour, texture and flavour. These properties are affected by the different product and process properties and interactions during frying.

Product level

The product is submerged in oil of 150-190°C, and heat is conducted via free convection from the oil to the product surface, and via conduction from the food surface to the interior. As the product surface reaches the boiling temperature, water will start to evaporate rapidly. The product surface will remain at the boiling temperature until all surface water is evaporated and the beginning of a crust is formed.

As water evaporation commences, the heat transfer of the oil to the surface will change from free convection to forced convection, due to the turbulence induced by the escaping vapour bubbles. This, besides the large temperature gradients, gives deep fat frying one of the highest heat transfer rates possible in food preparation. As water evaporation progresses, the crust will thicken, and form a thermally insulating layer between the oil and the moist interior of the product due to its low conductivity. This low conductivity is caused by the lack of water, which is highly thermally conductive, but also due to the porosity of the crust, formed by the explosive evaporation of water, and due to the convection of water vapour from the inside, counter to the heat transfer towards the inside.

The generated porosity greatly affects the texture of the final product, being perceived as the crispness of the product when consumed. As water is completely evaporated from the dry crust, the temperature will increase above the boiling temperature. This induces several reactions, of which the most important is probably the Maillard reaction. The Maillard reaction occurs between reducing sugars and amino acids, and produces a brown colour. Too little of this will result in a pale product, while too much will result in a burnt looking product. However, since reducing sugars are involved, this is mostly controlled by the blanching step where the reducing sugars are leached out.

Process level

Industrial, high-capacity frying operations are generally performed in continuous mode. These systems usually consist of a conveyor belt to propel the product through the fryer, a circulatory oil system to filter and transport the oil through the fryer, a heating system for the oil, and an exhaust for the water vapour emerging from the product. Oil is introduced into the fryer via one or multiple inlet points, and extracted at an equal amount of outlets. The oil flows through the fryer in co-current with the product to prevent any hold-up in the fryer. This usually leads to a temperature drop between 16 and 25 °C along the length of the fryer

(Moreira et al., 1999). It is therefore beneficial to have a high oil-to-product ratio, to reduce the relative amount of heat extracted from the oil and to minimise the temperature gradients. This can be achieved in a continuous system by decreasing the path length of the oil (e.g. having multiple in- and outlets) or increasing the oil circulation velocity.

1.4.Modelling of frying/drying

Modelling can serve as a tool to predict various process and product parameters and as an approach to obtain better insight in the mechanisms behind the process, reducing the need for numerous experimental trials.

To develop a model, a process may be approached as a black box, which is fitted with experimental data by using general correlations, by adapting a number of fitting parameters. In this case the fitting parameters do not have any physical meaning, and therefore such models are only useful for interpolation within the available experimental data range. Another approach is to identify the underlying mechanisms in the process, by observations, by hypothesis or both, and then use the appropriate fundamental relations which describe those mechanisms to construct a model containing parameters that have physical meaning and may be measured separately. Such a model may be used inside, but also outside the available experimental data range (of course, with continuous check for validity).

For frying, several types of models have been developed, ranging from simple to complex. Empirical models for water evaporation have been developed by Costa & Oliveira (1999) and Krokida et al. (2000), with time being the only independent variable. Even though these models result in accurate fits for their corresponding data sets, they are not suitable for extrapolation or use in other data sets. The fitting parameters do not have physical meaning and are simply a product of the regression analysis.

Farid (2001) developed an analytical model for water evaporation by neglecting the sensible heat, which is small compared to the latent heat of water evaporation. Since the model is based on fundamental heat transfer equations, it is generally applicable to evaporative processes and all input parameters have physical meaning. However, the model can only be used in evaporation-intensive processes with negligible temperature changes in the product. In addition, the temperature profiles and oil uptake are not described by the model.

Farkas et al. (1996) divided the fry into a crust and a core region with separate equations for heat transfer and moisture diffusion for each region. Additionally, they considered pressure

driven flow for the water vapour through the crust, thus including the major contributions to heat transfer and water evaporation. Their model however did not consider oil transport, even though the uptake of oil in fries is one of the most important quality parameters.

More elaborate models exist in the form of multiphase porous media models (Ni and Datta, 1999; Warning et al., 2012). These models incorporate the fluxes and physical properties of several species, namely oil, water, gas and solids, and account for pressure driven and diffusion driven flow. Though these types of models offer insight into all physical processes involved, they also introduce many parameters that are unknown or are hard to estimate. This makes them complex to use for predictions, and less appropriate for engineering purposes. Therefore, a mechanistic model that describes all phenomena that are relevant to the quality of the product, yet requires a minimum of input parameters, is not yet available.

This thesis is a result of the LEAF (Low Energy And Fat)-project, initiated by Aviko BV and was funded by EFRO, an initiative of the European Union. Partners in the project were Aviko BV, Machinefabriek Baltes Zutphen BV, van Lente Elektrotechniek BV, and Wageningen University. The overall aim of the LEAF project was to develop a new production process following an integral approach from raw material to product with focus on decreased energy consumption and reduced oil content in production of French fries, while maintaining a high quality product.

1.5.Research objective

The study described in this thesis aimed at gaining better insight in the frying process, on two scales:

1. Product scale. The aim was here to better understand which aspects of mass and heat transfer and structural changes are essential in the model-wise prediction of the result of frying and further studied the effect of an alternative cross-flow frying configuration on homogeneity of product quality. The physical phenomena not only relate to energy consumption, but also largely influence oil uptake and crispness formation, which determine final quality of the French fries.
2. Process scale. On larger scales, the aim was to understand the effect of the flow patterns in an industrial-scale pre-fryer, on product quality and its distribution, using a cross-flow pilot scale frying equipment.

1.6.Thesis outline

During frying, reduction in moisture and temperature changes forms the basis for structural and physicochemical changes in the fry. The moisture decrease due to dehydration leads to the formation of a crust, after which oil is taken up. Therefore, to gain more quantitative insight into the evaporation of water, in **chapter 2** a numerical crust-core model is developed for water evaporation inside a single fry. The model is governed by heat transfer, while the resistance in the crust to vapour transport is taken into account using Darcy's law. Additionally, an evaporation rate dependent heat transfer coefficient is implemented using a Nusselt relation for the spherical vapour bubbles. To minimise computational efforts, a cylindrical geometry is adopted, allowing a one-dimensional approach. Additionally, shrinkage is neglected. The model is validated using experimentally measured moisture loss curves and temperature profiles from cylindrical potato samples of varying diameter, fried at specific temperatures. This provides a model that describes the moisture loss and temperature change during frying, while also giving mechanistic insight into the process. The formation of pores due to evaporation also allows oil to start migrating into the fries, already during the frying process.

In **chapter 3** an analytical model is developed to predict an oil uptake during frying. The model follows from the hypothesis that oil uptake can be described with a pore-inactivation mechanism in analogy to pore inactivation during membrane emulsification. Additionally, the model takes into account that oil uptake increases due to thickening of the crust (i.e. lengthening of the pores). The model presents a better description of the oil uptake, especially for small time intervals, compared to the general assumption that oil uptake only takes place in the form of one on one replacement of water. As water evaporates, it leaves behind a dry crust, which is responsible for defines the textural properties of French fries.

Chapter 4 explores the structural changes in the crust during frying, while also quantitatively measuring the textural changes that occur during frying at different frying temperatures. X-ray tomography (XRT) is applied to visualize the crust formation and structure, while texture analysis is applied to give a relative description for crispness of the fry, to be used in a quantitative manner. We clearly show that increased pore size and porosity give rise to the crispy behaviour of the fries. Increased pore formation is also observed for higher temperatures for equal moisture contents. However, chemical changes induce plastic behaviour for frying temperatures around 195°C.

Besides the changes in the individual fries, the manner of oil-fry contact and oil distribution in the bath is also important in the overall process. Temperature gradients in the oil bath cause differences in the quality distribution of the fries. In **chapter 5** we apply a newly designed cross-flow frying unit to better understand oil-fry and fry-fry interactions. The bottom-to-top cross-flow contact mode of oil and fries was chosen from the logical assumption that a shorter path of the oil through the fries will result in smaller temperature gradients. For the final product quality, the moisture content of the fries is chosen as an indicator. As such, the standard deviation of the moisture content of different fries represented the quality distribution. It was found that increased oil flow velocities increased the homogeneity of the fry moisture content up to the point of fluidization of the fry bed. After this point, local packing due to the non-spherical shape of the fries and channelling of the oil caused the homogeneity to decrease again. This effect was visualised by using coloured fries, and observing the packing before and after frying.

A general discussion of the results obtained is given in **chapter 6**. Here, the main findings are highlighted and discussed. Recommendations for further research and potential improvements to frying systems are given. Additionally, since the oil-fry interactions were only experimentally studied, the possibility of using computational fluid dynamics (CFD) is discussed to connect the physical phenomena at the single fry scale and external oil flow in an all-encompassing simulation.

2. Modelling water evaporation during frying with an evaporation dependent heat transfer coefficient

This chapter has been submitted as: van Koerten, K.N., Somsen, D., Boom, R.M., Schutyser, M. A. I., (2015). Modelling water evaporation during frying with an evaporation dependent heat transfer coefficient. Journal of Food Engineering.

2.1.Abstract

Water evaporation is critical to the design of frying processes and is strongly related to quality parameters such as oil uptake. Modelling of water evaporation as a result of coupled heat and mass transfer during potato frying is therefore highly relevant. In this study we developed a crust-core frying model that includes an evaporation rate dependent heat transfer coefficient. For this, we applied a Nusselt relation for spherical bodies and view the release of vapour bubbles during the frying process as a reversed fluidised bed. The characteristic length and velocity for the Reynolds number are taken as the average diameter of the vapour bubbles and vapour bubble release frequency multiplied with the bubble diameter, respectively. The model assumes limited conductive heat transfer and convective water vapour flow through the crust following Darcy's law. The predictions of the temperature profiles and water losses in potato cylinders of different size and at varying frying temperature were in good agreement with the experimental data. Extensions to the crust-core model are suggested to improve the prediction of the heat transfer coefficient and water vapour flux; however this should be balanced to the simplicity of the model, important for engineering purposes.

2.2.Introduction

Deep-fat frying is a method to prepare food through rapid dehydration by completely submersion in hot oil. Heat is initially transferred from the oil to the product surface through free convection, and from the surface to the interior via conduction. As water starts to evaporate from the product, the external heat transfer changes from free to forced convection by the emergence and escape of water vapour bubbles. A dry crust forms, which hinders conductive heat transfer and provides a resistance for moisture loss. The latter results in a pressure gradient between the moist interior of the product and the surface (Sandhu et al., 2013; Vitrac et al., 2000). As the evaporation rate decreases due to increasing crust thickness, the pressure gradient over the crust also decreases and oil may enter the product (van Koerten et al., 2015a). When the product is removed from the frying medium, the pressure gradient is lost with the heat transfer driving it, resulting in significant oil uptake (Bouchon et al., 2003; Ziaiifar et al., 2008). Since the moisture evaporation forms the basis for frying and is connected to oil uptake, an accurate description of the kinetics of water loss during frying is important for optimal control of the frying process.

Various models have been developed to describe moisture loss during frying, ranging in complexity from simplified empirical equations to complex numerical models, which incorporate mechanistic equations for both heat and mass transfer. All models have their own advantages in describing the moisture loss during frying. The simplest empirical models fit very well with the data set that is used, but they have to be fitted for every new data set and are therefore not well suited for extrapolation and prediction (Costa and Oliveira, 1999; Gamble et al., 1987; Krokida et al., 2000a).

At the other side of the spectrum, numerical models have been developed based on heat and mass transfer in porous media (Halder et al., 2006). These models incorporate phenomena such as diffusion, Darcy flow, heat transfer, and volume reduction. While highly accurate, these models are computationally intensive and contain many input parameters. Meanwhile, also simpler models have been developed on the basis of additional assumptions that still provide accurate predictions. For example, Farid (2001) developed an analytical model based on the assumption that frying is limited by heat transfer.

A recurring problem in modelling moisture evaporation during frying is the lack of a thorough description of the external heat transfer coefficient during forced convection. Models either use constant values for the heat transfer coefficient (Lioumbas et al., 2012a; Ni and Datta, 1999; Warning et al., 2012) or variable values based on literature (Bansal et al., 2014). It

would be logical to assume that the heat transfer coefficient is a function of the evaporation rate, as bubble formation at the product surface enhances forced convection.

In this work we present a relatively simple, though mechanistic model assuming a sharp moving boundary between the dry crust and moist interior of potatoes, in which the external heat transfer coefficient is connected to the water evaporation rate via a Nusselt correlation. While the water evaporation is mainly considered to be heat transfer dependent, the convective flow resistance of the water vapour in the crust was modelled following Darcy's law. Both the moisture loss during frying and the temperature profile at the surface and the centre of the potatoes were compared to experimental values for model validation.

2.3.Materials & methods

2.3.1. Preparation of raw potato samples

Alexia potatoes purchased at a local supermarket were used. The potatoes were cut into uniform cylinders with a cork borer and a stainless steel knife into three different diameters: 8.5, 10.5, and 14 mm. The cylinders were cut to a length of 50 mm with a calliper. The cylinders were then soaked for 10 minutes in tap water to equilibrate the moisture content of the batch; tissue paper was used to remove excess surface water.

2.3.2. Frying experiments

Potato cylinders were fried in a professional fryer (Caterchef EF 4L) containing 3L of 100% sunflower oil as frying medium. Three different temperatures were used to fry the samples: 140, 160, and 180°C. The sample frying times were 20, 40, 60, 120, and 180 seconds. One sample was fried at a time, and three duplicates were performed for each sample. Combined with the varying potato diameters (section 2.1), this resulted in 9 data sets with different potato diameter – frying temperature combinations.

2.3.3. Moisture content

Prior to frying, the raw potato cylinders were weighed to determine their initial mass. After frying, the moisture content of the potato cylinders was determined by oven drying at 105 °C to constant weight (approximately 24 hours). Afterwards, all oil was extracted from the cylinders using Soxhlet extraction (Büchi extraction system B-811), leaving only the dry matter of the potato cylinders. To determine the amount of moisture evaporated from the cylinders during frying, the mass balance was solved assuming oil, water, and dry matter as the only components.

2.3.4. Temperature measurements

A thermocouple (Tempcontrol, 0.2mm) was inserted in the potato, either at the surface or at the centre. The potato with the thermocouple was lowered in the frying oil for four centimetres. Therefore, the thermocouple could not conduct heat directly from the oil to the measuring tip (Figure 2.1). After frying, the potato was cut to exactly determine the position of the thermocouple. A data logger (EL-USB-TC-LCD thermocouple data logger) was used to obtain a time-temperature profile from the thermocouples.

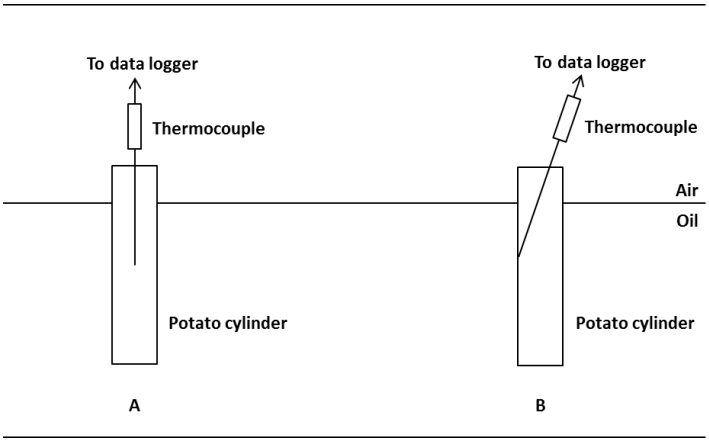

Figure 2.1. Schematic representation of the frying of a potato cylinder. A: Measuring the temperature at the centre. B: Measuring the temperature profile at the surface.

2.4.Model development

2.4.1. Model assumptions

To minimise computational effort, several assumptions were made for development of the model.

1) The evaporation front is modelled as a sharp boundary with a completely dehydrated crust on one side and a moist interior with the initial moisture content on the other side.
2) Shrinkage is neglected. Besides the fact that this reduces the computational effort, potatoes only experience around 10% shrinkage for the time intervals used in this work (Costa et al., 2001). The creation of pores is taken into account.
3) The model assumes a cylindrical geometry with infinite length, which allows for a one-dimensional formulation of the model.

Since the experiments were also performed using cylindrical fries, representative results are expected. The frying process itself is divided into 3 phases:

- Phase 1 (Initial heating): In this first phase no water evaporation takes place as the fry surface is heated to the boiling temperature of water. Heat is transported from the oil to

the fry surface through free convection, while conduction takes place from the fry surface to the interior.

- Phase 2 (Surface water evaporation): This phase starts as soon as the surface of the fry reaches the boiling temperature of the water (T_{boil}). Water starts evaporating while the surface temperature of the fry remains at T_{boil}.
- Phase 3 (Crust formation): As all the surface water is evaporated, crust formation begins and forms an additional barrier for heat transfer and vapour expulsion. The external heat transfer coefficient increases due to forced convection as a function of the evaporation rate. The sharp evaporation boundary migrates inwards, increasing the crust thickness.

2.4.2. Governing equations

During phase 1 of the process, only heat transfer takes place without water evaporation. Thus, the temperature profile inside the potato can be described using the general heat equation using cylindrical coordinates:

$$\rho_{co} c_{p,co} \frac{\partial T}{\partial t} = \frac{1}{r} \frac{\partial}{\partial r} (k_{co} r \frac{\partial T}{\partial r}) \quad (1)$$

Where ρ_{co}, $c_{p,co}$ and k_{co} are the density, specific heat capacity and the conductivity of the moist interior (core) of the potato respectively, T the temperature in the potato and r the radial position inside the cylindrical potato. The density and specific heat capacity of the potato are composed of the constituent mass-averaged values, assuming dry matter, moisture and water vapour as the only components. The following boundary conditions for the surface and core of the potato were applied:

$$-k_{co} \frac{dT}{dr} = h(T - T_{oil}) \text{ at } r = R \quad (2)$$

$$\frac{dT}{dt} = 0 \text{ at } r = 0 \quad (3)$$

With h being the external heat transfer coefficient, T_{oil} the oil temperature and R the radius of the potato cylinder. Since there is no water evaporation in phase 1, the Nusselt number (Nu), describing the ratio of convective to conductive heat transfer, is a function of the Rayleigh number (Ra) and the Prandtl number (Pr) using the diameter as the characteristic length. An empirical correlation that describes the external heat transfer coefficient for a wide range of Ra numbers was adapted from Churchill and Chu (1975) for free convection.

$$h = \frac{Nu}{2Rk_{oil}} \quad (4)$$

$$Nu_{free} = \left\{ 0.6 + \frac{0.387 Ra^{1/6}}{\left[1+\left(\frac{0.559}{Pr}\right)^{9/16}\right]^{8/27}} \right\}^2 \quad (5)$$

$$Ra = \frac{g\beta {\rho_{oil}}^2 c_{p,oil} \Delta T (2R)^3}{\mu_{oil} k_{oil}} \quad (6)$$

$$Pr = \frac{c_{p,oil}\mu_{oil}}{k_{oil}} \quad (7)$$

where ρ_{oil}, $c_{p,oil}$, k_{oil} and μ_{oil} are the density, specific heat, conductivity and the dynamic viscosity of the oil, respectively, g is the gravitational constant, β is the coefficient of thermal expansion and ΔT is the temperature difference between the potato surface and the bulk oil. The 'free' subscript indicates the Nusselt number accounting for free convection, while the Nusselt number for forced convection will be discussed below. The overall Nusselt number to calculate the heat transfer coefficient was calculated as the sum of the Nusselt numbers for free and forced convection.

When at the beginning of phase 2 the surface temperature of the fry reaches the evaporation temperature of water, surface evaporation starts and the boundary condition at the surface changes into:

$$-k_{co}\frac{dT}{dr} - \frac{dm_w}{dt}H_{vap} = h(T_{boil} - T_{oil}) \quad (8)$$

This boundary condition accounts for the energy lost due to water evaporation, H_{vap} is the evaporation enthalpy of water and m_w is the amount of water inside the potato. Note that the surface temperature of the potato is now constant at the boiling temperature of water. Again, the same solution approach is adopted.

This relatively short period ends as soon as the water in the outer layers is completely evaporated, and crust formation has started. This is the start of phase 3. Equation 8 can then be replaced by equation 2 again, with the only exception that the conductivity has to be changed to that of the dry crust (k_{cr}). Also, there is a new boundary condition, namely for the sharp evaporation front:

$$k_{cr}\left(\frac{dT}{dr}\right)_{r=R_{Y,cr}} - k_{co}\left(\frac{dT}{dr}\right)_{r=R_{Y,co}} = \frac{dm_w}{dt}H_{vap} \text{ at } r = R_Y \quad (9)$$

Where R_Y represents the position of the evaporation boundary and the cr and co subscripts refer to the outer radius of the dry crust and moist interior respectively. As vapour diffusion

through the crust is taken into account, the temperature at $r = R_Y$ will not remain at T_{boil} due to pressure build up. As a consequence, one equation is lacking, which is solved by explicitly calculating the evaporation rate with Darcy's law, while using a small time step for the implicit iterations.

The evaporation rate can be described as a pressure driven flow with a pressure gradient between the evaporation front and the surface of the potato. In this case, the pressure at the evaporation boundary is given by the saturation pressure for the local temperature (P_{sat}) while the pressure at the surface is assumed to be atmospheric (P_0). The saturation pressure was calculated from the governing temperature using the Antoine equation:

$$P_{sat} = e^{A-\frac{B}{C+T}} \tag{10}$$

Where A, B and C are the Antoine constants for water vapour. Subsequently, Darcy's law describing loss of water due to vapour flow through the crust is formulated as:

$$\frac{dm_w}{dt} = \rho_v \frac{2\pi\kappa L}{\mu_v \ln\left(\frac{R}{r}\right)} (P_{sat} - P_0) \tag{11}$$

Where ρ_v and μ_v are the density and viscosity of the water vapour at temperature T, κ is the permeability of the crust layer and L is the length of the fry. By calculating the evaporation rate explicitly the above system of equations can now be solved.

The final step is to account for the change in heat transfer, which has shifted from free to forced convection due to bubble formation and release at the potato surface. Since the oil flow around these vapour bubbles is deterministic for the heat transfer coefficient, the Nusselt relation developed by Dincer (1995) for spherical bodies was adopted:

$$Nu_{forced} = 0.267 Re^{0.432} Pr^{1/3} \tag{12}$$

An important aspect for using this equation is to apply a representative characteristic length and velocity for the Reynolds number. We chose to view the release of vapour bubbles during the frying process as a reversed fluidised bed, i.e. with oil being the stagnant fluidization medium and the vapour bubbles as the moving packed bed. In this case, the characteristic length is the average diameter of the vapour bubbles, while the characteristic velocity is the frequency with which the bubbles are released from the product multiplied by the bubble diameter (Forster and Zuber, 1955):

$$Re = \frac{\rho_{oil} v_b L_b}{\mu_{oil}} \quad (13)$$

$$v_b = \frac{\frac{dm_w}{dt}}{\rho_v} \frac{6}{\pi L_b^2} \quad (14)$$

Where, v_b and L_b are the average velocity and diameter of the escaping vapour bubbles respectively. In this case, the diameter of the vapour bubbles was taken as a constant, assuming that this is mostly a function of the interfacial tension between water vapour and the oil, which is constant. Moreover, also other work showed that the bubble diameter is practically constant for different frying times (Lioumbas and Karapantsios, 2015).

2.4.3. Model implementation

The above system of equations was discretized using a Crank-Nicolson scheme and solved using the Thomas algorithm, similar to Suárez et al. (2008). The potato cylinders were divided into 200 slices for the discretization of the spatial domain, while a time step of 0.00005 s was used for discretization of the temporal domain. Both discretization intervals were chosen for their resulting resolution in the output parameters and the simulation time, based on preliminary simulations. An increase of the number of spatial slices by 100 did not result in different results; the same was true for the time steps, decreased by a factor 0.2.

The system was initialized with a homogeneous temperature inside the potato of 20 °C and a water content of 0.8 (w/w total). All other physical parameters used as input for the model are listed in Table 2.1. All calculations were performed with MATLAB version 7.10.

Table 2.1. Physical parameters used in the model.

Parameter	Value	Units
Density		
Oil (180°C)	810	kg/m^3
Water	1000	kg/m^3
Dry matter (starch)	1600	kg/m^3
Water vapour	Ideal gas	kg/m^3
Specific heat capacity		
Oil	2518	J/kg/K
Water	4200	J/kg/K
Dry matter	1750	J/kg/K
Water vapour (100 °C)	1900	J/kg/K
Thermal conductivity		
Oil (180°C)	0.146	W/m/K
Moist interior[1]	0.95	W/m/K
Crust region[1]	0.14	W/m/K
Viscosity		
Oil (180°C)	0.0013	Pa·s
Water vapour (100 °C)	0.000012	Pa·s
Thermal expansion coefficient of oil	0.0007	K^{-1}
Antoine constants (Temperature in °C)		
A	23.295	
B	3885.7	
C	230.17	
Permeability of the crust to vapour[1]	10^{-13}	m^2
Vapour bubble diameter[2]	0.0006	m
Evaporation enthalpy of water (100 °C)	2260000	J/kg
Boiling point of water	100	°C

1. Lioumbas et al. (2012a)
2. Ni & Datta (1999)
3. Lioumbas & Karapantsios (2015)

2.5.Results & Discussion

To validate the model, the simulation output was compared to experimental data. Since the temperature profiles and moisture loss can easily be measured, these were used for the comparison. Additionally, the temperature and moisture content of the fries are also very relevant for the final product quality parameters. Since the evaporation rate dependent heat transfer coefficient is the most notable new aspect of the model, a closer look is taken at the evaporation rate and the heat transfer coefficient predicted by the model.

2.5.1. Temperature profiles

Figure 2.2 shows the temperature change in time for the core and surface of 3 different combinations of frying temperature and fry diameter. The surface temperature of the potato cylinders rapidly increases in time due to the high initial temperature difference between the oil and the potato cylinder. Due to the resistance to heat transfer in the potato cylinder, the temperature increase in the core is delayed, but finally reaches a plateau value around 100 °C, which is maintained due to the high evaporation enthalpy of the water present in large amounts in the potato interior.

The same plateau can be observed for the surface temperature, but the duration is much shorter than for the core. The reason for this is fast dehydration of the material close to the oil, and crust formation; when all water is evaporated, the evaporation can no longer act as an energy sink and the temperature starts to increase. The temperature increase in the crust is very slow and far below the temperature of the frying oil. This is because the moisture located deeper inside the fry still acts as a cooling source, and the heat transfer through the oil requires a difference in temperature between the oil and the surface of the potato cylinder.

The trends in temperature increase and plateau values are in agreement with observations by others (Farid and Kizilel, 2009; Lioumbas and Karapantsios, 2012; Sandhu et al., 2013). The model predictions for the different frying temperature–fry diameter combinations are also shown in Figure 2.2. The model provides an adequate description of the temperature evolution in both the core and the surface for all data sets. It can be observed that the model values for the surface temperatures do not produce smooth lines as water evaporation ensues. This is a direct consequence of the explicit incorporation of the water evaporation rate into the model, in combination with the discretization of the spatial coordinate. As the water in a numerical slice is evaporating, the temperature will remain practically constant. A slight increase in temperature is observed when the evaporation boundary moves further into the fry due to the relation between crust thickness and the temperature at the evaporation boundary (equation 10

and 11). It can also be observed in Figure 2.2 that the experimentally measured core temperature reaches a slightly higher plateau value than the model predicts. This may be explained by boiling point elevation due to the presence of dissolved components, which was not taken into account in the model, or by the higher local pressures generated by the water vapour generated locally, and which is then expelled forcefully through the pores into the oil. A local temperature of 105℃ would indicate a local overpressure of 0.2 bar, when this would be the only cause, which seems a physically realistic value.

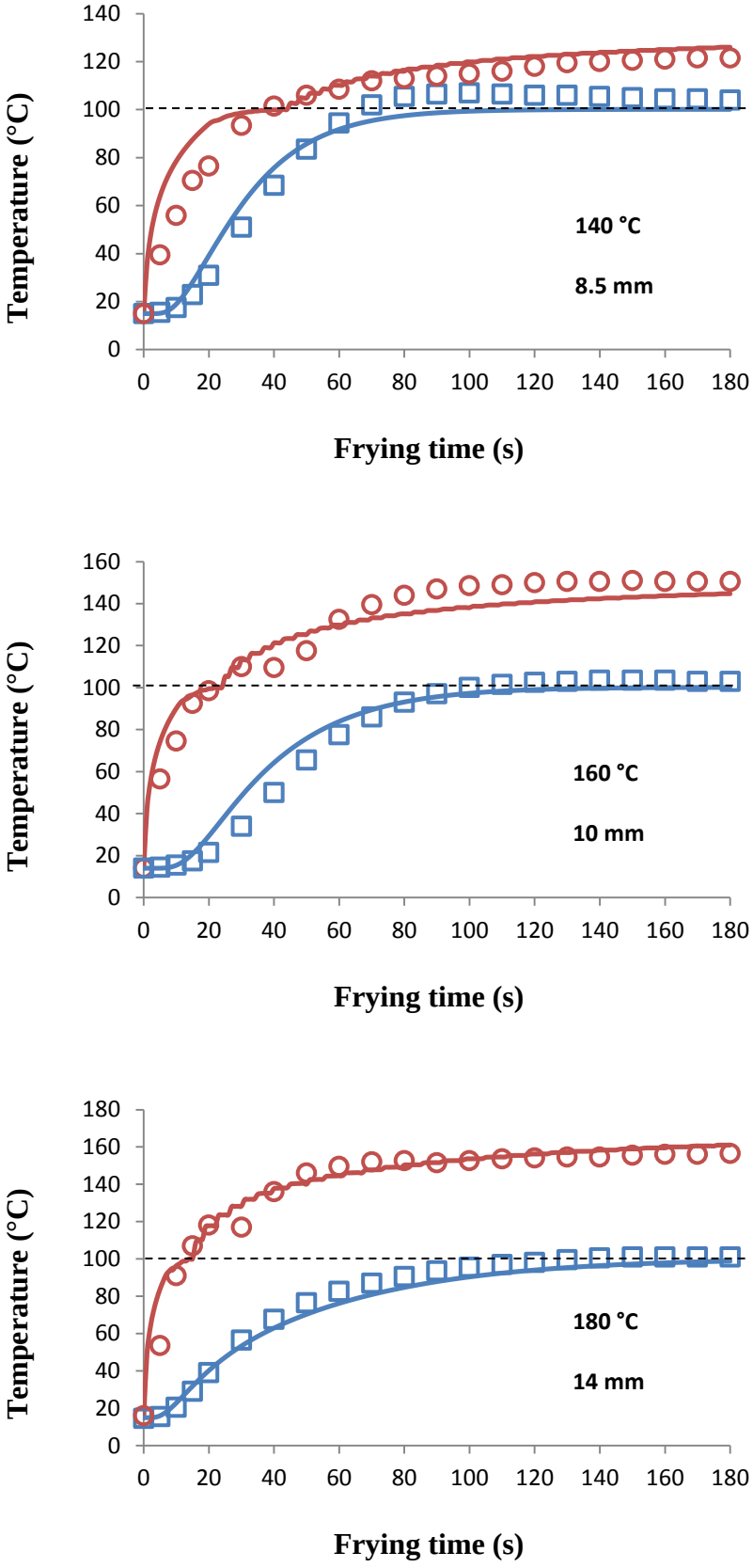

Figure 2.2. The measured evolution of temperature in time plotted for the centre (□) and the surface of the potato cylinders (○) for three different frying temperature and cylinder diameter combinations. The solid lines represent the model predictions.

2.5.2. Moisture loss

The moisture losses over time for all combinations of frying temperatures and fry diameters are shown in Figure 2.3. The rate of water loss increases with frying temperature due to the higher driving force for heat transfer. Next to this, the evaporation rate increases with decreasing diameter, because the surface-to-volume ratio of the potato cylinders is inversely proportional to the diameter of the cylinders.

Besides the experimental values, Figure 2.3 also shows the model predictions for water evaporation. Good agreement is observed between the experimental values and the model predictions. It is emphasized that model parameters are not fitted to the experimental data; it is a true prediction. When comparing these results to those obtained by fitting empirical relations (Costa and Oliveira, 1999; van Koerten et al., 2015a, 2015c) our model compares favourably. Even though our current mechanistic description is not as elaborate as some porous media based approaches, it is truly predictive and, having few parameters, it is useful from an engineering point of view (Bansal et al., 2014; Warning et al., 2012).

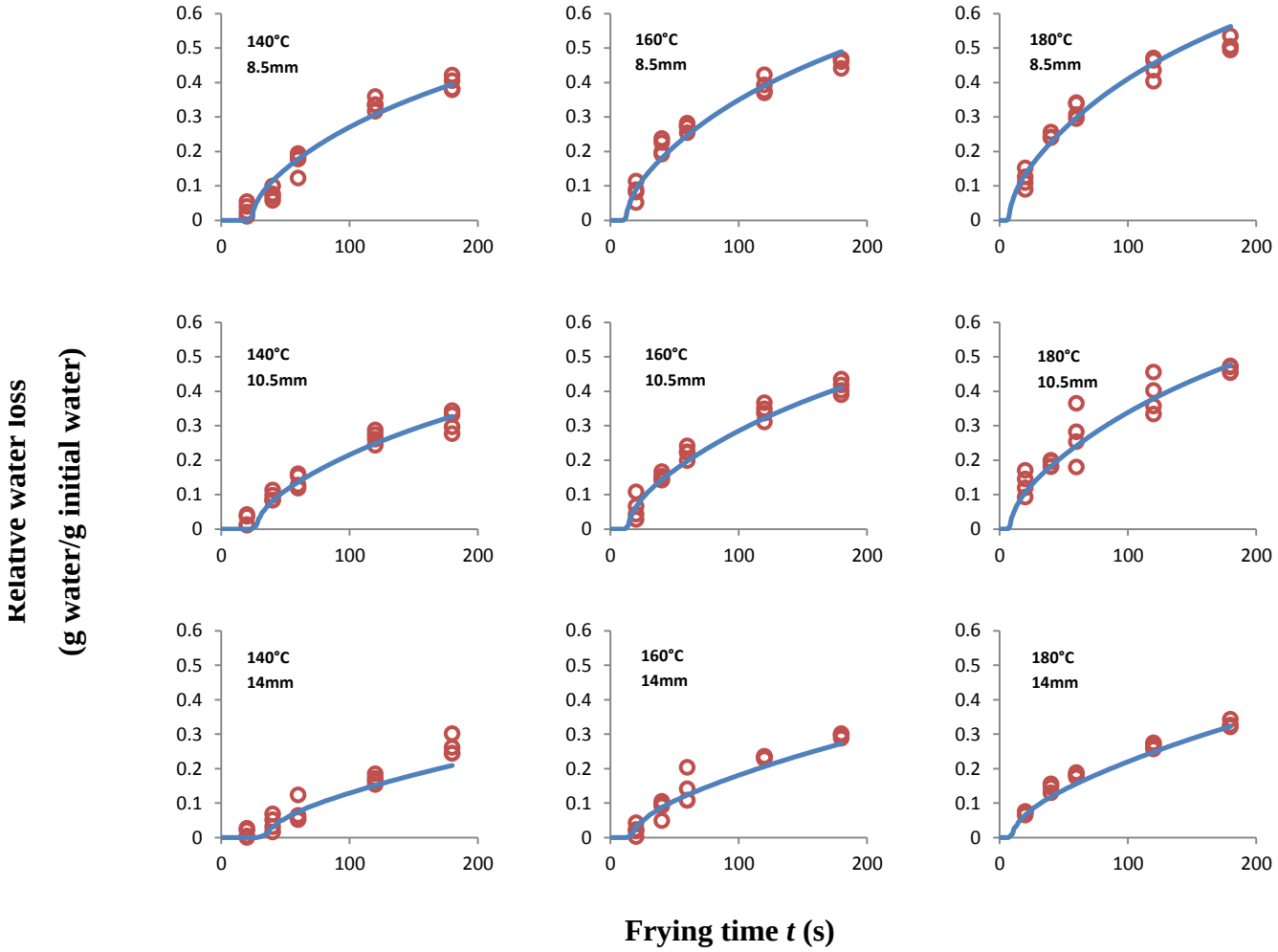

Figure 2.3. Water loss as function of frying time for different temperature and fry diameter combinations. Experimental data are represented by symbols (o) and model predictions by a line (-).

2.5.3. Vapour flux and heat transfer coefficient

To further assess the validity of the model, the calculated evaporation rate and the heat transfer coefficient were evaluated. Figure 2.4 shows the evaporation rate over time for potato cylinders with a diameter of 8.5 mm, fried at 140, 160 and 180 °C. There is a short delay, larger for lower frying times, which represents phase 1, the initial heating period. In this period the outer temperature of the potato increases to the boiling temperature of water, after which evaporation starts. Obviously, this period will last longer if the driving force for heat transfer is smaller.

The evaporation rate immediately moves to a maximum value after the initial heating period. This is because initially the surface water can evaporate freely, without any limitation by a crust. Additionally, the temperature difference between the oil and the surface of the potato is at a maximum during this second phase.

After the initial surface water has been evaporated, the surface temperature will exceed the boiling point of water (Figure 2.2). This initiates phase 3. The evaporation rate now drops drastically. This is caused by the formation of a crust and the resulting resistance to evaporation in the porous crust layer. The evaporation rate keeps decreasing, although at a slower pace, mostly due to the growth of the crust, and with it the resistance to heat transfer as a result of water loss (Figure 2.3). The decrease in evaporation rate is also partly caused by the decreasing temperature difference between oil and potato surface (Figure 2.2), which lowers Nu_{free}.

Decreasing the frying temperature results in a lower maximum evaporation rate, because of the decreased driving force from the oil-fry temperature gradient. However, during the period at which the water evaporation becomes more stable, the values practically merge. This indicates that after the initial crust formation, the frying process is now fully controlled by internal heat transfer.

The predicted trends for the evaporation rate by our model generally agree with experimental observations reported in other studies, although the evaporation rate in phase 2 is larger (Costa et al., 1999). The explanation for this may be that in the current model it is assumed that no evaporation takes place before the potato surface reaches the boiling point of water. However, in practice it has been observed that surface water evaporation already is initiated before this time. Possible reasons are the formation of nucleation sites due to the roughness of the potato surface, and escape of dissolved air: the expulsion of dissolved air out of the aqueous potato tissue due to the temperature increase, meaning that bubbles of gas can form at temperatures below the boiling point of water (Lioumbas et al., 2012b). As a consequence, the model underestimates the evaporation in phase 1, and overestimates the evaporation rate in phase 2.

The heat transfer coefficient for potato cylinders with an 8.5 mm diameter fried at 140, 160 and 180 °C, is plotted in Figure 2.5A as function of the frying time. During the initial heating phase, a small decrease in the heat transfer coefficient can be observed. In this period there is only free convection, so the decrease in the outer temperature gradient will lead to a reduction of the heat transfer according to equations 4-7. After the initial heating phase, the trend for the heat transfer coefficient is similar to that for the evaporation rate (Figure 2.4). This observation reflects the outcome of equations 13 to 15, which describe the dependence of the heat transfer coefficient on the evaporation rate.

Even though similar trends are observed in literature, the absolute values observed in this work are relatively high (Costa et al., 1999; Farkas and Hubbard, 2000). A reason for this may be the sharp evaporation boundary used in this work, while a diffusive evaporative zone may be more realistic (van Koerten et al., 2015b). As water migration in the fry and water evaporation at multiple locations are not taken into account, a larger heat transfer coefficient is necessary to obtain an adequate amount of water loss.

Another reason may be related to the low diameter of the vapour bubble used in the model, which was 0.6 mm assumed on the basis of literature data (Lioumbas and Karapantsios, 2015). This diameter differed from our own camera observations as we determined an average bubble size of 2 mm using a frying unit with transparent windows. The reason for this difference is probably that the literature data originate from measurements above a ceramic porous matrix, while our own observations are done during potato frying. From Figure 2.5b it is clear that a larger bubble diameter leads to a significant decrease of the heat transfer coefficient with peak values similar to those observed by Lioumbas et al. (2012a), who used a comparable model based on heat transfer limitation.

Additionally, it is noted that reported heat transfer coefficients in literature are usually determined with indirect methods involving assumption based and simplified equations leading to underestimation of the actual value.

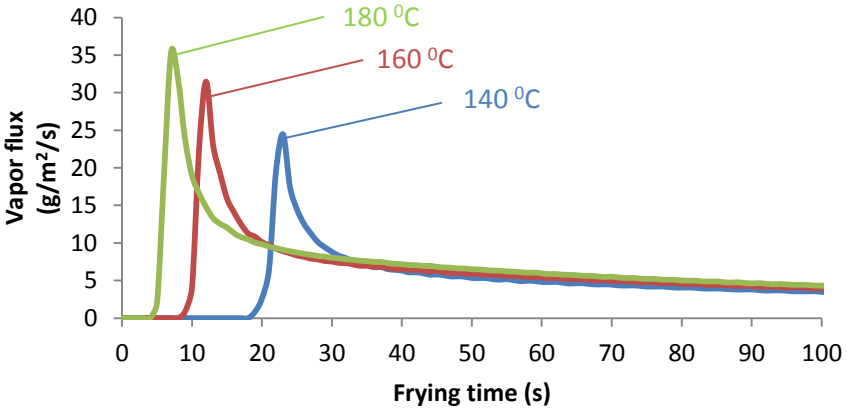

Figure 2.4. Vapour flux over time for potato cylinders with a diameter of 8.5 mm, fried at 140 (-), 160 (-) and 180 °C (-).

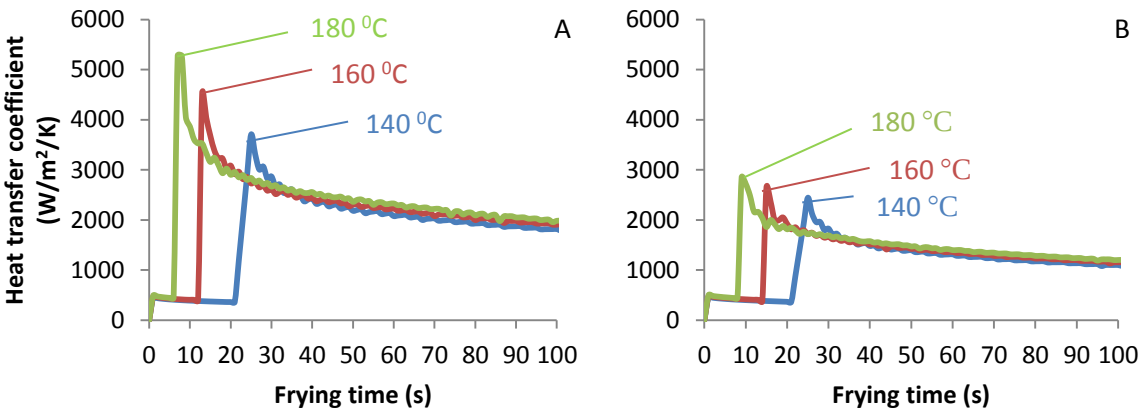

Figure 2.5. Heat transfer coefficient over time for potato cylinders with a diameter of 8.5 mm, fried at 140 (-), 160 (-) and 180 °C (-). A: Results for a bubble diameter of 0.6 mm. B: Results for a bubble diameter of 2 mm.

2.6.Conclusions

A water evaporation model was developed based on the assumption that frying is limited by heat transfer. An explicit Nusselt relation was included to describe the heat transfer coefficient during frying due to evaporation. Resistance of the crust towards water vapour flow was taken into account following Darcy's law. The model was numerically implemented using the Crank-Nicolson method with a sharp moving evaporation boundary.

The model accurately predicted the experimental temperature profiles and water loss during frying of potato cylinders without the use of heat transfer coefficients from literature or parameter estimation. The absence of fitting parameters and the limited number of physical parameters make this model suitable for engineering purposes. Moreover, since water evaporation is connected to oil uptake, it could also be applied for optimal control of the frying process.

Based on the vapour flux results, the model could still be extended with a better description of the initial evaporation process of the surface water. Additionally, the use of a diffusive evaporation zone instead of a sharp evaporation boundary could lead to calculation of more realistic heat transfer coefficients and provide more smoothened temperature profiles. However, the drawback of such extensions is that the model becomes perhaps again too complex to use it for engineering purposes.

2.7.Acknowledgements

This study was funded by *GO Gebundelde Innovatiekracht* and EFRO, an initiative by the European Union. Co-partners in the study were Aviko B.V., Machinefabriek Baltes and van Lente elektrotechniek. The authors also acknowledge Annelieke Bot and Dane te Hennepe, Msc students from Wageningen University, for their help with the experimental work.

3. A pore inactivation model for describing oil uptake of French fries during pre-frying

This chapter has been published as: van Koerten, K. N., Schutyser, M. A. I., Somsen, D., & Boom, R. M. (2015). A pore inactivation model for describing oil uptake of French fries during pre-frying. Journal of Food Engineering, 146, 92-98.

3.1.Abstract

The reduction of oil uptake during deep-frying is a subject with societal relevance, given the trend towards lower-fat foods. Since research into oil absorption during frying is limited, we here report on developing better mechanistic understanding of this process. The oil uptake for different frying temperatures and fry dimensions was measured as a function of the water evaporation rate and water loss. A pore inactivation model was developed based on the hypothesis that the crust is a porous layer through which the exuding moisture vapour flow inhibits oil migration. Decreases in water evaporation rates will cause pores to inactivate, allowing oil to penetrate into the crust. The model provides good predictions to the experimental data. Since the model has two parameters, a purely statistical comparison with a simple linear fit having one parameter, does not show a significant benefit; however, the model better describes the overall trend of oil uptake.

3.2.Introduction

In the last decades, deep-fat frying has become one of the most popular methods to prepare food, not only because of the method's ease but also because of the distinctive palatability and mouth feel of oil fried products. Globally, potatoes are easily the most established fried product and, as French fries and potato chips, are an integral part of many western cultures. One of the most important quality parameters of fried foods is the oil content. While the oil gives fried products their specific flavour, consumers tend to move towards lower-fat food products, creating the need to also reduce the fat content in industrial-scale food processing. To minimize the oil content without losing the popular characteristics of fried products, it is essential to understand the mechanisms by which the oil penetrates the product during frying.

The oil uptake into French fries can be divided into 3 parts: (1) the internal oil, which is the oil that is absorbed by the fries during the frying itself; (2) the absorbed surface oil, which is the oil absorbed by the fries directly after their removal from the oil; and (3) the surface oil, which is the oil that adheres to the surface of the fry after cooling (Bouchon et al., 2003). Previous research showed that the final oil content is determined to large extent by the adsorbed surface oil, while during frying itself, oil penetration into the product is partly hindered by water evaporation and expulsion from the fry (Moreira et al., 1997; Pedreschi et al., 2008; Ufheil and Escher, 1996). After the fries are removed from the oil, cooling leads to condensation of the water vapour in the pores, which causes an under-pressure and thus a suction of oil from the surface into the pores of the fries (Vitrac et al., 2000).

Measures have been developed to prevent uptake after frying, mostly revolving around fast removal of the surface oil to minimize the oil uptake due to condensation of the water vapour in the fries. The oil uptake during frying, however, is a phenomenon that has been less well studied and is more difficult to prevent. Previous investigations only empirically described the oil uptake during frying using a first order equation or simply by proposing that the amount of oil absorbed is proportional to the amount of evaporated water (Gamble et al., 1987; Krokida et al., 2000; Moyano and Pedreschi, 2006). Although this gives adequate results for higher frying times, it does not match the experimental data for smaller time intervals, which are the relevant times for industrial pre-frying processes. To better understand this counter-current migration of oil and water vapour, a more mechanical description is proposed in this study.

We here report on a mechanistic description of the oil uptake during frying, by drawing an analogy to the way that pore inactivation is modelled during cross-flow membrane emulsification. This is a new process that is proposed to produce emulsions with narrow droplet size distributions, by pressing a to-be-dispersed fluid through the pores of a membrane that is wetted by the continuous phase. The continuous phase flows over to the receiving side of the membrane. In many studies, it was found that only a small fraction of all pores in the membranes were active, i.e., had dispersed phase flowing through, while most of them were inactive (Vladisavljevic and Schubert, 2002;Yasuno et al., 2002). During emulsification with microsieves (micro-engineered precision membranes) it was observed that lower transmembrane pressures lead to inactivation of a large fraction of the pores, even when all pores are exactly the same (Abrahamse et al., 2002). The reason for this is that droplets at the surface of a pore need a minimum pressure to be released, i.e. the critical Laplace pressure, which is higher than the pressure that is needed to sustain the oil flow and continuous detachment of droplets, as soon as the oil flow has started. If the supplied pressure across the membrane is lower than the critical Laplace pressure, not all pores can be sustained, and inactivation of pores occurs. Similar phenomena have been seen with the formation of foams with membranes (Kukizaki and Goto, 2006).

We here draw the analogy to frying of French fries. Here, water vapour is forced through the pores in the crust of the fry into the oil phase. During frying the pressure across the pores in the crust decreases due to the decreasing heat transfer and water evaporation rate, since the crust slowly become thicker. This will cause some of the pores to become inactivated, and will allow oil to be taken up due to capillary pressure.

We first report on the measurement of water evaporation and oil uptake as function of frying time for different frying oil temperature and dimension of the French fries. Then, the mechanistic approach is presented and used to describe the oil absorption during frying based on the principle of pore inactivation. This approach is then evaluated and compared to the empirical approach assuming linear relation between absorbed oil and amount of water evaporated.

3.3.Materials & methods

3.3.1. Preparation of raw potato samples

Alexia potatoes purchased at a local supermarket were used in this study. Potatoes were cut into uniform cylinders with a cork borer and a stainless steel knife into three different diameters: 8.5, 10.5, and 14 mm. The cylinders were cut to a length of 50 mm with a calliper. Samples were then soaked for 10 minutes in tap water to equilibrate the moisture content of the batch, and tissue paper was used to remove excess surface water.

3.3.2. Frying experiments

Potato samples were fried in a professional fryer (Caterchef EF 4L) containing 3L of 100% sunflower oil as frying medium. Three different temperatures were used to fry the samples: 140, 160, and 180°C. The sample frying times were 20, 40, 60, 120, and 180 seconds. One fry was fried at a time, and three duplicates were performed for each sample.

3.3.3. Surface oil determination

Directly after frying, the potato cylinders were dipped for 1 second in a reaction tube containing petroleum ether in order to remove all the adhering surface oil. Afterwards, the petroleum ether was left to evaporate in a fume hood and the weight gain of the reaction tube was used to determine the amount of surface oil that had adhered to the sample (Moreira et al., 1997).

3.3.4. Moisture content

Prior to the frying step, the raw potato cylinders were weighed to determine their initial mass. After the adhered surface oil had been removed, the potato cylinders were weighed once more and oven dried at 105 °C to constant weight (approximately 24 hours). To determine the amount of moisture evaporated from the cylinders during frying, the mass balance was solved assuming oil, water, and dry matter as the only components.

3.3.5. Oil uptake during frying

After removing the adhered surface oil, the only remaining oil in the potato cylinders was the oil that had been absorbed during frying. This oil was determined using a Büchi Extraction system B-811 with 200 mL of petroleum ether as the extraction medium (boiling range 40-60 °C). The samples were ground and subjected to the extraction (3 hours) in pairs to obtain a more significant amount of oil, and thus decrease the relative errors.

3.3.6. Water evaporation rate

Different methods to determine the water evaporation rate have been documented. Costa et al., 1997 proposed a method to obtain the evaporation rate by recording the frying process in a

glass container on video. Since larger amounts of vapour bubbles resulted in lighter patches in the grayscale images, they could well correlate the average lightness with the amount of evaporating water. However, a more reliable method is gravimetric analysis. This has been done during frying by putting the entire frying system on a scale and directly monitoring the weight loss during frying (Farkas and Hubbard, 2000). However, since the weight of the frying setup is much larger than the weight of evaporating water per time unit, this method is not very accurate.

We here use an offline gravimetric analysis to obtain the water evaporation rate. This was done by measuring the water loss at different times and subsequently fitting a line through the obtained data points. The water content obtained at different frying times was fitted using a compartmental model proposed by Costa and Oliveira, 1999:

$$\frac{M_0 - M}{M_0} = 1 - \alpha[e^{-K_c t}(1 + K_c t)] - (1 - \alpha)[e^{-K_e t}(1 + K_e t)] \qquad (1)$$

In which M_0 is the initial amount of water in the fry (g), *t* the frying time (s), *M* the amount of water in the fry (g) at time *t* and α, K_c (s^{-1}) and K_e (s^{-1}) are fitting constants. By taking the derivative of the compartmental model we obtain an expression for the evaporation rate:

$$\frac{M}{t} = -\alpha {K_c}^2 t[e^{-K_c t}] - (1 - \alpha){K_e}^2 t[e^{-K_e t}] \qquad (2)$$

Since these relations are empirical in nature it should be noted that the fitting constants cannot be directly correlated with the process parameters (i.e. temperature and fry diameter) and the data sets need to be fitted separately. For the same reason, extrapolation should be avoided, since the fit is not validated outside the data range.

3.3.7. Modelling oil uptake

Since existing models for oil absorption during frying all rely on purely empirical relations, a new mechanistic interpretation is useful. For this, we approach the crust as a series of parallel linear pores which connect the moist core of the French fry with the frying medium. As the internal pressure decreases, due to decreasing evaporation rate, pore inactivation occurs (Figure 3.1).

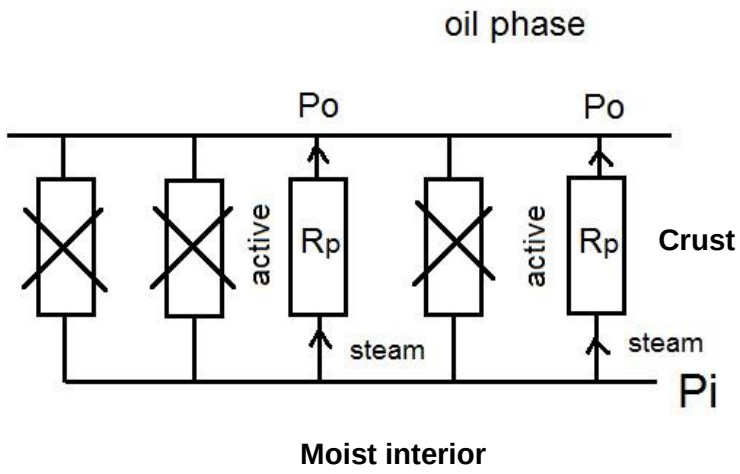

Figure 3.1. Schematic representation of the model that describes the crust as a series of parallel pores. R_p: pore flow resistance; P_i: pressure in the moist interior below the crust; P_o: oil pressure. As P_i decreases, not all pores can be sustained and pore inactivation occurs.

Some additional assumptions are needed. The first one is that oil cannot be taken up through pores which are still expelling water vapour, since it would be displaced by the vapour flow. Second, the total amount of pores is formed at the maximum evaporation rate, at which point all pores are active. Abrahamse et al., 2002 showed that there is a linear relationship between the pressure gradient over a membrane and the percentage of active pores. Additionally, from Darcy's law we know that the flux through a porous medium is proportional to the pressure gradient. Following this we can relate the water evaporation rate and the amount of active pores using:

$$\frac{w}{w_{max}} \sim \frac{N}{N_T} \qquad (3)$$

where w is the evaporation rate (g/s), w_{max} the maximum evaporation rate (g/s), N the number of active pores and N_T the total amount of pores. Since oil is only taken up through the inactivated pores (N_T-N) the oil uptake using the water evaporation rate is given by:

$$\boldsymbol{S = a \cdot N_T \cdot \frac{w_{max} - w}{w_{max}}} \quad (4)$$

In this, *S* is the total oil uptake in a single fry (g) and a is the oil taken up by a single inactive pore (g). It was found from preliminary experiments that there is already some oil uptake before the maximum evaporation rate is reached, so an additional term for initial oil content should be added. The amount of fat/oil present in raw potatoes was found to be negligible, being less than 10% of the initial oil uptake.

Additionally, the amount of oil taken up by a single inactive pore is considered to change during frying due to the increasing thickness of the crust. The pores were therefore assumed to be uniform cylinders perpendicular to the length of the potato tubers. Since the crust thickness increases almost linearly with the amount of evaporated water in cylindrical fries with length >> radius, equation 4 can be modified into:

$$\boldsymbol{S = \frac{M_0 - M}{M_0} \cdot K \cdot \frac{w_{max} - w}{w_{max}} + oil_0} \quad (5)$$

With

$$\boldsymbol{K = N_T \rho_{oil} A r} \quad (6)$$

where K represents the amount of oil uptake when no water remains in the fry (kg), ρ_{oil} the density of the frying oil (kg/m^3), A the average pore surface area (m^2), r the radius of the potato cylinder (m) and oil_0 is the amount of oil already taken up when the maximum evaporation rate is reached (g). Shrinkage of the potatoes may be assumed to be negligible for the frying times used in the experiments (Costa et al., 2001). For comparison, a simple linear model is evaluated as well, assuming that the oil uptake is simply proportional to the water loss, as proposed by Gamble et al., 1987:

$$S = \frac{M_0 - M}{M_0} \cdot S_{max} \quad (7)$$

Where S_{max} is simply the maximum amount of oil that can be absorbed during frying.

3.3.8. Model fitting & comparison

The pore inactivation model has two parameters; K and oil_0, while the linear model only has one parameter; S_{max}. All models were fitted using nonlinear least squares regression in Excel. Although the pore inactivation model would be preferred as it rests on physical phenomena, both models were compared using a statistical criterion. For this a corrected Akaike criterion

was used for smaller data sets, comparing the models, while taking the different number of parameters in account (van Boekel, 2008):

$$\mathbf{AIC_c} = \mathbf{n} \cdot \mathbf{ln}\left(\frac{\mathbf{SS_r}}{\mathbf{n}}\right) + \mathbf{2} \cdot (\mathbf{p} + \mathbf{1}) + \mathbf{2} \cdot (\mathbf{p} + \mathbf{1}) \cdot (\frac{\mathbf{p+2}}{\mathbf{n-p}}) \qquad (8)$$

Here AIC_c is the corrected Akaike criterion, p is the number of fitting parameters used in the nonlinear regression, n the sample size of the dataset and SS_r the residual sum of squares. The criterion balances the goodness of fit of the model with the complexity of the model. For two models, the one with the smallest value for the Akaike criterion is the most desired.

3.4.Results & Discussion

3.4.1. Moisture loss

The moisture loss was determined during frying at different time intervals: 20, 40, 60, 120 and 180 seconds. Figure 3.2 shows the relative water loss during frying for nine different combinations of frying temperature and fry diameter. The compartmental model (equation 1) describes the results well. The slope of the curves increases with increasing temperature, which is to be expected, since the heat flux is proportional to the temperature gradient, according to Fourier's law. Further, the slope of the water evaporation curves increases with decreasing fry diameter, which may be explained by the increasing area-to-volume ratio of the fries, since the length of all the fries is the same. If there is more area per volume, there will be more heat transferred per unit of water present in the fry, hence the evaporation rate increases.

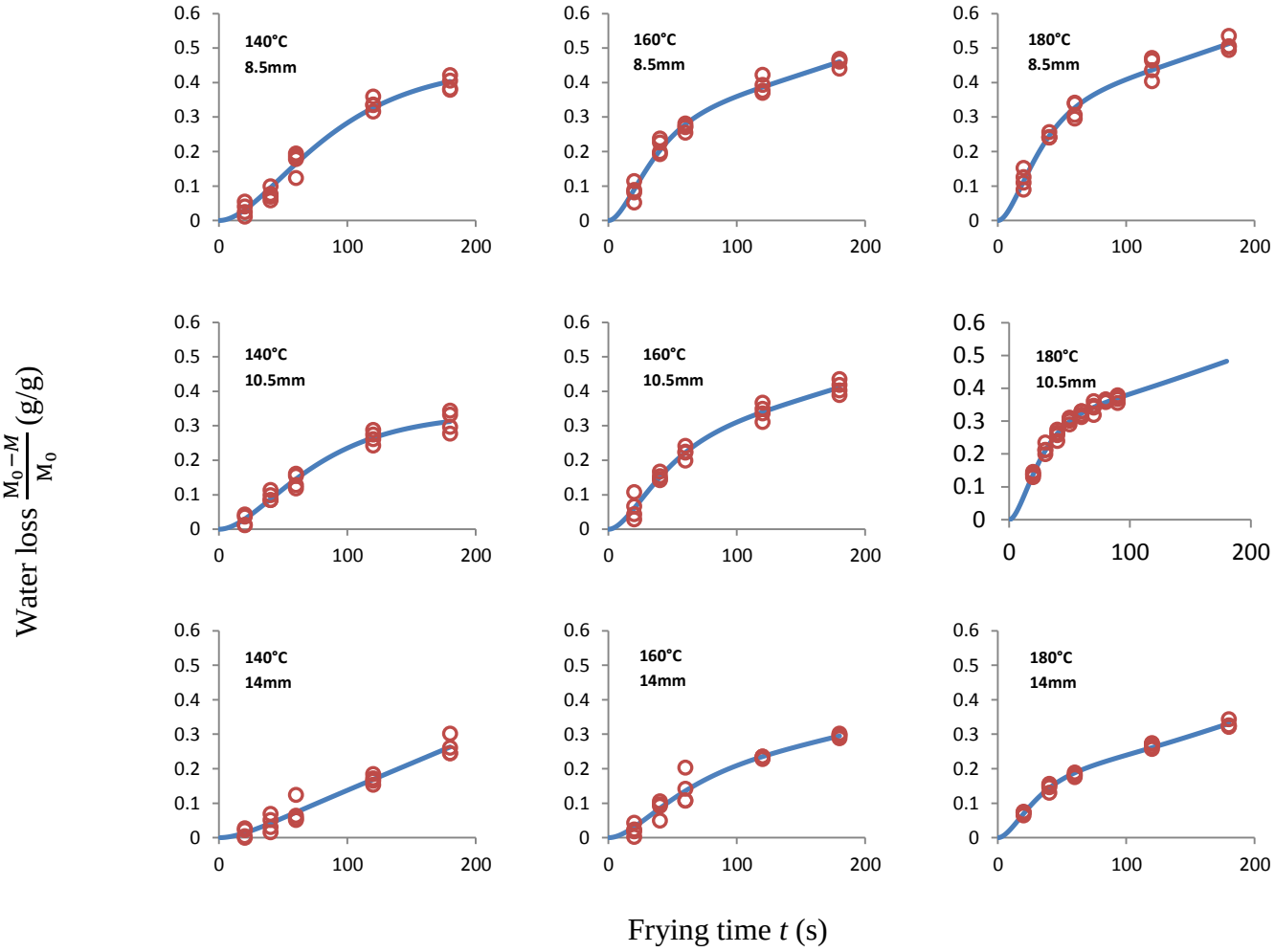

Figure 3.2. The water loss over time for the different temperature-fry diameter combinations. With the experimental values (o) and the curve fitted using the compartmental model (equation 1) (-).

To obtain the water evaporation rate, the derivative of the fitted curves was determined (equation 2), which is simply an equation for the slopes visible in Figure 3.2. Initially, there is a rapid increase as vapour bubbles start to appear at the surface of the fry, increasing the local turbulence and thus increasing the heat transfer coefficient (Farkas and Hubbard, 2000; Lioumbas and Karapantsios, 2012). After the maximum evaporation rate has been reached, heat transfer decreases due to formation of the crust, which has a much lower conductivity than the frying oil (Ziaiifar et al., 2009). As the moisture evaporation continues, less vapour bubbles appear at the surface, the local turbulence decreases, the heat convective heat transfer decreases, and the moisture evaporation rate decreases almost to a lower plateau value (Vitrac et al., 2002). The values and trend for water evaporation rate correspond well with literature data (Costa et al., 1999;Farkas and Hubbard, 2000). Also, in addition to the increasing slope with higher temperature and decreasing fry diameter, the maximum evaporation rate is reached earlier for higher temperatures and decreasing fry diameter.

Since the heat transfer coefficient is proportional to the temperature gradient and the surface area of heat transfer, it is possible to calculate an apparent heat transfer coefficient by dividing the water evaporation rate by the temperature gradient and the surface area of heat transfer where we assume that all heat is transferred to the fries as latent heat. In Figure 3.3 the calculated heat transfer coefficients for three different temperatures and three different fry dimensions are shown. It is clear from Figure 3.3 that the heat transfer coefficient decreases with increasing fry diameter. This may be explained by the fact that larger fries require relative more energy to heat and thus less energy is available to generate vapour, which results in a lower calculated heat transfer coefficient. For the frying oil temperatures of 180 ^{o}C, 160 ^{o}C 140 ^{o}C the time-averaged heat transfer coefficients were 58, 69, and 89 W/m^2/K, respectively. It can be concluded that this time-averaged heat transfer coefficient actually decreases with increasing temperature, which is in agreement with previous investigations (Yıldız et al., 2007). They explained that this decrease is related to the increasing water evaporation rate with increasing oil temperature, leading to more energy loss with the vapour, leaving less energy available for internal heating. Additionally, a critical vapour bubble concentration near the fry surface may be reached for higher oil temperatures. At this critical vapour concentration a thin film of vapour is formed with a lower conductivity than the oil, thus reducing the apparent heat transfer coefficient.

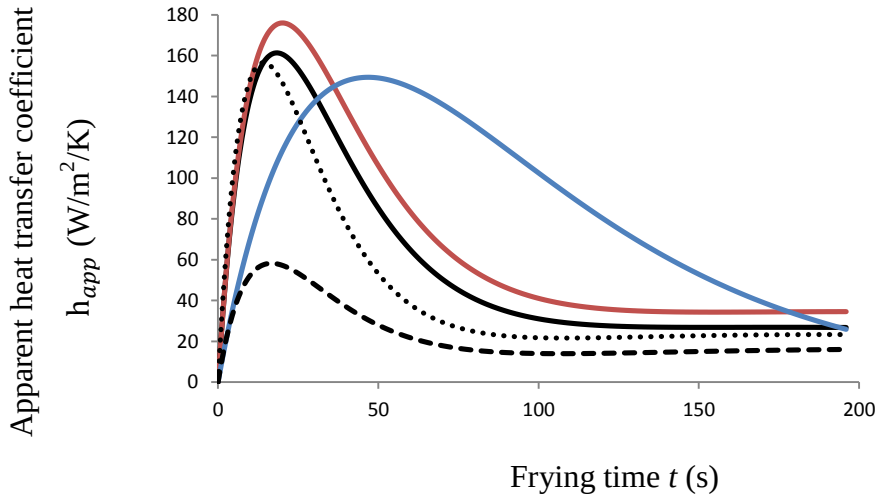

Figure 3.3. The apparent heat transfer coefficient for different oil temperatures and fry dimensions, i.e. 180 °C and 8.5 mm (-), 160 °C and 8.5 mm (-), 140 °C and 8.5 mm (-), 180 °C and 10.5 mm (··), and 180 °C and 14 mm (--).

3.4.2. Oil uptake

The values of K_c, K_e and α that were found by using equation 1 in Figure 3.2, were used to estimate the time-dependent moisture evaporation rates. In Figure 3.4 these values are plotted against the oil uptake during frying, starting with the maximum evaporation rate (i.e., the values in the initial heating period are omitted, for reasons of clarity). The graphs should be interpreted from right to left, as the water evaporation decreases from the maximum evaporation rate onwards, and from bottom to top, as the amount of oil taken up increases.

The values obtained for the oil uptake are in line with those found by Ziaiifar et al. (Ziaiifar et al., 2008;Ziaiifar et al., 2010). In Figure 3.4, the graphs for 160°C-10.5mm, 180°C-10.5mm and 180°C-14mm again show the disadvantage of adopting an empirical model. Here, at the final stage of the frying where the evaporation rate should go towards a plateau value, the water evaporation rate suddenly increases again by a small amount. As this is physically not possible with constant frying conditions, this must be an artefact from the fitted equation 2. However, since this occurs only at the final stage of water evaporation where the change in water evaporation rate goes towards zero, the error is not significant.

The trends observed in Figure 3.4 seem to be in agreement with the proposed pore inactivation model (equation 5). Initially there is a linear relation between the water evaporation rate and the amount of oil absorbed ($S \propto w$), as suggested. Subsequently, when the amount of inactivated pores approaches N_T, the right side of equation 5 equals 1 and the oil uptake becomes completely dependent on the absolute amount of water loss: the number of filled pores is constant, but they still grow in length. Concurrently, the trend becomes a vertical line, independent of the water evaporation rate.

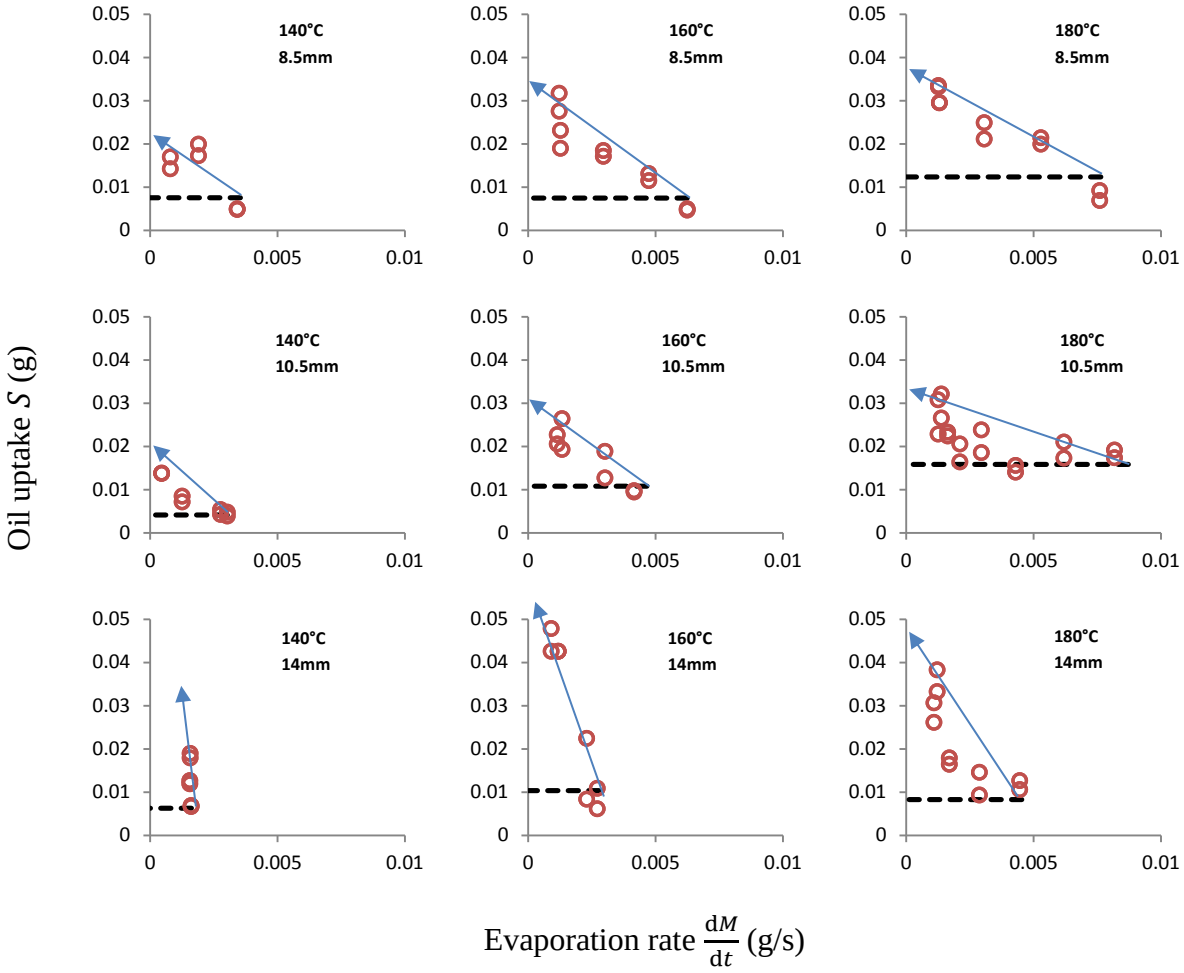

Figure 3.4. The oil uptake in a single fry (with a fat free dry matter content of 0.20 g/cm^3 of total fry volume) plotted against the water evaporation rate obtained from equation 2. With the experimental data (o), a dashed line representing the initial oil uptake oil$_0$ (--) and a line to guide the eye, indicating the chronological order of frying (→).

3.4.3. Oil uptake model comparison

In Figure 3.5, for three frying conditions, the two models predicting the oil uptake as function of the water loss are plotted together with the experimental data. Both the linear model and the pore inactivation model fit the experimental data, but the pore model seems to capture the initial flat stage of the frying more accurately. This initial stage is in agreement with the hypothesis that oil uptake is hindered by the flux of water vapour emerging from the pores. This hindrance is stronger at higher water evaporation rates, or in this case at lower values for absolute water loss. As the number of inactive pores approaches N_T, no more new pores can be filled, and the oil uptake can only increase by the increase of their length, due to the absolute water loss. This correlates well with the linear part of the curves in Figure 3.5 at higher values for water loss. Also interesting to note is that Figure 3.2 shows higher total water losses for higher temperatures. If the oil absorption would be just a linear function of the amount of moisture loss, higher frying temperatures would also lead to more oil

absorption. However, looking at Figure 3.4, this is not that evident for the frying temperatures of 160°C and 180°C. For the fry diameter of 14mm, the frying temperature of 160°C even shows a higher amount of oil absorption than the temperature of 180°C. However, because of the experimental variation it is difficult to draw conclusions on which model statistically describes the data most accurately.

To compare the linear model to the pore inactivation model proposed in this work the Akaike criterion was used. As the Akaike criterion takes into account the residual sum of squares, the sample size and the number of parameters, it provides a statistical comparison between the two different models. However, it does not take into account the fact that the parameters of the new model describe the physical properties of the potato, while the parameter for the linear model is a fitting constant without any physical meaning, and in parts of the process does not behaves physically (*see above*).

The calculated fitting parameters and Akaike values for the different models are provided in table 3.1, together with the Akaike criterion differences. Since a lower Akaike criterion value suggests a model with higher statistical quality, positive numbers favour the linear model while negative numbers favour the pore inactivation model. On average, the linear model describes the experimental data slightly better, due to the fact that the linear model has only one fitting parameter. Another factor is that most data points are in the linear part of the oil uptake vs. water loss, which is best described by the linear model. Indeed, the linear model seems to especially fit the 8.5 mm data sets very well, and, as mentioned before, the maximum evaporation rate is reached sooner with thinner fries and higher temperature. Since the sampling times are the same, this also means that more data points are in the linear part of the graph. However, the pore inactivation model better explains the initially slow increase of oil uptake and its fitting parameter (K) has physical meaning, which is not so for the S_{max} in the linear model.

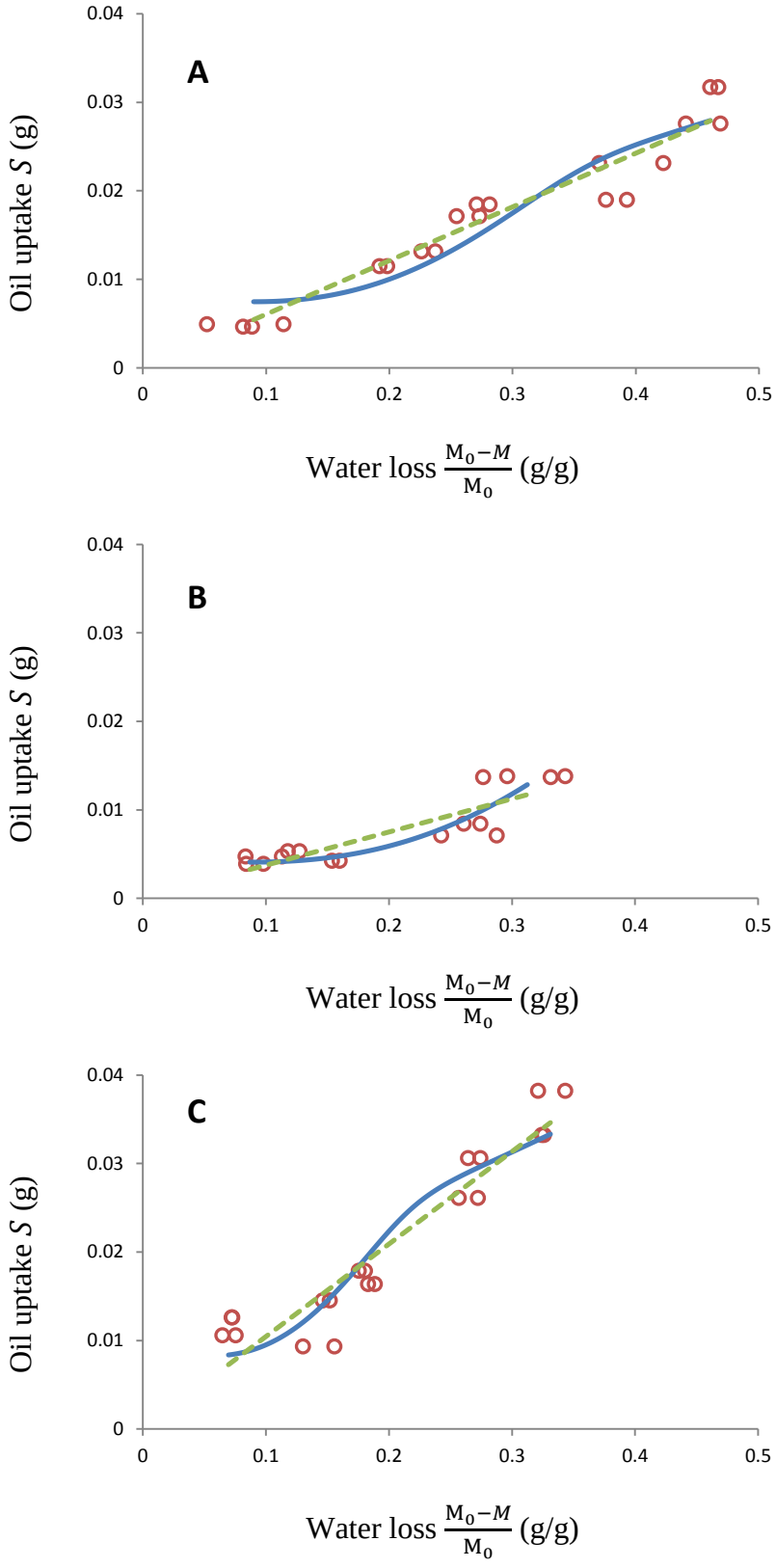

Figure 3.5. The oil uptake in a single fry (with a fat free dry matter content of 0.20 g/cm^3 of total fry volume) plotted against water loss for three different temperature-fry diameter combinations: 160 °C and 8.5 mm (A), 140 °C and 10.5 mm (B), 180 °C and 14 mm (C). With the experimental data set (o) fitted using both the linear model (--) and the pore inactivation model (-).

Table 3.1. Calculated values of the fitting parameters and the Akaike criterion for the pore inactivation model and the linear model fitted to the experimental data. The difference in Akaike criterion was taken as pore model minus linear model. Therefore positive numbers statistically favour the linear model while negative numbers statistically favour the pore model.

T (C)	*d* (mm)	**Pore model**		**Linear model**	**Akaike criterion**		
		K	oil_0	S_{max}	Pore model	Linear model	Difference
140	8.5	0.035	0.008	0.044	-99.1	-108.0	8.9
160	8.5	0.055	0.007	0.061	-101.1	-110.8	9.7
180	8.5	0.050	0.012	0.068	-99.2	-106.6	7.5
140	10.5	0.033	0.004	0.038	-122.9	-116.0	-6.8
160	10.5	0.041	0.011	0.060	-101.9	-103.8	1.9
180	10.5	0.023	0.016	0.072	-201.9	-199.8	-2.1
140	14	1.618	0.006	0.071	-118.6	-118.1	-0.5
160	14	0.196	0.010	0.155	-91.5	-92.8	1.3
180	14	0.104	0.008	0.105	-173.5	-175.2	1.7
Average		0.239	0.009	0.075	-123.3	-125.7	2.4

3.5.Conclusions

A pore inactivation model was proposed to describe the oil uptake during frying as an alternative to the commonly used assumption that oil uptake during frying is a linear function of absolute water loss. Whereas the pore model has a mechanistic basis and better describes the initial stage with less oil absorption, in combination with high initial water evaporation rates, the linear model is purely empirical.

However, since the linear model has just one parameter, and the pore inactivation two, a purely statistical comparison slightly favours the linear model. We expect that the pore inactivation model will be better in the description of the total frying process, especially at

lower frying times, where the oil uptake shows a clear deviation from the apparent linear behaviour observed for longer frying times. Also, since the model takes into account the partial replacement of water in the fry with oil, a better reliability with respect to extrapolation to longer frying times is expected.

3.6.Acknowledgements

This study was funded by GO *Gebundelde innovatiekracht* and EFRO, an initiative by the European Union. Co-partners in the study were Aviko B.V., Machinefabriek Baltes and van Lente elektrotechniek. The authors also acknowledge Annelieke Bot, Msc student from Wageningen University, for her help with the experimental work.

4. Crust morphology and crispness development during deep-fat frying of potato

This chapter has been published as: van Koerten, K. N., Schutyser, M. A. I., Somsen, D., & Boom, R. M. (2015). Crust morphology and crispness development during deep-fat frying of potato. Food Research International, 78, 336-342.

4.1.Abstract

Crust formation is an important factor in determining the crispness of French fries. This study aimed at unravelling detailed structural and textural properties of the crust in relation to crispness during frying as a function of the process temperature and time. X-ray tomography showed a larger overall pore volume at higher frying times, while a lower final moisture content mainly resulted in an increase in the amount of large pores. Texture analysis revealed that the increase in porosity, due to the increased formation of pores, results in more crispy behaviour after frying with oil of up to 180 °C. At temperatures above 180 °C crispness is actually found to decrease again, which is explained by the increased plastic behaviour of the crust. This may be related to the reduced glass transition temperature of the crust because of increased sugar degradation at very high temperature.

4.2.Introduction

Deep frying is one of the most popular methods to prepare foods. Its popularity is related to the short and easy preparation and the attractive taste of the products. The attractive taste of for example French fries is especially related to its crispy crust. This and also other sensory attributes of French fries are strongly related to crust formation during the frying process. During frying raw strips of potato are exposed to hot oil, which results in rapid heat transfer from the oil to the water and consequent dehydration. Because the evaporation at the product surface is fast compared to the moisture migration within the product a crust is formed. While the outer layer of the potato is converted into a crispy crust, the core region remains moist and soft. The crust also to large extent determines the amount of oil that is taken up during and after the frying process (Ziaiifar et al., 2008). On the one hand uptake of some oil may be desired from taste perspective, uptake of large amounts of oil are undesired from health perspective. Both the large influence on sensory attributes and oil uptake during frying make it important to study the crust morphology and its formation process during frying in more detail.

When French fries are removed from the oil bath, oil uptake occurs due to capillary action (Bouchon et al., 2001) and due to a sudden pressure drop in the pores as a result of steam condensation (Gamble et al., 1987). The porosity of the crust and the size of the pores co-determine how much oil is taken up. During frying oil uptake is hindered by the counter current vapour flow from the pores. However, because the evaporation rate during frying decreases this leads to a lower vapour pressure (Vitrac et al., 2000) and therefore not all pores will still release vapour, i.e. pores become inactive, allowing oil uptake (van Koerten et al., 2015a). Earlier more empirical studies showed that oil uptake is strongly correlated to final crust porosity (Pinthus et al., 1995; Ziaiifar et al., 2010), but a description of the mechanism of oil uptake through the crust was not provided. Other studies used scanning electron microscopy (SEM) and Confocal Laser Scanning Microscopy (CLSM) to obtain more details of the pore structure (Bouchon and Aguilera, 2001; Bouchon and Pyle, 2004) and location of the oil in the crust (Bouchon et al., 2001; Dueik et al., 2012). Unfortunately, the latter methods provide only a qualitative impression. Kalogianni and Papastergiadis (2014) used a dynamic wicking method and fitted the capillary flow with the Lucas-Washburn equation to measure an effective pore size in French fries. Although the structure of the crust was not fully characterised, some more quantitative insight on oil penetration in the crust was obtained in this study. A new non-invasive technique to visualise crust morphology is X-ray

tomography (XRT). This technique employs X-ray imaging to construct a three dimensional density map of the scanned object. It allows distinguishing between air-filled pores and the solid parts of the fry and thus visualization of the crust morphology. In a recent study Vauvre et al. (2014) already used XRT to image the structure of the crust. However, the development of structure was not studied as function of the frying conditions. This information would provide better understanding of the oil uptake and development of crispness as a result of frying conditions.

As mentioned before, the crust morphology is an important factor in the sensory properties of French fries. Sensory attributes are often evaluated via sensory panel tests. Unfortunately, sensory evaluations provide usually a more qualitative rather than a quantitative comparison. Therefore, many studies use for example texture analysis to assess physical properties related to perceived crispness. During texture analysis, a force can be exerted on a fried sample as a probe moves through it, i.e. mimicking a first bite. Subsequently, the force-deformation curve is used to calculate quantitative parameters related to the crispness of the fry (Miranda and Aguilera, 2006). These parameters include the maximum force until fracture, the initial slope in the stress-strain curve and the number of peaks or fracture incidents while straining. The effect of the frying conditions on textural properties has been studied before. However, most of these studies were empirical of nature and did not include a systematic approach that provided more mechanistic insight (Aguilar et al., 1997; Lima and Singh, 2001). A more step-wise approach would be useful, i.e. first defining how the physical properties (e.g. moisture content, oil content and crust structure) of the product arise due to different frying conditions and from this explain the observed textural properties using these physical properties.

Following, the aim of this study was to study the crust formation in terms of the detailed structural development and textural properties during frying as a function of the process temperature and time. To better compare the effect of frying temperature on the crust formation variations in moisture content were minimized. Additionally, the oil was removed by dipping the finished fries in petroleum ether after frying. Subsequently, texture and XRT analyses were carried out to obtain the force-deformation curves and porosity, crust thickness and pore size distribution data, respectively. Finally, crust morphology data were compared to the textural property data, which provided new insight on how the crust develops during frying.

4.3.Materials & Methods

4.3.1. Frying experiments

Alexia potatoes purchased at a local supermarket were used in this study. The potatoes were cut with a cork borer and a stainless steel knife, into cylinders with a diameter of 10 mm and a length of 50 mm. The samples were then rinsed with tap water followed by a blanching step at 80 °C for 30 minutes. This blanching time is relatively long to ensure that the potatoes were completely cooked. This blanching treatment was preferred as it allows studying the effect of crust formation during frying without interference with an initial cooking process that softens the tissue. After blanching, the potato tubers were fried at different frying temperatures for varying times in sunflower oil. The tubers were fried one at a time and experiments were carried out in triplicate. The frying step was performed using a professional fryer (Caterchef EF 5L, EMGA, the Netherlands) containing 4 litres of sunflower oil (Horeca Select, Makro, the Netherlands), and with a build-in thermostat controlled at ± 2 °C. After frying, the potatoes were dipped in petroleum ether 40-60 (bp≥90%, Sigma-Aldrich, USA) for 1 second to remove any surface oil and thus remove any possible effects of oil on the subsequent measurements.

4.3.2. Calibration moisture content

To remove the influence of moisture content while studying the effect of frying temperature, the water loss for the different frying temperatures was measured and fitted empirically to estimate the necessary frying times to obtain similar moisture content. The water loss was determined by oven drying and defined as the mass of water lost during frying divided by the initial mass of water before frying. The frying times for 180 °C were used as reference times, being: 10, 20, 30, 40, 50, 60 and 120 seconds. After obtaining the corresponding frying times for 150, 165 and 195 °C from the empirical water loss curves, they were also experimentally confirmed again in duplicate to ensure similar moisture content.

4.3.3. XRT measurement

For the X-ray tomography scans, French fries were fried at 180 °C for 10, 60 and 120 seconds. Additionally, fries were fried at 150, 165 and 195 °C, all to the moisture content that the fries have after frying for 60 seconds at 180 °C. After frying, the samples were dipped in petroleum ether to remove most of the oil, which increases the resolution of the XRT scans. In addition, a control sample which was blanched but not fried was scanned.

The XRT scans were performed with an X-ray microfocus CT system (Phoenix v[tome]x m, General Electric, USA) with a voxel size of 10 μm. Reconstruction software was used to

calculate the 3D structure via back projection (Phoenix datos|x reconstruction software, General Electric, USA), which resulted in a 3D-volume element of the fry as shown in Figure . After this, Avizo 3D software for materials science (version 8.0, FEI, USA) was used to extract the X,Y and Z position and volume of each individual pore. For further analysis, 2 regions of 1 cm in length were probed. The porosity was accordingly defined as the cumulative volume of all pores divided by the whole volume of the fry (pores included). The crust was defined as the porous region of the fry. Therefore, crust thickness was determined by measuring the thickness of the porous region, using the obtained X, Y and Z position of the pores. To determine the pore size distribution, 6 cross-sectional slices were extracted from the individual sample scans and the pore sizes were quantified using Matlab (version 7.10.0 with image processing toolbox, Mathworks, USA).

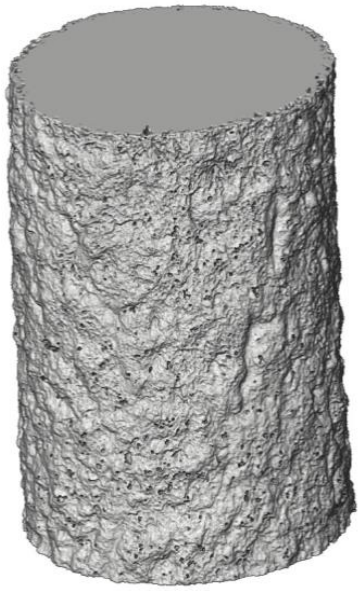

Figure 4.1. Volume element extracted from the XRT scan of a French fry.

4.3.4. Texture analysis

Texture analysis measurements were performed using an Instron testing instrument (Instron-5564Series-Table-ModelSystems-Twin-column-design, USA). Fries were fried at 180 °C for 10, 20, 30, 40, 50, 60 and 120 seconds, and at 150, 165 and 195 °C for frying times that yielded the same moisture contents as at 180 °C (as in section 2.2). After frying, the samples were dipped in petroleum ether to remove the variability caused by oil located in the crust. The fries were fractured within 30 seconds after frying using a wedge-shaped 3 mm probe on a flat surface. The probe velocity was 0.1 mm s^{-1}. A schematic force-deformation curve is shown in Figure 4.2, in which several parameters that can be derived from the curve are also indicated. The maximum force (N) is an indication for the overall hardness of the French fry, while the initial slope (N mm^{-1}) represents the stiffness of the surface layer. Finally, the frequency of the peaks or breaking incidents may be correlated to the crispness of the fry.

Since we are only interested in the crispy behaviour of the crust, only the first millimetre of deformation is evaluated for the peak count. All fracture tests were performed in triplicate.

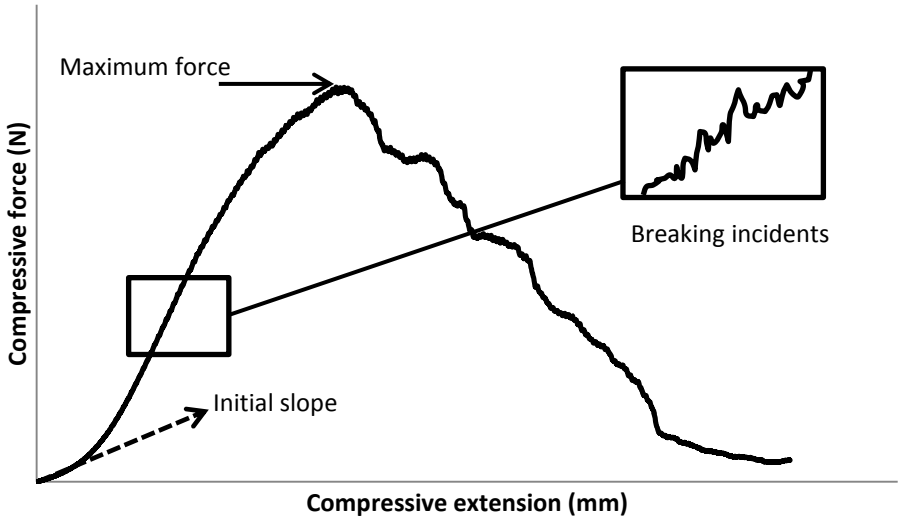

Figure 4.2. Schematic force-deformation curve obtained from texture analysis.

4.4.Results & Discussion

4.4.1. Calibration curves

To eliminate the effect of the moisture content during comparison of the influence of frying temperature on crust formation, water loss curves were fitted to estimate the frying time required to achieve similar final moisture content at each frying temperature. The water loss data, together with the empirical fitting curves, are shown in Figure . Obviously, water is removed more rapidly at higher temperatures due to a higher heat transfer rate. After estimating the required frying time for each temperature from the curves shown in Figure , the final moisture content was experimentally measured for confirmation. The comparison of the moisture content of fries fried at 180 °C at the reference frying times of 10, 20, 30, 40, 50, 60 and 120 seconds and the other frying temperatures is shown in Figure . The frying times estimated from the water loss curves indeed resulted in similar moisture content for each applied frying temperature.

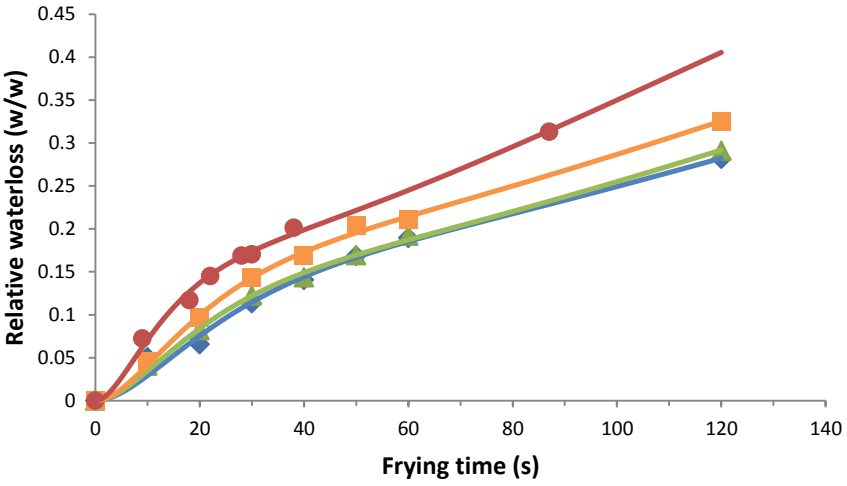

Figure 4.3. Relative water loss as a function of time for fries fried at different frying temperatures: ◆ 150, ▲ 165, ■ 180.and ● 195 °C. The lines of corresponding colour indicate the fitted water loss curve which was used to determine the required frying times to obtain equal moisture contents.

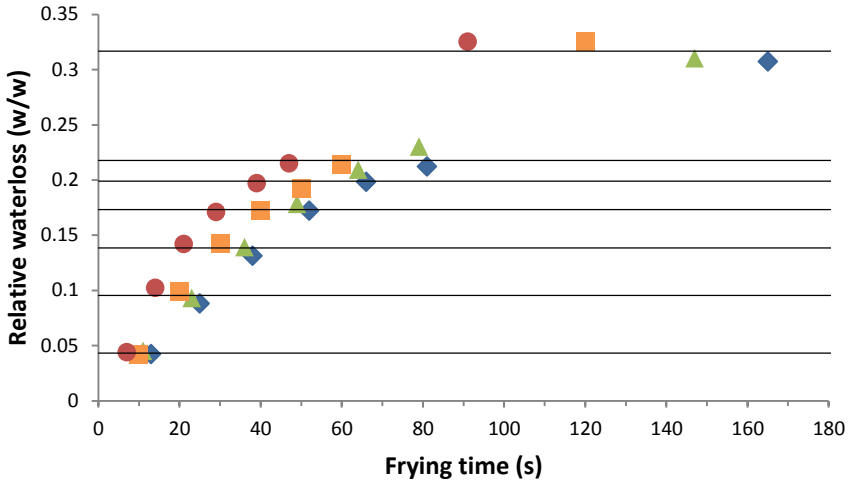

Figure 4.4. Experimental confirmation of the relative water losses obtained from the water loss curves as function of frying time at different frying temperatures: ◆ 150, ▲ 165, ■ 180 and ● 195 °C. The black lines indicate the desired moisture contents.

4.4.2. Crust analysis using XRT

For the XRT analyses, potato strips were fried at 180 °C for 10, 60 and 120 seconds. Additionally, a sample that was only blanched, representing a sample fried for 0 seconds, was subjected to XRT analysis. Cross-sectional slices of the XRT scan for the different frying times are shown in Figure 4.5. The thickness of the porous layer becomes larger with increasing frying time, which is expected since longer frying times correspond to more water loss, leaving a thicker porous region. For the 0 second sample it can be observed that there is already some initial structure. The 10 second sample also mainly shows the initial structure without any visible new or larger pores. This can be explained by surface water evaporation in

the initial stage of frying, which does not increase the actual potato porosity (Lioumbas et al., 2012b). Also, the temperature of the fry needs to reach the boiling point temperature before evaporation from the fry can take place and structure formation begins. To assess the influence of frying temperature, fries were fried at 150, 165, 180 and 195 °C to equal moisture content, corresponding to the moisture content of fries fried at 180 °C for 60 seconds. The cross-sectional slices of the XRT scan for these different frying temperatures are shown in Figure 4.6. One can visually observe a small increase in porosity with increasing frying temperature, with the lower porosity only clearly observed for the 150 °C sample. Concluding, the frying temperature seems to have an effect also at similar final moisture levels, but quantitative data is desired to further confirm this.

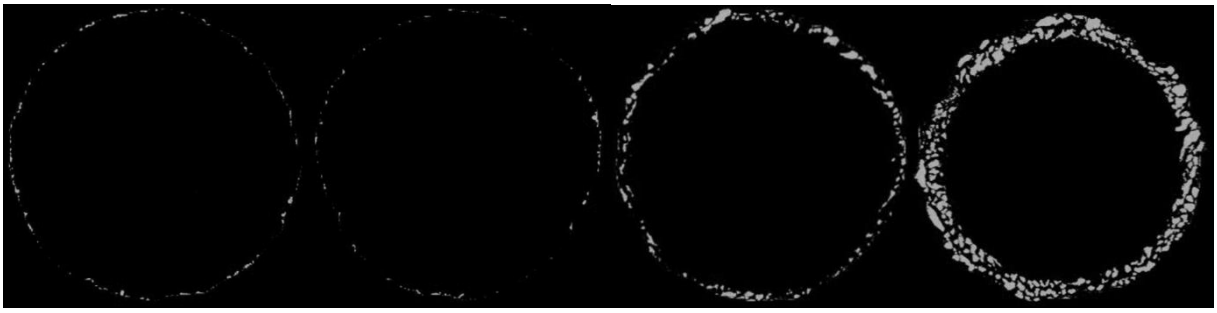

Figure 4.5. Cross-sectional slices obtained from the XRT scans of fries fried at 180 °C. With frying times from left to right of: 0, 10, 60 and 120 seconds.

Figure 4.6. Cross-sectional slices obtained from the XRT scans of fries fried to the same moisture content corresponding to fries fried at 180 °C for 60 seconds. With frying temperatures from left to right of: 150, 165, 180 and 195 °C. With respective frying times of 81,79, 60 and 47 seconds.

4.4.2.1. Crust thickness

We defined the crust as the porous region of the fry. Accordingly, the crust thickness was obtained by measuring the maximum distances between the inner and outer pores in the porous regions. Figure 4.7 shows the crust thickness as a function of time for potato strips fried at 180 °C. As observed before, the crust thickness increases with time due to water evaporation from the fry, leaving behind the dry and porous crust. The obtained values are large compared to values in literature. A crust thickness of approximately 0.4 mm is generally observed for frying times around 2 minutes, compared to the 0.95 mm we found and presented in Figure 4.7. The explanation for this difference is most probable related to the

method used to measure crust thickness, which in literature is mostly done by either physical measurement of the harder part of the fry (Ziaiifar et al., 2010) or by image analysis of cross-sections (Kalogianni and Smith, 2013), while we defined the total porous region as the crust. This means that not just the completely dehydrated part of the fry, but also the evaporative zone where just enough water is evaporated to create pores, is considered te be crust. Lioumbas and Karapantsios (2012) found that the evaporation front moves faster into the fry than the crust thickness increased, as observed through measurements using a micrometre and image analysis.

The evolution of the crust thickness using different frying temperatures is shown in Figure 4.8. Even though the moisture contents are equal for all the temperatures shown, crust thickness does increase with increasing frying temperature. This may be explained by the larger heat transfer rates and consequent moisture loss at higher temperatures. The higher vapour fluxes will exert a greater force on the potato structure, enabling the formation of larger visible pores in the fry. Additionally, the separation between crust and core may not be a sharp evaporation boundary but rather a zone where water is evaporating and pores are already formed (Halder et al., 2007). As a consequence, the evaporative zone can migrate deeper into the fry and becomes larger at higher temperatures due to a higher heat transfer rate, creating a thicker porous region, even though the same amount of water was evaporated.

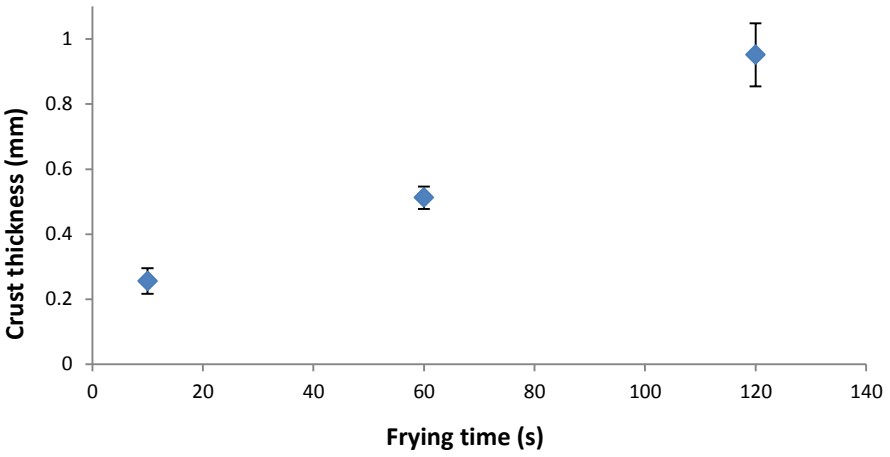

Figure 4.7. Crust thickness as a function of the frying time for fries fried at 180 °C.

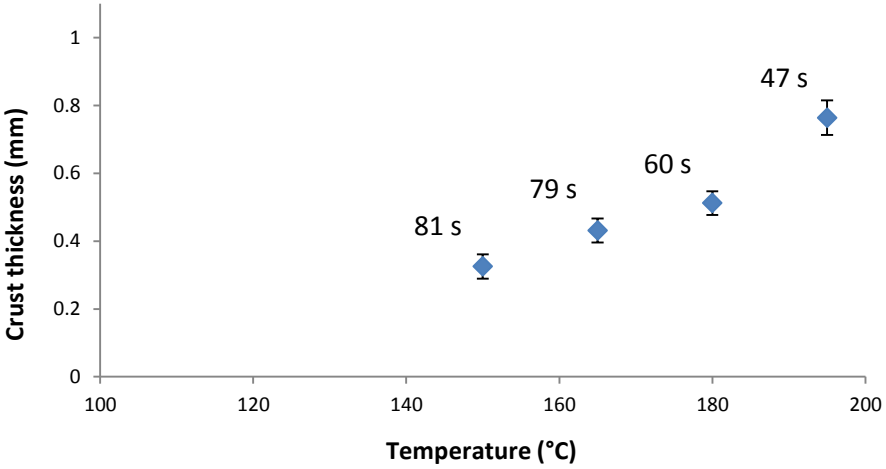

Figure 4.8. Crust thickness as a function of frying temperature for fries fried to an equal moisture content, corresponding to 60 seconds frying at 180 °C. The numbers in the graph represent the actual frying times used.

4.4.2.2. Porosity

The porosity was defined as the cumulative volume of all the pores relative to the volume of the entire fry. In Figure 4.9 the porosity is plotted as a function of frying time for a frying temperature of 180 °C. Analogous to the crust thickness, the porosity increases with frying time. This is to be expected since the crust is the porous region of the fry. There is no porosity increase in the first 10 seconds as only surface water is being evaporated at this stage (Farkas and Hubbard, 2000). When comparing the determined porosities to data from other studies the values we obtained are relatively low; for example, we found 12% porosity around 2 minutes while others found a porosity between 20 and 30% (Krokida et al., 2000b; Pinthus et al., 1995). The reason for this is most likely related to the resolution of the XRT method, which was 10 µm. Kalogianni and Papastergiadis (2014) for example obtained an average pore size between 2 and 3 µm using dynamic wicking, which implies that we do not take the smallest pores into account, resulting in a lower porosity compared to literature. Figure 4.10 shows the porosity as a function of the frying temperature. As with the crust thickness, the porosity also increases again. This supports our initial observations in Figure 4.6, where the cross-sections showed larger pores as the temperature increases. It should be noted that extrapolation of the data set in Figure 4.10 suggests that a minimum temperature is required for porosity development.

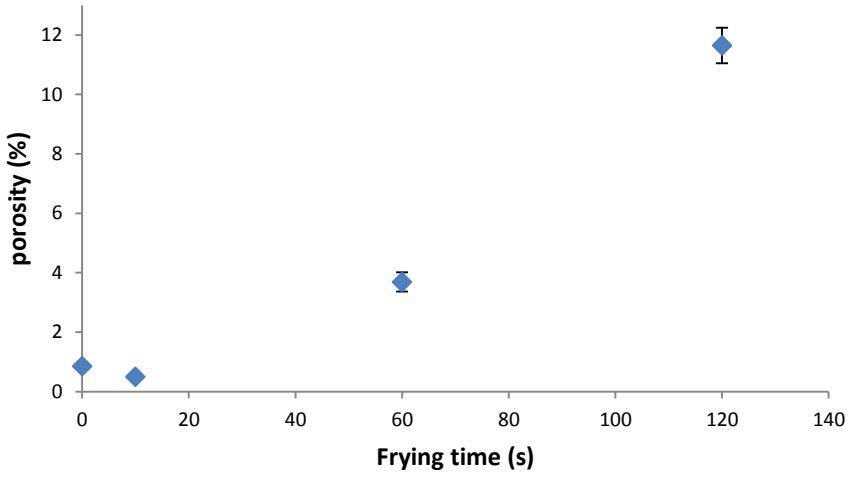

Figure 4.9. Porosity as a function of the frying time for fries fried at 180 °C.

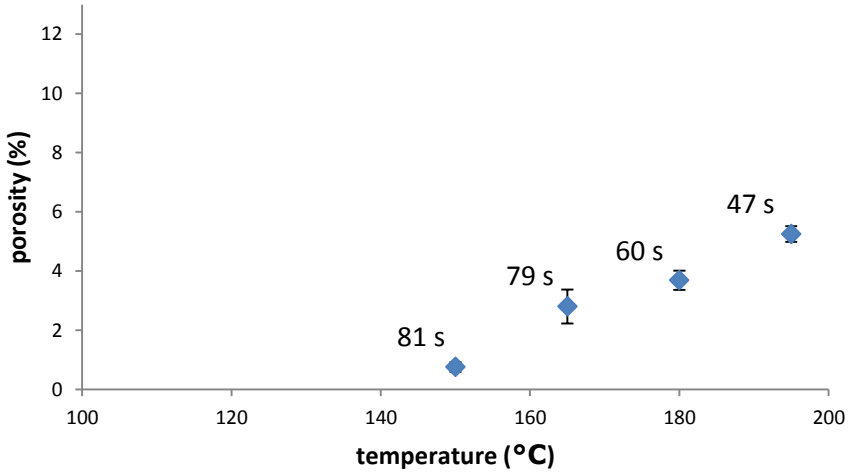

Figure 4.10. Porosity as a function of frying temperature for fries fried to a similar moisture content, corresponding to 60 seconds frying at 180 °C. The numbers in the graph represent the actual frying times used.

4.4.2.3. Pore size distribution

The pore size distribution per sample was obtained by sampling the pore sizes in 6 different cross-sectional slices. Figure 4.11 shows the cumulative pore size distribution for potato strips fried at 180 °C for 0, 10, 60 and 120 seconds. Analogous to the porosity, there is no significant change in the total pores volume from 0 to 10 seconds. From 10 seconds onwards more and larger pores are being formed. This indicates that during frying pores are continuously growing and merging together due to internal water evaporation. Additional, the left side of the graph also shows an increase in smaller pores from 10 seconds onwards, so new pores are also being formed. The cumulative pore size distribution for different frying temperatures is shown in Figure 4.12, where the moisture content was constant for all frying temperatures. It can be observed that there is a larger amount of small pores present in the 195

°C sample. Combining this with the results from the porosity and crust thickness it may be concluded that increasing frying temperatures widen the evaporative zone inside the fry, and create a larger number of pores. The 195 °C sample also has pores with the largest size, while the largest pore diameters for the other temperatures are quite similar. For the 165 °C sample the largest diameter is even slightly larger than the diameter for the 180 °C sample. From Figure it can also be seen that some of the largest pores in the 165 °C cross-section are the same size as those in the 180 °C slice. Larger pores at higher temperatures may be explained by the more vigorous water evaporation, which increases the damage to the crust. Surprisingly, also a high number of large pores at 165 °C is observed. The reason for this might be that the largest pores are mainly formed by growth of pores formed early in the frying process. Meanwhile, increasing the frying temperature is correlated to a higher number of new pores formed. However, when considering the volume occupied by large pores with increasing frying time, an increasing trend is observed. The increase is not linear, as there is a large jump in the number of large pores from 150 to 165 °C. This suggests that a minimum force is required to disrupt the initial potato structure and enable the formation of large pores. This is in line with the observation in Figure 4.10, where a minimum temperature is needed for the formation of noticeable pores.

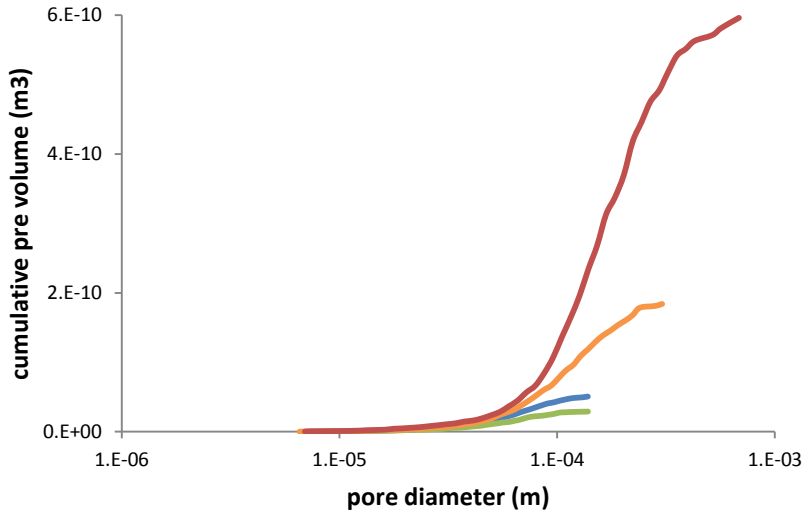

Figure 4.11. Pore size distribution of fries fried at 180 °C for varying frying times: 0, 10, 60 and 120 seconds.

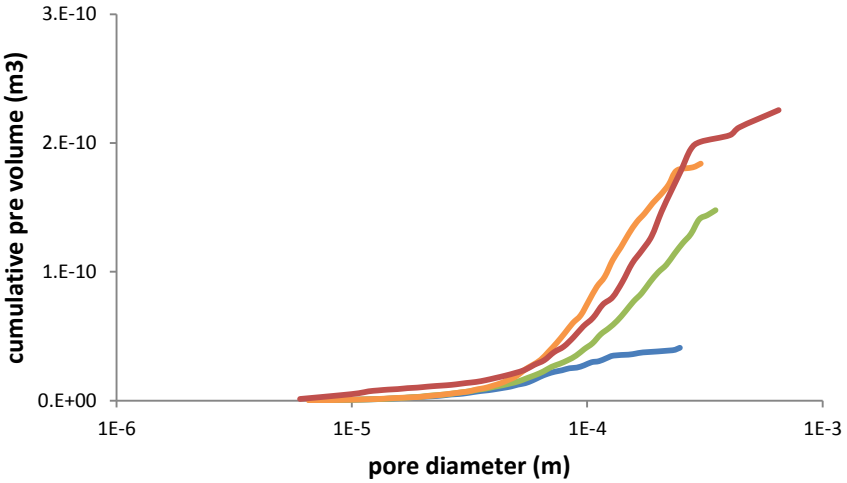

Figure 4.12. Pore size distribution of fries fried to similar moisture content for varying frying temperatures: 150, 165, 180 and 195 °C.

4.4.3. Texture analysis

During texture analyses the frying times of 10, 20, 30, 40, 50, 60 and 120 seconds for frying at 180 °C were used as reference times. For the other frying temperatures, the fries were fried to the same moisture content as the references according to Figure 4.4. The measurements were performed directly after frying and in triplicate.

4.4.3.1. Maximum force

The maximum force measured by the texture analyser is an indication for the overall hardness and cohesiveness of the fry. Figure 4.13 shows the maximum fracture force for the different frying temperatures plotted against the reference frying times of 180 °C. A decreasing trend is observed for all frying temperatures, caused by starch gelatinization during frying which softens the tissue, and the increased porosity as observed in Figure 4.10 which will lower the breaking resistance. Other studies confirm this for the investigated time interval; for larger time intervals (>5 minutes) the breaking force will eventually increase again due to a significant crust being formed (Lima and Singh, 2001; Teruel et al., 2015). There are no differences in the maximum force at breakage for the frying temperatures of 150, 165 and 180 °C, which indicates that the hardness of the fry is mostly determined by the overall moisture content in this temperature range. The maximum force at breakage for 195 °C is much higher than the other temperatures but still decreasing, indicating gelatinization and porosity increase. It was noted during the experiments that the samples for 195 °C were deformed to a greater extent before the initial breaking point compared to the other temperatures. This suggests that a tougher, more cohesive crust layer is formed when frying at 195 °C. A reason for this may be that the crust layer is still in a rubbery state for the higher temperatures while

it is in the glassy state for the lower temperatures. As the glass transition temperature (T_g) decreases with molecular weight (van der Sman and Meinders, 2011), the degradation of sugars may have resulted in a lower T_g (Jiang et al., 2008; Le Meste et al., 2002). Given the temperature range in which frying takes place, the degradation may be due to the Maillard reaction and caramelization. Maillard reactions become significant above temperatures of 120 °C and the reaction rate increases at higher temperatures (Achir et al., 2008). Additionally, the caramelization temperature for several mono- and di-saccharides lies between 160 and 180 °C, causing the sugars to pyrolyse. However, this does not completely explain the sudden increase from 180 to 195 °C, as a similar increase could be expected from 165 to 180 °C due to increased degradation rates. A possible explanation is the decomposition of sucrose, which generally is the most abundant sugar in potatoes (Truong Van et al., 1986) and decomposes around 186 °C (Perry et al., 1997). The decomposition of sucrose to glucose, and the consequent caramelization of glucose could explain a sudden increase in the T_g.

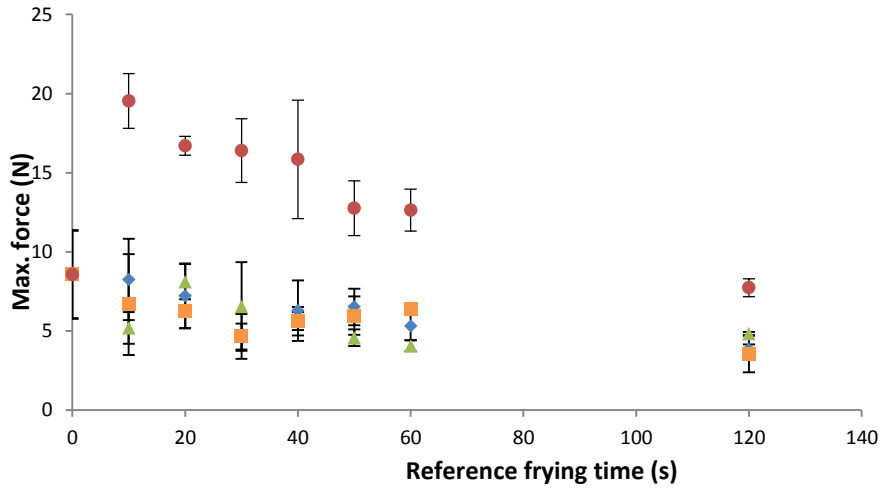

Figure 4.13. Maximum breaking force of French fries for different frying temperatures: ◆ 150, ▲ 165, ■ 180 and ● 195 °C. The breaking force is plotted against the reference frying time of 180 °C, meaning that all other temperatures have the same moisture content at the same reference frying time.

4.4.3.2. Initial slope

To assess the stiffness of the surface of the fry, the slope of the initial millimetre of strain was extracted from the force-deformation curves. The result of this for all frying temperatures is shown in Figure 4.14. In the first part no real change is observed. At longer frying times the stiffness decreases, which indicates that the surface of the fry becomes either softer or more brittle. This is in line with the increase in crust thickness and porosity observed with XRT, as a more porous crust is also expected to be more brittle. There is however not much difference

between the frying temperatures. But this does reflect the greater increase in porosity with frying time compared to the increase in porosity with frying temperature.

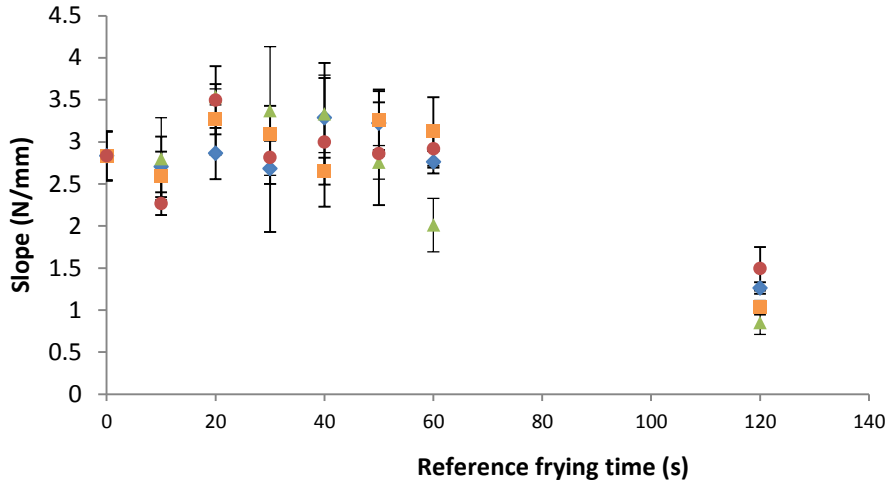

Figure 4.14. Initial slope of French fries for different frying temperatures: ◆ 150, ▲ 165, ■ 180 and ● 195 °C. The slope is plotted against the reference frying time of 180 °C, meaning that all other temperatures have the same moisture content at the same reference frying time.

4.4.3.3. Crispness

Sensory crispness is hard to define using reproducible quantitative methods. As the use of trained sensory panels is time consuming and may introduce some subjectivity, crispness is often evaluated by the amount of peaks in the force-deformation curve (Thanatuksorn et al., 2007). These peaks basically represent numerous small fracture incidents during deformation, which a consumer would perceive as crispness. Since crispy behaviour in fries is mostly determined by the brittle crust, only the peaks in the first millimetre of the force-deformation curve are relevant. The result peak density is plotted in Figure 4.15 for the varying frying temperatures. Only after about 60 seconds, any significant crust is formed, similar to the results in Figure 4.14 where the weakening effect of the brittle crust on the surface layer is not noticeable at first. As more moisture is continually lost, the crust thickens, and more fracture incidents occur. This shows that the crust is indeed responsible for the crispy behaviour of the fries. As with the maximum force at breakage and the initial stress-strain slope, the differences between the different frying temperatures are quite small. However, this might just be a consequence of the relatively short frying interval that was chosen. Since the differences for frying temperature are visible in the XRT measurements, but the differences observed for frying time are larger than for frying temperature, meaning that the texture analysis needs greater differences in crust morphology before any effect is observable.

The graph for the peak density is practically the inversed of that to the initial slope. This indicates that the decrease in stiffness of the fry is indeed caused by the increasing brittleness of the surface layer as the porosity increases. Additionally, the apparent tougher crust for 195 °C, as observed from the breaking force, can be related to less breaking incidents at 120 seconds. This reflects the behaviour of more rubbery material, supporting our explanation that at this high frying temperature the surface layer could be above the T_g.

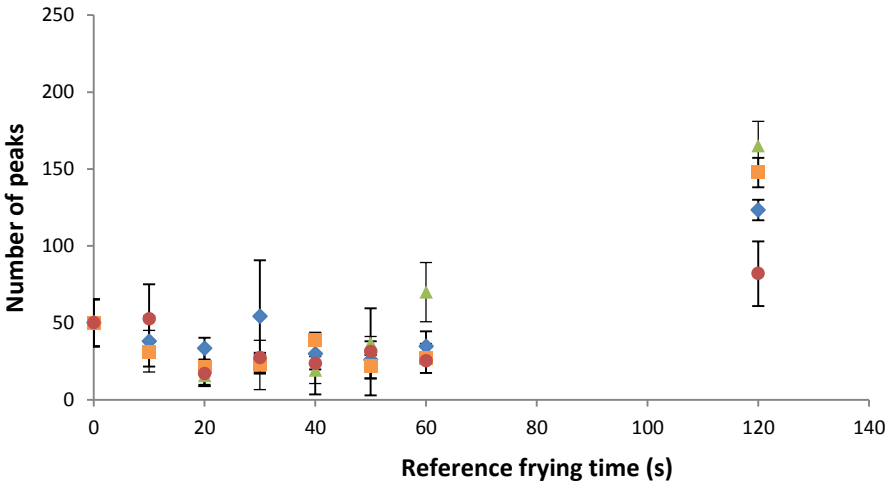

Figure 4.15. Amount of peaks within first millimetre in the force-deformation curves for French fries at different temperatures. : ◆ 150, ▲ 165, ■ 180 and ● 195 °C. The amount of peaks are plotted against the reference frying time of 180 °C, meaning that all other temperatures have the same moisture content at the same reference frying time.

4.5.Conclusions

The effects of the frying time, corresponding to moisture content, and frying temperature on the crust morphology and textural properties were evaluated. XRT measurements showed that the decreasing moisture content causes the growth of a brittle crust and an increase in porosity. Higher frying temperatures lead to a thicker crust and a higher porosity, which is explained by the increased water evaporation rate.

The pore size distribution derived from the XRT measurements supported visual observations, showing that increased evaporation rate leads to formation of more pores, even at the same final moisture content. In addition to new pore formation, also earlier formed pores grew in size because of continuing evaporation of moisture. This suggests that higher frying temperatures mainly lead to formation of larger number of pores, whereas increased frying times, or moisture loss, mainly contribute to the growth of larger pores. The potato structure also has an inherent inertia, which limits pore formation for frying temperatures of 150 °C or lower.

Texture analysis showed that the porosity and crust thickness enhanced the crispness of the fries due to weakening of the surface layer by the growing brittle crust. However, the structure of the crust is not the only factor in determining crispness. The composition of the crust is also important, as too high temperatures can result in a tougher crust with rubbery properties. This is most likely the effect of sugar degradation and consequent increase of the T_g.

Concluding, increased frying temperatures will improve the crispy properties of the fries due to the formation of more and larger pores, but only until a certain maximum between 180 and 195 ^{0}C.

4.6.Acknowledgements

This study was funded by GO *Gebundelde innovatiekracht* and EFRO, an initiative by the European Union. Co-partners in the study were Aviko B.V., Machinefabriek Baltes and van Lente elektrotechniek. The authors also acknowledge Amber van Veghel and Xingying Li, students from Wageningen University, for their help with the experimental work. Also CAT-AgroFood is acknowledged for providing accessibility to the XRT equipment and software.

5. Cross-flow deep fat frying and its effect on fry quality distribution and mobility

This chapter has been published as: van Koerten, K. N., Schutyser, M. A. I., Somsen, D., & Boom, R. M. (2015). Cross-flow deep fat frying and its effect on fry quality distribution and mobility. Journal of Food Science and Technology, available online since 4 November 2015. doi: 10.1007/s13197-015-2070-2

5.1.Abstract

Conventional industrial frying systems are not optimised towards homogeneous product quality, which is partly related to poor oil distribution across the packed bed of fries. In this study we investigate an alternative frying system with an oil cross-flow from bottom to top through a packed bed of fries. Fluidization of rectangular fries during frying was characterised with a modified Ergun equation. Mixing was visualized by using two coloured layers of fries and quantified in terms of mixing entropy. Smaller fries mixed quickly during frying, while longer fries exhibited much less mixing, which was attributed to the higher minimum fluidization velocity and slower dehydration for longer fries. The cross-flow velocity was found an important parameter for the homogeneity of the moisture content of fries. Increased oil velocities positively affected moisture distribution due to a higher oil refresh rate. However, inducing fluidization caused the moisture distribution to become unpredictable due to bed instabilities.

5.2.Introduction

Deep fat frying is one of the more important unit operations in the food processing industry. As for other technologies, also for frying technology there is a continuous need for innovation in terms of process efficiency and product quality (Blumenthal and Stier, 1991). The fried product with the highest market share is without doubts French fries with a worldwide production of 11 million tonnes in 2003 (Huffaker, 2003), a number expected to increase with the increase in world population and spreading of western culture.

One of the major challenges with large scale frying systems is to obtain products of consistent quality. Variations in raw materials, but also frying conditions are sources of quality variation (Stier, 2004). For state-of-the-art industrial frying operations, especially the oil flow conditions are not well defined. This may be obvious since industrial fryers work at high production capacity and hot oil is continuously injected, while the cooled oil is removed for reheating. Depending on the exact design details, variations in frying conditions may occur as a result of the characteristic flow of the oil, which can affect the local temperature, convective heat transfer and the residence time in the frying unit. Inefficient oil flow conditions can give rise to an undesired distribution of final fry quality.

The best way to ensure homogenous heat transfer from the frying oil to the fries would be to subject each fry to exactly the same amount of oil with a steady temperature. If the fries are transported horizontally, then the most appropriate way to do this is by applying a vertical oil flow. This is analogous to continuous fluidized bed drying. Fluid bed drying can be used for the uniform drying of powders with high heat and mass transfer rates (Senadeera et al., 2000). Additionally, fluidization enhances the mixing of the particles ensuring more homogeneous conditions (Nitz and Taranto, 2007; Srinivasakannan and Balasubramanian, 2008). An important parameter to control is the horizontal transport rate of particles in the continuous fluidised bed. In industrial fryers the horizontal transport is carried out with a conveyer belt that moves the French fries slowly through the oil (Vitrac et al., 2000). With increasing fluidization the horizontal transport rate would be reduced such that the residence time becomes uncontrollable.

The objective of this study is to quantify and control the effect of convective oil flow on the quality distribution of French fries, which is achieved by applying an upward oil flow through a packed bed of fries at increasing flow rates. First, the influence of flow conditions is studied in a model packed bed system to find the minimum fluidization velocities as function of the

geometry. Subsequently, a newly developed pilot-scale frying unit with upward convective oil flow is used to study the influence of hydrodynamic conditions and particle geometry on fluidization behaviour and quality distribution in terms of moisture content. Finally, the influence of hydrodynamic conditions on packed bed mobility under different oil flow velocities is investigated.

5.3.Materials & methods

5.3.1. Fluidization of fry shaped particles

Initial fluidization experiments were carried out with bar-shaped (fry-shaped) objects fluidised in a tall column filled with water. The system consists of the column (10 cm internal diameter), a centrifugal pump (Iwaki MDH-401) to control the flow speed, a rotameter to measure the flow rate and a water reservoir. The minimum fluidization velocity was determined by changing the flow speed of the water while measuring variations in the . Since the dimensions of the column and particles are known, the void fraction can be directly determined from the measured bed height. Varying void fractions and particle sizes were used to validate calculations on the minimum fluidization velocity.

Bar shaped polycarbonate (PC) with a density of 1125 kg/m^3 and polyvinylchloride (PVC) with a density of 1375 kg/m^3 with different dimensions were used to establish the fluidization behaviour of fry shaped particles. PC and PVC were chosen for their ease of fabrication and their difference in density. The materials used and their ratios are summarized in table 5.1. The different combinations were chosen to observe the fluidization behaviour for different geometries and different densities.

Table 5.1. Overview of the different particle geometries and combinations (in number of particles) used during the packed bed flow experiments. PC indicates use of polycarbonate particles, while PVC indicates polyvinylchloride particles.

Run	16x4x4mm PC	20x4x4mm PC	24x4x4mm PC	20x4x4mm PVC
1	503	0	0	0
2	0	395	0	0
3	0	0	387	0
4	0	0	0	477
5	254	0	170	0
6	0	203	0	280

5.3.2. Ergun equation

The superficial velocity at which the pressure drop across a packed bed is just high enough to support the entire weight of the bed is called the minimum fluidization velocity. This velocity can be obtained by relating the pressure drop over a packed bed to the pressure drop across a completely fluidized bed. The latter can be obtained by balancing the net weight of the bed against the upward force exerted on the bed:

$$\frac{\Delta P}{L} = (\rho_s - \rho_f)(1-\varepsilon)g \qquad (1)$$

In which ΔP is the pressure drop (Pa) across the fluidized bed height L (m), ρ_s the density of the fluidized material (kg/m^3), ρ_f the density of the fluid phase (kg/m^3), ε the void fraction of the fluidized bed and g the gravitational constant (9.81 m/s^2).

A frequently applied semi-empirical relation to characterise the pressure drop across a cylindrical packed bed of particles is the Ergun equation (Eq. 2) (Ergun, 1949). This relation is mostly consistent with experimental data, where the pressure drop is a continuous function of the superficial velocity and is as follows:

$$\frac{\Delta P}{L} = 150\frac{(1-\varepsilon)^2}{\varepsilon^3}\frac{\eta u}{d^2} + 1.75\frac{(1-\varepsilon)}{\varepsilon^3}\frac{\rho_f u^2}{d} \qquad (2)$$

Where ΔP is the pressure drop (Pa) and L is the length for the pressure drop measurement (m). The first term on the right hand side represents the viscous loss while the second term represents the inertial loss. In this expression 150 and 1.75 are the Ergun constants, η the dynamic viscosity of the fluid phase (Pa·s), u the superficial velocity of the fluid phase (m/s) and d the diameter of the fluidized particles (m).

Since the Ergun equation describes the pressure drop across a packed bed of spherical particles, it cannot be directly applied to a packed bed of non-spherical particles. A generally accepted approach to modify the Ergun equation for this situation is to replace the diameter d in equation 2 by the equivalent diameter and multiplying it with the sphericity of the particles (Li and Ma, 2011; Ozahi et al., 2008). The equivalent diameter of a particle is defined as the diameter of a sphere of equal volume to the particle while its sphericity is defined as the ratio of the surface area of the equivalent-volume sphere to the surface area of the actual particle (Hewitt, 2002). As mentioned before, at the minimum fluidization velocity the pressure drop across the fixed bed will provide the onset of fluidization. This means that at the minimum fluidization velocity equation 1 will equal equation 2 and an expression for the minimum fluidization velocity is obtained:

$$u_{m=}\frac{150(1-\varepsilon_m)}{3.5}\frac{\nu}{\bar{\phi}\bar{d}_p}\left(\sqrt{1+\frac{7}{150^2}\frac{{\varepsilon_m}^3}{(1-\varepsilon_m)^2}\frac{(\bar{\rho}_s-\rho_f)}{\rho_f}\frac{\bar{\phi}^3\bar{d}_p^3 g}{\nu^2}}-1\right) \quad (3)$$

With

$$\bar{\phi}=\sum_{i=1}^{n}x_i\varphi_i \quad \text{and} \quad \varphi_i=\frac{\pi^{\frac{1}{3}}(6V_{pi})^{\frac{2}{3}}}{A_{pi}} \quad (4)$$

$$\bar{d}_p=\sum_{i=1}^{n}x_i\,d_{pi} \quad \text{and} \quad d_{pi}=\frac{6V_{pi}}{\varphi_i A_{pi}} \quad (5)$$

$$\bar{\rho}_s=\sum_{i=1}^{n}x_i\rho_{si} \quad (6)$$

Where u_m is the minimum fluidization velocity (m/s), ε_m the void fraction of the packed bed, ν the kinematic viscosity (η/ρ_f, m^2/s), φ the sphericity of the particles, d_p the equivalent particle diameter (m), ρ_s the particle density (kg/m^3), x_i the volume fraction of particle fraction i, V_{pi} the volume of a particle from particle fraction i (m^3) and A_{pi} the surface area of a particle from particle fraction i (m^2).

The expression can be extended for materials of mixed size and/or composition by averaging the material properties by volume fraction, as shown in equations 4-6 (Asif, 2011). Thus the minimum fluidization can be calculated as a function of the initial void fraction if the fluid properties and particle dimensions are known.

5.3.3. Frying experiments

The frying experiments were carried out in a newly designed frying unit that allows accurate control of the upward oil flow (Figure 5.1). The frying unit has a close-coupled pump (KSB Etabloc SYT) to regulate the flow speed, a flanged immersion heater (Cetal) to control the oil temperature and a Coriolis mass flow meter (Rheonik RHM-20) to measure the flow rate.

Additionally, the frying compartment is equipped with two glass windows to observe the French fries during frying. A video camera is positioned in front of one window to monitor the initial fluidization behaviour of the French fries. Sunflower oil was chosen as the frying medium, as this is mostly used in industry.

Alexia potatoes purchased at a local supermarket were cut to a thickness of 0.8 by 0.8 cm and three different lengths; 3, 4 and 5 cm. For mobility frying experiments, half of the fries were coloured red by mixing these in an aqueous solution of Rhodamine B (0.01% w/w) for 10 minutes while the other fries were treated for the same time with normal tap water. Afterwards tissue paper was used to remove the excess of surface water from the fries, after which they were placed in the frying basket to create two separate layers of coloured fries (see Figure 5.2). A product to oil ratio of approximately 1 to 6 was used. The fries were fried for 1 minute at 180 °C, as these are common pre-frying conditions in industry, with oil flow velocities varying between 0.007 and 0.07 m/s.

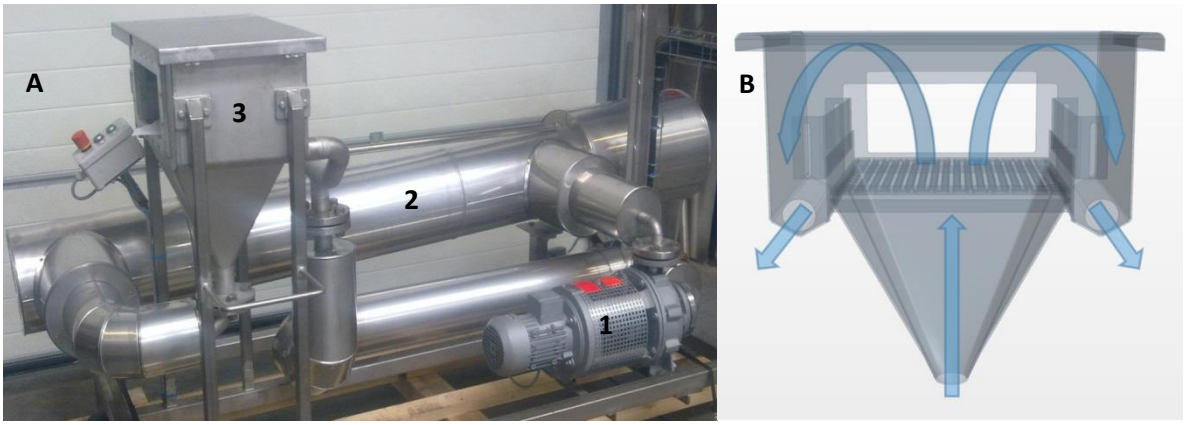

Figure 5.1. A: Cross-flow frying unit with pump (1),heat exchanger (2) and frying compartment (3). B: Schematic drawing of the frying compartment with two glass windows; the arrows indicate the direction of the circulating oil flow.

5.3.4. Quality distribution

In defining the quality of French fries, the most important parameters are moisture content, oil content, colour and texture. Since the water content and total oil content are to a large extent determined by the method of frying, these two quality parameters were used as an indication of the quality distribution of the fries after frying. After frying, 10 fries were taken from the frying basket for further analysis. These fries were transferred to aluminium trays, weighed and dried to constant weight in an oven at 105 °C. The recorded loss in weight was used to represent the remaining water after frying. The dried fries were then submerged in petroleum ether (20 mL per fry) for 3 days to remove all the oil from the fries. Although this method of oil extraction differs from the more generally applied soxhlet extraction, it reduces the amount

of solvent wasted. Moreover, it was examined in preliminary experiments that this method extracted the same amount of oil as conventional soxhlet extraction. The final weight after the oil extraction was used to represent the fat-free dry matter mass of the fry. After this the water content and total oil content after frying could be calculated by dividing the water remaining after frying and the oil removed from the fries by the fat-free dry matter mass.

5.3.5. Degree of mixing

Before and after frying a picture of the top view was taken from the frying basket. The obtained pictures were cropped to obtain only the packed bed with fries and divided into grid cells (Figure 5.2).

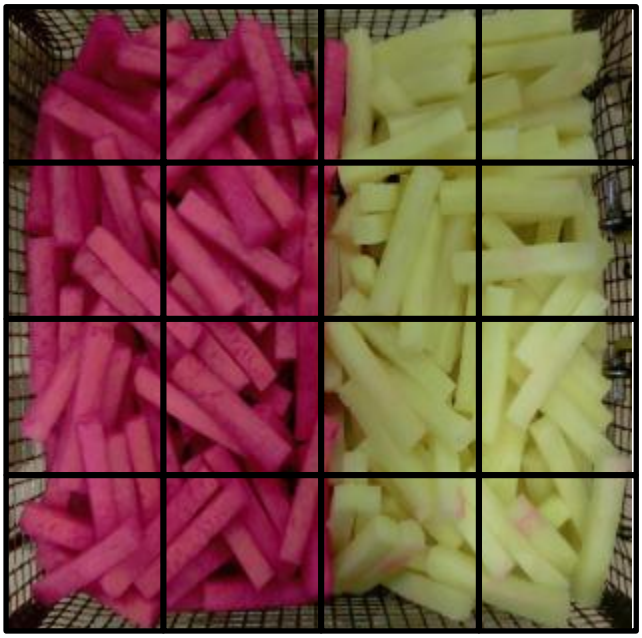

Figure 5.2. Division of image used for image analysis into 16 grid cells to determine mixing entropy

An in-house developed routine in Matlab (version 7.10.0 with image processing toolbox) was used to determine the amount of red and yellow pixels in each grid cell. To quantify the degree of mixing the mixing entropy was used (Schutyser et al., 2001). The mixing entropy for a single grid cell was calculated using:

$$S(i,j) = p_r(i,j)\log\left(p_r(i,j)\right) + p_y(i,j)\log\left(p_y(i,j)\right) \qquad (7)$$

Where *S(i,j)* is the mixing entropy in cell (i,j), $p_r(i,j)$ the fraction of red pixels in cell (i,j) and $p_y(i,j)$ the fraction of yellow pixels in cell (i,j). The total mixing entropy was then calculated using:

$$S_{tot} = \frac{1}{-\log 2}\sum_{i,j} S(i,j)\left(\frac{N_{cell}(i,j)}{N}\right) \qquad (8)$$

With S_{tot} being the total mixing entropy, $N_{cell}(i,j)$ the amount of red and yellow pixels in cell (i,j) and N the amount of red and yellow pixels in the entire image. The ratio between the coloured pixels per cell and total amount of coloured pixels is used to correct for cells with a relatively low amount of coloured pixels. The –log(2) factor is the mixing entropy at maximum mixing and is used to scale the calculated mixing entropies from 0 to 1. When the grid cell size is too small then the total mixing entropy will remain 0, as only one fry will fit each cell, whereas when the grid cell size is too large then the entropy will be already close to 1 at the beginning of the mixing. Using a square grid it was found that 16 grid cells gave the best result, with fewer cells causing values to converge towards 1, while more cells caused values to move towards zero.

5.4.Results & Discussion

5.4.1. Predicting the minimum fluidization velocity

The flow rate was varied while the bed height was monitored to obtain the minimum fluidization velocities for different materials. The obtained void fractions as a function of the superficial velocity are presented in Figure 5.3. It can be seen that the void fraction remains constant until a certain point after which the bed starts to expand. This point represents the transition from a packed to a fluidized bed. The minimum fluidization velocity is the superficial velocity at which the void fraction starts to increase. Run 4 clearly shows the highest minimum fluidization velocity, followed by run 6. This can be explained by the amount of PVC particles in these two runs, since the PVC has a higher density than the PC, it will require a higher fluid velocity to fluidize. Other differences are less obvious, as the other runs only represent differences in geometry and thus the fluidization behaviour depends primarily on the specific packing. Run 5 shows the lowest fluidization velocities, which may be attributed to the binary composition of the system. Mixing of two differently sized particles can result in densely packed beds (Asif, 2011), which in turn decreases the fluidization velocity due to a higher pressure drop.

Minimum fluidization velocities (u_m) were also calculated using equation 3 and depicted in Figure 5.3. The Ergun equation could predict the experimentally determined minimum fluidization velocity of fry shaped particles with a difference of at maximum ± 10%. This is in agreement with other studies describing the minimum fluidization velocity of non-spherical particles using the adjusted Ergun equation (equation 3) (Li and Ma, 2011; Ozahi et al., 2008). Though better predictions might be obtained by fitting modified Ergun-type equations, this is

always done for a specific set of materials, shapes and possible wall effects, which makes them less appropriate for extrapolation to other data sets.

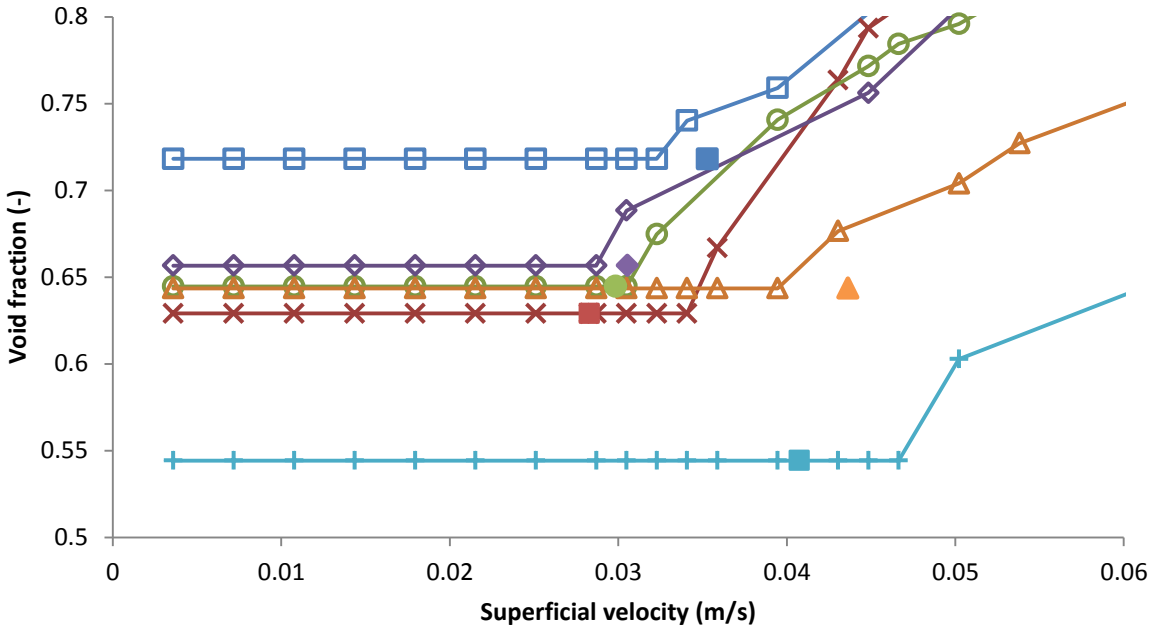

Figure 5.3. The void fraction of the fixed/fluidized bed as a function of the superficial velocity for different rectangular particle shapes, as listed in table 5.1: run 1 (□); run 2 (X); run 3 (○); run 4 (+); run 5 (◇) and run 6 (△). The minimum fluidization velocity calculated using equation 3 for the different runs is indicated with a corresponding filled data point.

5.4.2. Initial fluidization during frying

Batches of 3, 4 and 5 cm long fries were subjected to vertical oil flow velocities between 0.007 and 0.07 m/s at 180 ^{o}C to experimentally determine the minimum fluidization velocity during frying. Video recordings of the initial seconds, before water evaporated, showed either a fixed bed of fries or a fluidized bed of fries. By considering the largest flow rate that still showed a fixed bed and the smallest flow rate that showed a fluidized bed, a region was found that should contain the minimum flow rate required for fluidization (Figure 5.4). Additionally, the minimum fluidization velocity was predicted using equation 3 and plotted in Figure 5.4. Input parameters are derived from the bed and fry dimensions, while the density was 1030 kg/m^3 determined by means of weighing and the water displacement method.

The experimentally determined regions in which the minimum fluidization velocity is expected overlaps with the predicted minimum flow rate required for fluidization, taking into account a 10% relative error. This is in accordance with the findings in section 3.1, where the validity of a modified Ergun equation was confirmed for rectangular particles.

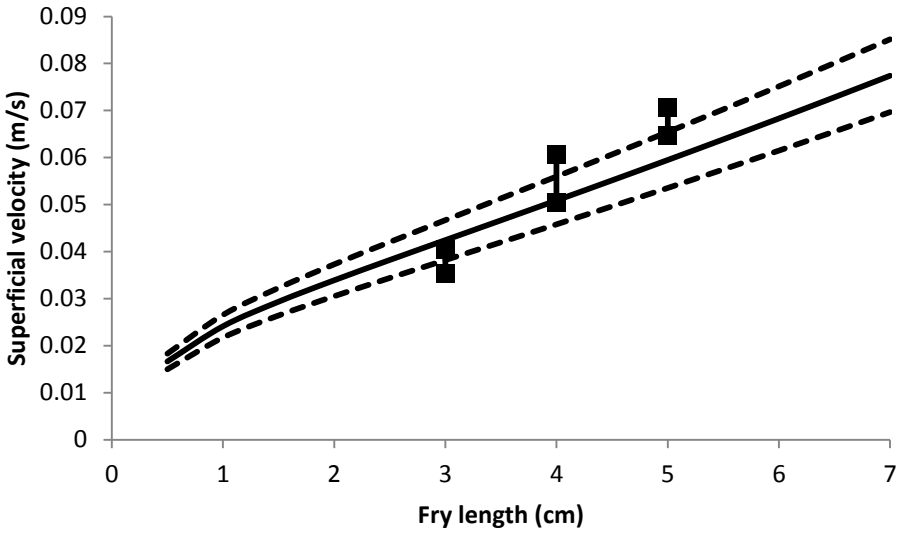

Figure 5.4. Minimum fluidization velocity calculated using equation 3 plotted against the fry length(-). The dotted lines indicate a 10% relative error. The connected blocks (■) represent the maximum flow velocity at which no fluidization was observed and the minimum flow velocity at which fluidization was observed for the fry lengths of 3, 4 and 5 cm.

5.4.3. Quality distribution

The final moisture and oil contents on fat-free dry matter base are plotted in Figure 5.5 against the different oil flow velocities for different fry lengths. The final moisture content was observed to be equal for different flow rates. This is expected since water evaporation is a function of the heat transfer rate which in turn depends on the temperature differences, fry size and frying time. Since the oil temperature, fry size and frying time are all constant within each data set, similar amounts of water loss are expected. A parameter that could cause variation in water loss is the increasing oil flow rate, which should positively affect the external convective heat transfer coefficient. However, most of the heat transfer will take place in the boiling phase during which water is evaporating and at that moment the heat transfer coefficient is dominated by the local turbulence close to the surface of the fry, induced by vapour bubble formation (Costa et al., 1999; Farkas and Hubbard, 2000). Similar values for the moisture content are found in literature studies in the absence of forced convective oil flow (Krokida et al., 2001, 2000a; van Koerten et al., 2015a).

The final oil content was also expected not to vary much for different flow rates. This can be observed from the results shown in Figure 5.5. There is more overall variation in the oil content than in the water content. A possible explanation for this is related to the rate at which the frying basket is removed from the hot oil. At a higher removal rate, less oil remains adsorbed onto the surface of the fry, yielding a lower total oil content (Krozel et al., 2000).

Still, the oil content values obtained are within the range of total oil contents as observed in other studies (Moyano and Pedreschi, 2006; Ziaiifar et al., 2010).

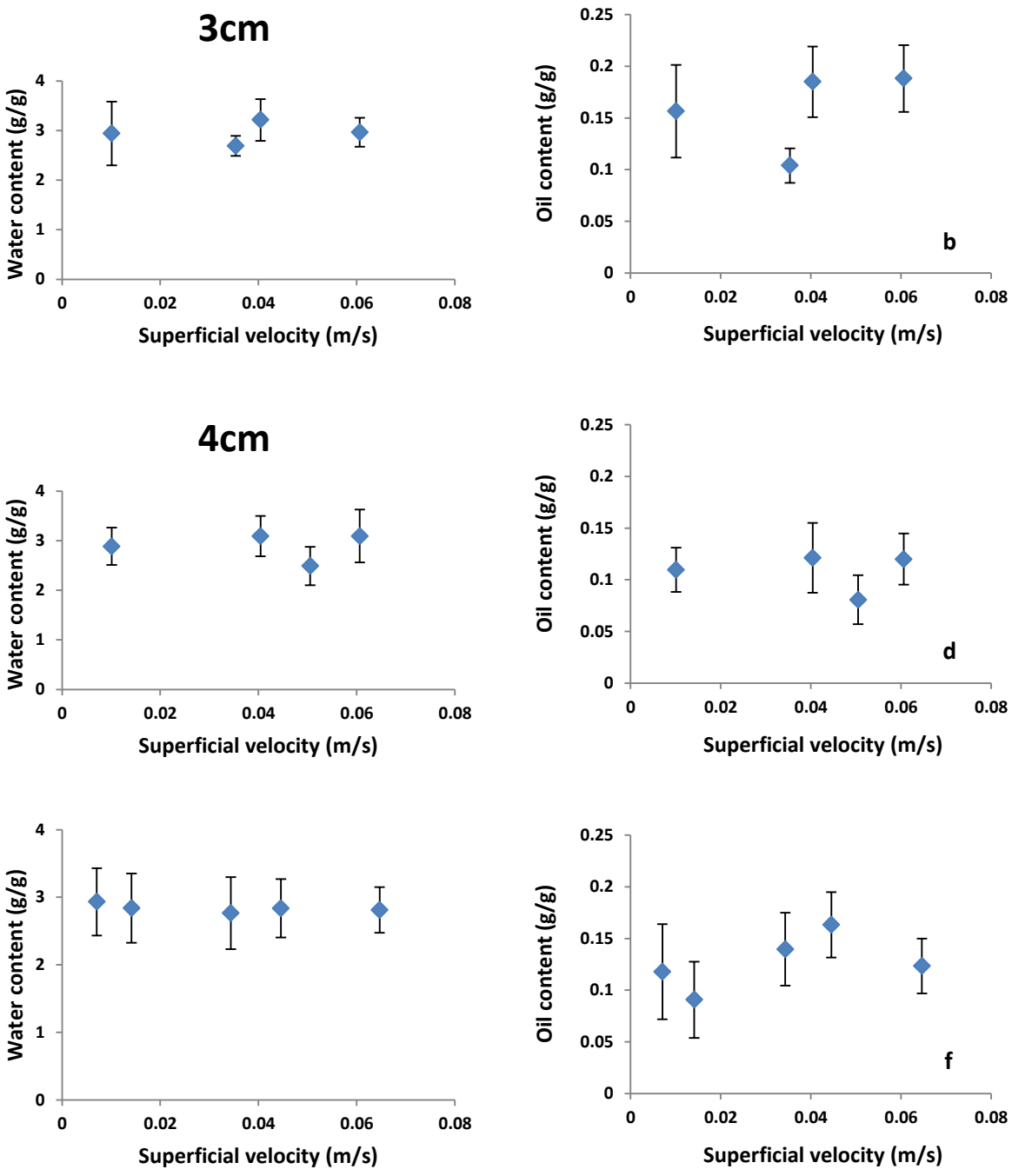

Figure 5.5. Left side: Water content per fat-free dry matter with standard deviation plotted against the superficial oil velocity for 3 (a), 4 (c) and 5 (e) cm fries. Right side: Oil content per fat-free dry matter with standard deviation plotted against the oil flow velocity for 3 (b), 4 (d) and 5 (f) cm fries. All fries were fried at 180 °C for 1 minute.

To assess the variability in the quality of the fried French fries, we use the measured variations within each data set, as indicated by the standard deviation. In Figure 5.6, the standard deviations of the moisture content data are plotted versus the oil flow velocity.

Additionally, the minimum fluidization velocity obtained from the initial fluidization experiments is indicated in Figure 5.6. There is a decreasing trend in the standard deviation for flow velocities higher than 0.03 m/s for the 5 cm fries. Note that this is before initial fluidization is achieved. The standard deviation also decreases for the 3 cm fries before the initial fluidization, but actually increases after this fluidization point. The latter is also observed for the 4 cm fries. However, the standard deviation of the 4 cm fries shows no significant change before fluidization is achieved.

For 5 cm fries it can be clearly observed that increasing oil flow velocity has a positive influence on the quality distribution as the standard deviation is continuously decreasing for flow velocities higher than 0.03 m/s (Figure 5.6). This can be attributed to the increased oil refresh rate, which in turn will lead to lower temperature gradients inside the frying compartment. The 3 cm fries also show a decrease in distribution before the minimum fluidization velocity is reached, but this is already visible after flow velocities higher than 0.01 m/s. This suggests that the void fraction of the bed of fries can already partially increase before actual fluidization is reached, which increases the oil flow through the bed, and that this happens earlier for beds with a lower minimum fluidization velocity. However, this effect is not visible for the 4 cm fries, which would then be expected to decrease for flow velocities between 0.01 and 0.03 m/s. Additionally, a clear trend of decreasing homogeneity is observed for the 3 and 4 cm fries when they start to fluidize. It may be expected that upon fluidization more mixing is achieved and the fries would be fried more equally. One explanation for this increase is the limited height of the fluidization compartment (approximately 1.5 times the packed bed height), with air at the surface. If fluidization takes place and the bed expands, some fries are pushed to the surface and experience a smaller contact area with the oil, thus achieving different drying rates. Another reason for the increased quality distribution might be bed instabilities. Such bed instabilities are related to non-homogenous packing and enhanced by resulting unequal upward oil flow distribution. Bed instabilities are predominant in systems with a high diameter ratio between the fluidization compartment and the fluidized particles as is the case in this work (Duru et al., 2002). Non-homogenous packing with different void fractions will results in varying exposure of fries to oil, which consequently affects the drying rates.

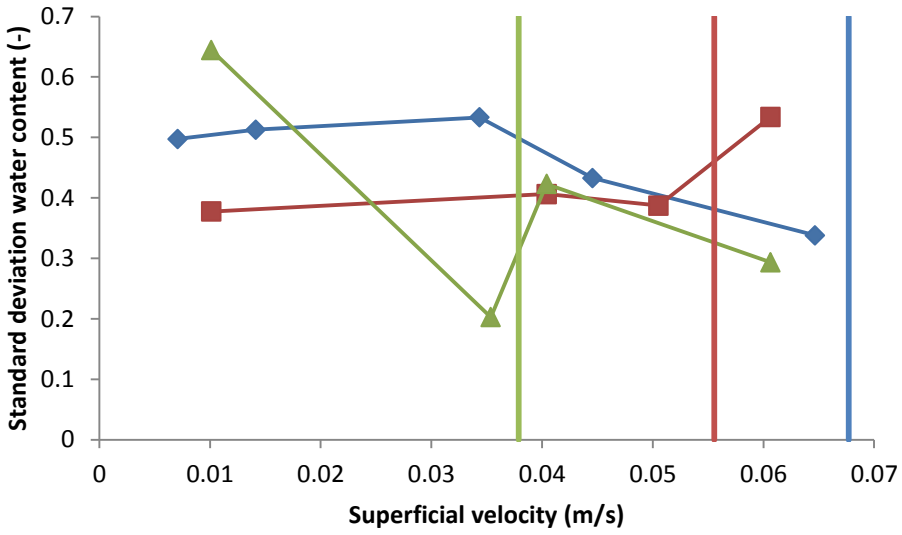

Figure 5.6. Standard deviations of the water content at different oil flow velocities for 3 (▲), 4 (■) and 5 (◆) cm fries. The vertical lines indicate the experimentally obtained minimum fluidization velocity for the different fry lengths, where increasing superficial velocity corresponds to increasing fry length.

5.4.4. Mobility of French fries during frying

In Figure 5.7 the mixing after frying is visualised using coloured French fries as function of the fry length and the oil flow velocity. The smaller fries mix to a greater extent and at lower flow velocities than the larger fries. The red line in Figure 5.7 indicates the experimentally obtained minimum fluidization velocities for the different fry lengths.

The degree of mixing was also quantified in terms of mixing entropy, which was determined by image analyses after frying fries of 3, 4 and 5 cm at different oil flow rates. These results are plotted in Figure 5.8. The entropy starts with a value of 0.074, representing the non-mixed situation, and then asymptotically moves towards a maximum degree of mixing (normalised to 1). In line with the visual observations, it can be concluded that the mixing of entropy increases less fast with increasing flow rate for the 5 cm fries.

These results are in line with section 3.2, where the fluidization velocity was shown to be lower for smaller fries, thus more mixing is expected. However, Figure 5.7 also shows that for 3 and 4 cm fries, mixing already takes place before the minimum fluidization velocity is reached. This can be partly attributed to the water evaporation during frying which will cause the fries to decrease in density. As the fries decrease in water content from 4 to 3 g/g dry matter during the 1 minute of frying, the density is expected to decrease by 50 kg/m^3 (Costa et al., 2001). According to equation 3, a density decrease of 50 kg/m^3 would result in a decrease in minimum fluidization velocity of approximately 10% for the different fry lengths. However, this does not explain the mixing at velocities lower than 90% of the minimum

fluidization velocity. In a previous study it was observed that before fluidization of the entire bed already some particles were fluidised at the top of the bed, while the bottom of the bed remained stagnant (Duru et al., 2002). Since emerging vapour bubbles increased turbidity in the oil above the bed, only the lower part of the bed could be clearly monitored for initial fluidization experiments. This means that there might already be minor bed movement before any observed fluidization takes place. This confirms the suspected increase in void fraction at velocities below the minimum fluidization velocity discussed in section 3.3.

The faster observed mixing of the shorter fries, already at low flow rates, can also explain why the standard deviations in the moisture content for these fries do not decrease consistently with increasing flow rates. The degree of mixing for the 4 cm fries is already close to that of 3 cm fries at a flow rates around 0.04 m/s. This suggests that application of even a small oil flow to the 3 and 4 cm fries provides a more homogeneous quality distribution due to a higher oil refresh rate. At higher flow velocities, when the fries start to fluidize, the quality variation becomes subject to the bed instabilities at the corresponding flow velocities, and becomes independent of the oil flow velocity.

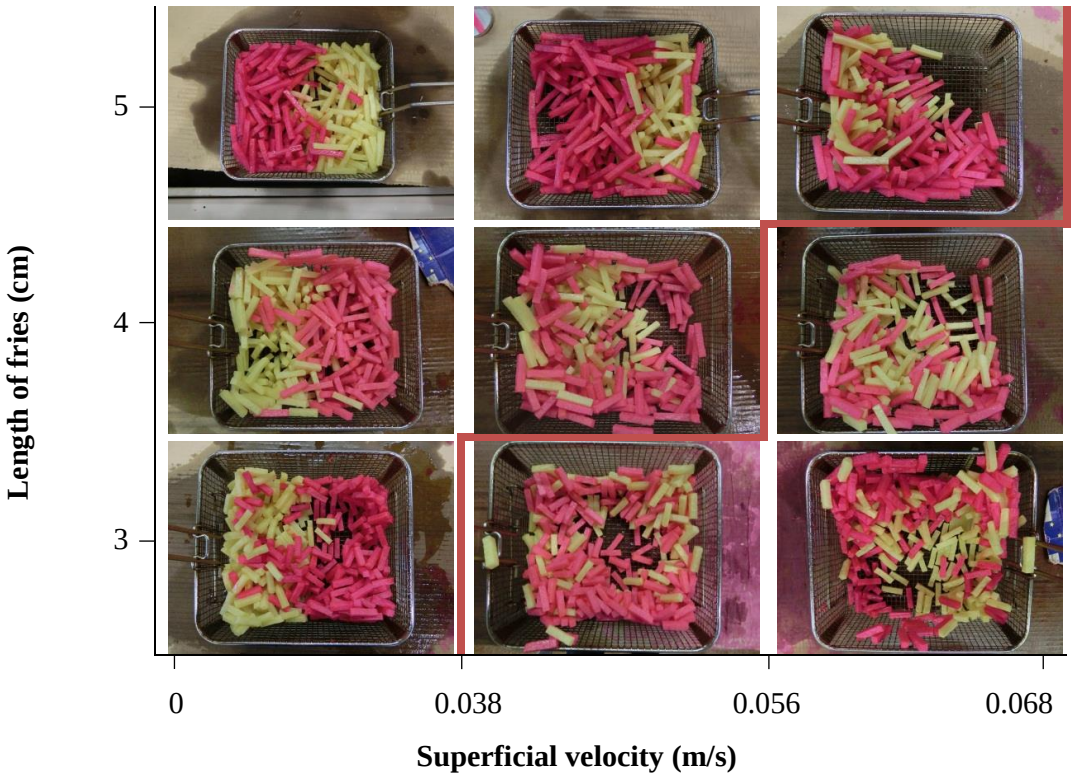

Figure 5.7. Pictures visualizing the degree of mixing after 1 minute of frying at different oil flow velocities and fry lengths. The red line indicated the location of the experimentally obtained minimum fluidization velocity for the different fry lengths.

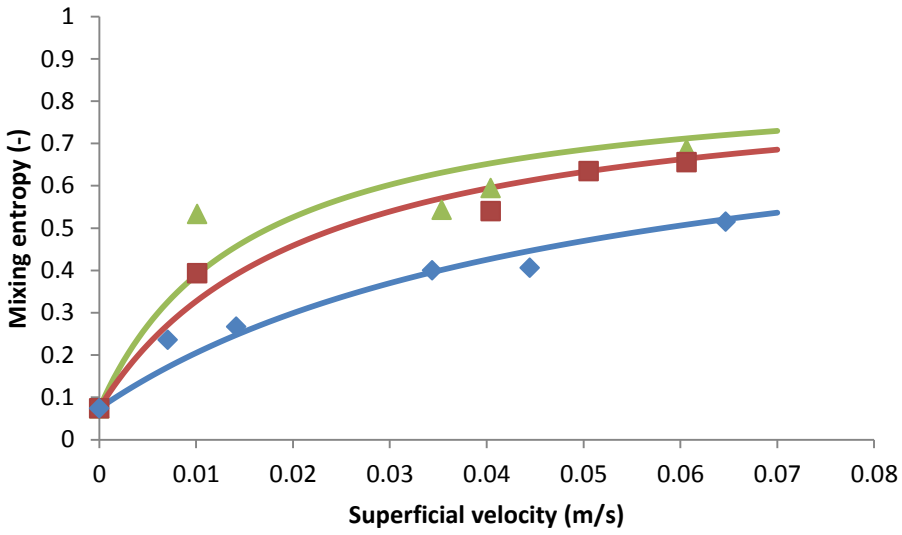

Figure 5.8. Mixing entropy as calculated by equation 8 plotted against the oil flow velocity for fry lengths of 3 (▲), 4 (■) and 5 (◆) cm. Lines of are drawn to guide the eye.

5.5.Conclusions

A modified Ergun equation was found to accurately describe fluidization of rectangular shaped particles in a water column and used to characterize initial fluidization behaviour of French fries during frying in a cross-flow frying set-up.

Subsequently, the effect of varying flow conditions on the quality distribution as represented by the moisture content and the oil content was studied. For fries of 3 and 5 cm long, an increased oil flow velocity improved the homogeneity of the fries, while this was not observed for fries of 4 cm.

The smaller fried were found to mix quickly during frying, while longer fries exhibited much less mixing. This is because of two effects: the higher minimum fluidization velocity for longer fries, due to their stronger entanglement in the bed, and the smaller surface area of long fries leading to a slower dehydration and thus later fluidization during the frying process.

The crossflow velocity was found to be an important parameter for the homogeneity of the quality of French fries. Increased oil flow velocities positively affect the quality distribution due to a higher oil refresh rate. However, inducing fluidization caused the quality distribution to become unpredictable due to the bed instabilities caused by the system dimensions.

5.6.Acknowledgements

This study was funded by GO *Gebundelde innovatiekracht* and EFRO, an initiative by the European Union. Co-partners in the study were Aviko B.V., Machinefabriek Baltes and van Lente elektrotechniek. The authors also acknowledge Hua Shan, Msc student from Wageningen University, for his help with the experimental work.

6. General discussion

6.1.Introduction

The aim of this thesis was to gain insight in the frying process on both product and process scale.

- At product scale, the influence of mass and heat transfer on the structural changes and subsequent oil uptake and crispness formation was studied.
- At the process scale, the aim was gaining understanding of the flow patterns and how these influence the product quality and its distribution in a new cross-flow frying apparatus.

This chapter reports on the major findings of this thesis. Subsequently, it discusses how product and process scale results obtained in this thesis may be connected via a multi-scale modelling approach. Finally, based on the findings and discussion, future directions of research and application are suggested.

6.2.Summary of the conclusions in this thesis

All physicochemical changes that occur during the frying of French fries are influenced by the evaporation of water. Several models with varying degree of complexity have been developed to describe heat transfer and consequently water evaporation during frying. In this thesis the choice was made to develop a so-called crust-core model with a variable heat transfer coefficient (Lioumbas et al., 2012a). This modelling approach was preferred as it has a mechanistic basis, but still can be implemented and validated in a relatively straightforward manner. In previous studies usually a constant external heat transfer coefficient was assumed, even though it is known to vary greatly during the frying process. This variation is caused by the vapour bubbles which emerge at the fry surface, causing turbulence and thus influence the heat transfer coefficient. Therefore, a crust-core model is developed (chapter 2) that incorporates the heat transfer coefficient as a function of the evaporation rate by means of a Nusselt relation. The crust-core model assumes that frying is heat transfer limited, while internal water diffusion may be neglected since this occurs on a larger timescale for deep fat frying. A sharp moving boundary was used to describe the transition from wet matrix to crust due to water evaporation.

The model was found to be in close agreement with the experimental data of both moisture loss and temperature profiles of the centre and surface of the potatoes. The model correctly captures the initial heating of the product to the boiling point without evaporation Subsequently, rapid water loss occurs as the heat transfer switches from free to forced

convection in the absence of internal heat transfer limitation. However, as the crust thickens, internal resistance in the fry becomes the dominant factor in determining the heat transfer rate. At this stage the contribution of the external heat transfer coefficient becomes less relevant.

Good description of water evaporation is very relevant for understanding the uptake of oil during frying. The uptake of oil during frying and shortly after is very relevant for presence of oil in the final product. While previous studies often focused on oil uptake after frying, the focus of this thesis was to understand the oil uptake *during* frying following a new modelling approach (chapter 3). The model is based on a similar pore inactivation mechanism as observed during membrane emulsification. The main idea is that a pore requires a minimum pressure to produce a droplet and when the transmembrane pressure is too low, pores will be inactivated. Similarly, a pressure is formed across the crust layer due to the resistance towards vapour flow. Since according to Darcy's law the pressure gradient across the crust is proportional to the vapour flux, pore inactivation will occur with decreasing evaporation rates. Subsequently, oil uptake could be linked to the water evaporation rate. The model also took into account thickening of the crust, meaning inactivated pores can take up more oil as they grow.

The model was in agreement with the experimental data and with the more often reported observation that oil uptake is linearly correlated to the absolute amount of moisture lost. The new model could also accurately describe the oil uptake during the initial phase of frying when the evaporation rate is still relatively high. After this phase, pores become inactivated, and the oil uptake becomes practically linear related to the moisture loss. This means that if the evaporation rate is kept constant, the amount of inactivated pores should decrease, and with it the amount of oil taken up..

To connect the heat and mass transfer phenomena that occur during frying to product quality, in chapter 4 the effect of crust formation was studied in relation to the crispness. For this, a systematic study was carried out to the influence of frying conditions on crust structure formation and consequent textural properties. X-ray tomography was used to visualize the evolution of crust structure at different frying temperatures. It was observed that porosity, crust thickness and the amount of large pores all increased during frying. Moreover, it was found that also at higher frying temperatures porosity and crust thickness increased, albeit to a lesser extent. The latter may be explained by the increased vapour fluxes at higher

temperatures exerting a larger force on the potato structure, resulting in formation of more and larger pores.

Pore size data analyses further showed that a temperature of around 150 °C was at least necessary to produce any pores of noticeable size, suggesting a minimum resistance of the potato towards deformation and generation of pores. Texture analysis was applied to have an indication of the influence of structural changes on sensory properties such as crispness. Force deformation curves obtained by fracturing fried fries indicated an increase in crispy behaviour during frying. Probably, due to the lack of sensitivity of the texture analysis method, increased crispness was not observable for increased frying temperatures. This is however expected, given the strong correlation between increased pore size and more crispy behaviour. An exception to this was found for temperatures around 195 °C, where a clear decrease in crispy behaviour was observed, together with more plastic behaviour of the crust. This was attributed to the degradation of sucrose and consequent caramelization of glucose, leading to plasticization and a reduction of the glass transition temperature.

While the previous studies on frying of single fries assume homogeneous frying conditions, this is not the case in industrial frying systems. Therefore the distribution of product quality during frying was explored. For this a cross-flow pilot fryer was developed, which was used to investigate the effect of oil flow on quality distribution and bed mobility, (chapter 5). The oil flow direction was chosen from bottom to top, as to minimize the path of the oil through the fry bed, and thus minimizing temperature gradients in the oil. The water content of the fries was chosen as an indicator for the quality distribution.

Increased oil flow velocities resulted in an overall more homogeneous water content. However, around the fluidization point of the fry bed, less homogeneity in the bed was observed. Higher oil flow velocities increase the refreshment rate of oil and thus temperature differences in the bed decrease. Next, it would be expected that rigorous mixing of the fries and the oil, through fluidization, would have similar effect, as the system moves towards ideal mixing. However, the exact opposite was observed. From image analysis of the fry bed before and after frying, it was observed that at flow rates around and above the fluidization point very heterogeneous packing occurred probably due to entanglement of the non-spherical particles and resulting bed instabilities. Increasing the oil flow through the bed is therefore only beneficial up to the fluidization point of the fry bed.

6.3.Multi-scale understanding of industrial frying behaviour

In the previous section models were discussed that described the water evaporation and oil uptake at the single fry scale. In these models, constant boundary conditions were assumed, reflecting a constant oil temperature (i.e. ideally mixed systems). However, in industrial pre-frying systems, large temperature gradients exist depending on the construction details, but also due to the finite oil-to-fry ratio as presented in chapter 5. To facilitate the operation and design of large-scale frying systems, ideally a multi-scale model should be developed which incorporates a coupling of the generated insight at the product and process scale. In the following sections, steps are discussed that should be taken to develop such a modelling tool.

6.3.1. CFD Modelling of fluid flow through a packed bed of French fries

CFD modelling of fluid flow through a packed bed of French fries is a first step in the development of such a multi-scale model. For this a commercial CFD package, STARCCM+, was used to describe fluid flow through a bed of rectangular-shaped particles. Flow in a column filled with water and a packed bed of polycarbonate rectangular particles with dimension of 24x4x4 mm was modelled. The porous structure of the packed bed was scanned with X-ray tomography (XRT). Subsequently, the 3D image from the XRT scan was converted to a surface mesh and imported into STARCCM+.

Figure 6.1 visually depicts the extraction of the fluid phase from the imported geometry, followed by the simulation results. To check the results obtained using STARCCM+, the simulated pressure drop across the bed was compared to the Ergun equation, which accurately described experimental results in our previous research for different cross-flow velocities (Figure 6.2). From this Figure 6.2 it can be observed that the predicted pressure drop across the bed of plastic fries and thus the predicted fluid flow is in very good agreement with the Ergun equation.

Figure 6.1. Scheme for running a simulation on a scanned geometry in STARCCM+. From left to right: Imported geometry from XRT measurements; Extracted fluid volume; Cross-section with impression of the velocity distribution in the bed.

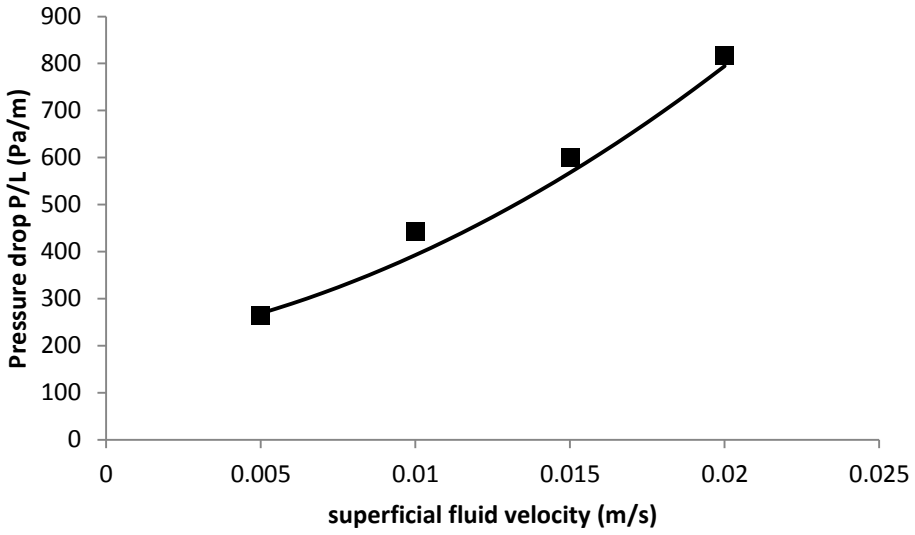

Figure 6.2. Pressure drop across a packed bed of rectangular particles as a function of superficial water velocity, predicted with STARCCM+ simulations (■) and calculated with the Ergun equation (-).

6.3.2. Modelling of heat transfer

The next step is the implementation of heat and mass transfer between the oil and the packed bed. However, to reduce complexity, first the heat transfer was implemented in STARCCM+. Additionally, predictions were in first instance carried out for a single fry and compared to measured temperature profiles in the core and surface of fries heated at 50 and 80 °C in the absence of evaporation.

A screenshot of the simulation for 1 minute at 80 °C is shown in Figure 6.3. A temperature gradient exists in the fry and in a small layer of oil around the fry. Additionally, a convective plume can be observed above the fry where the oil has slightly lower temperature, indicating the presence of convective flows due to temperature gradients. The predictions of the temperatures were found in good agreement to the experimental measurements as shown in Figure 6.4. Slight differences, especially for the temperature near the surface, may be explained by small differences in the exact location of the thermocouple in the experiments and the model. Although we can conclude here that CFD well predicts convective heat transfer, the implementation of mass transfer is more challenging. This will be discussed in the next section.

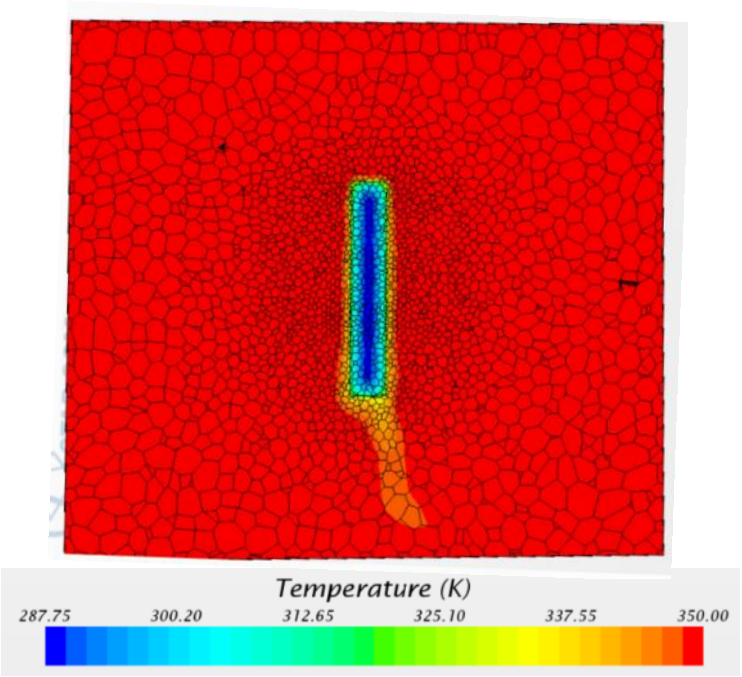

Figure 6.3. Simulation screenshot of heat transfer between oil at 80 °C and a single fry after 1 minute using STARCCM+.

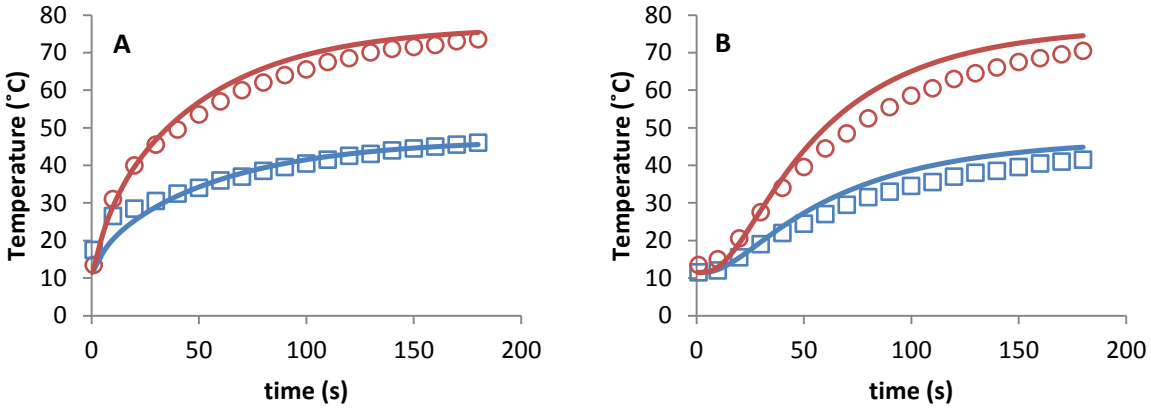

Figure 6.4. Temperature profiles of fry surface (A) and core (B), for frying temperatures of 50 °C (□) and 80 °C (○). The lines of equal colour represent the data from STARCCM+ simulations.

6.3.3. Modelling of mass transfer and momentum

Modelling of coupled heat and mass transfer is more complicated. Implementing water evaporation into the heat transfer equation is possible by feeding the oil-fry boundary values, obtained from STARCCM+, into single fry models for heat transfer and water evaporation, and explicitly return the calculated values for heat transfer as an energy sink. This means an iterative exchange between updating the oil velocity and temperature profiles and calculating the amount of heat transferred and water evaporated using the single fry models. Since this is an explicit procedure, the iterative time step must be low to prevent excessive error, making it a computationally intensive process. Additionally, a software package is needed which is capable of coupling the general numerical algorithms for single fries to the CFD model.

The next issue is then to incorporate the force from the vapour bubbles exerted onto the oil into the CFD model, which is multiphase flow. Though standard multiphase formulations are available in current CFD software packages, these formulations are not always accurate for a specific system. A lot of benchmark studies are needed to elucidate the correct interphase force formulations, and the model should be able to incorporate the complex hydrodynamics of the different flow regimes (Wang, 2010).

A further complication is that the fries are not stationary in a fixed packed bed, but in fact move and the bed is continually re-arranged. Due to the oil flow and rigorous water evaporation, the product will also experience momentum and will consequently exert a force on the oil and in between product units.

One way in which the movement of solid, non-deformable particles can be modelled is by use of the Discrete Element Method (DEM), which calculates the particle movement from Newton's equations of motion (Schutyser et al., 2001). This method is based on the use of spherical particles, but can also be applied to non-spherical particles (Kodam et al., 2009; Langston et al., 2004). The coupling of these DEM models to CFD models is not trivial, and though some progress has been made, the general implementation is still in the exploratory phase (Ho et al., 2013). Nonetheless, a multiphase model like this would be invaluable for optimisation and design of industrial frying processes.

6.4. Future directions for research and application

Even though a good description of the overall moisture loss was obtained in chapter 2, the prediction of the surface water evaporation could still be improved. More accurate in-line measuring methods would be helpful to better describe this phase of the frying process. Surface roughness plays an important role in the surface evaporation, so it would be very useful to link initial vaporization data to the XRT scans of raw potato tubers (Lioumbas et al., 2012b). Additionally, if the surface roughness could be manually varied, the effect of surface roughness on initial moisture loss can be analysed.

The evaporation rate dependent nature of the oil uptake during frying, as proven in chapter 3, could be used to optimise industrial frying units. An idea could be to vary the temperature during the course of frying to keep the evaporation rate at a constant level. This would probably require some adaptation to establish different temperature regimes inside the frying unit. However, fryers with multiple temperature zones already exist in industrial applications

(Moreira et al., 1999). This could expand the possibilities for the frying industry to further reduce the oil content of their products.

In chapter 4, the effect of higher temperatures on the crust structure was clearly visible with advanced XRT analysis. However, the connection to crispy behaviour was less obvious. Since an increase in crispy behaviour was only observed for large decreases in moisture content, it may be concluded that texture analysis methods are not accurate enough to identify small differences in crispness. However, better results might be achievable with a different probe, as the probe used in this thesis was relatively large compared to the sample. A smaller probe might give more resolution in the measurements. Otherwise, additional acoustic measurements might also be useful in increasing the measuring sensitivity (Van Vliet et al., 2007).

In chapter 5, the overall bed movement was visualized using images before and after frying. Due to the turbidity induced by vapour bubble formation, the movement during frying could not be observed through the windows of the pilot fryer. The quantification of the motion of in the bed would be very useful, as it not only shows the local packing occurs in a bed, but also how this packing is created and changes in time. This may be achieved with Positron Emission Particle Tracking (PEPT), which uses radioactive tracer particles combined with multiple detectors to triangulate particle coordinates in three dimensions (Schutyser et al., 2003). Though the steel construction of the pilot fryer might cause difficulties in this type of measurement, similar setups have been successful in applying PEPT measurements (Ingram et al., 2007).

6.5.Conclusions

.This thesis gives a description of the frying process using a modelling approach combined with experimental data. The most important parameters for heat transfer were described and quantified. Most notably a variable heat transfer coefficient was implemented, which is usually reduced to a constant in modelling approaches, despite its pivotal role in heat transfer. Additionally, oil uptake during frying was found to be function of evaporation rate. This widens the possibility of reducing oil uptake in commercial frying systems by using effective designs. XRT measurements showed that higher frying temperatures produce a more porous crust with larger pores. Though higher porosities were also correlated to more crispy behaviour using texture analysis, too high temperatures caused plastic behaviour due to chemical changes and subsequently increased glass transition temperatures.

The influence of oil flow was also studied. Increased oil circulation increased homogeneity in final moisture content. However, the non-spherical shape of the fries caused local packing upon fluidization, decreasing homogeneity in the moisture content. Though some initial steps towards an all-encompassing multiscale model for frying using CFD were made together with suggestions for additional steps, much work is still needed.

7. References

Achir, N., Vitrac, O., Trystram, G., 2008. Simulation and ability to control the surface thermal history and reactions during deep fat frying. Chem. Eng. Process. 47, 1953–1967.

Aguilar, C.N., Anzaldua-Morales, a., Talamas, R., Gastelum, G., 1997. Low-temperature Blanch Improves Textural Quality of French-fries. J. Food Sci. 62, 568–571.

Asif, M., 2011. Effect of volume-contraction on incipient fluidization of binary-solid mixtures. Particuology 9, 101–106.

Bansal, H.S., Takhar, P.S., Maneerote, J., 2014. Modeling multiscale transport mechanisms, phase changes and thermomechanics during frying. Food Res. Int. 62, 709–717.

Blumenthal, M.M., Stier, R.F., 1991. Optimization of deep-fat frying operations. Trends Food Sci. Technol. 2, 144–148.

Bouchon, P., Aguilera, J.A., 2001. Microstructural analysis of frying potatoes. Int. J. Food Sci. Technol. 36, 669–676.

Bouchon, P., Aguilera, J.M., Pyle, D.L., 2003. Structure Oil-Absorption Relationships During Deep-Fat Frying. J. Food Sci. 68, 2711–2716.

Bouchon, P., Aguilera, J.M.M., Pyle, D.L.L., 2001. Structure Oil – Absorption Relationships During Deep-Fat Frying. J. Food Sci. 68, 2711–2716.

Bouchon, P., Pyle, D.L., 2004. Studying Oil Absorption in Restructured Potato Chips. J. Food Sci. 69, FEP115–FEP122.

Bunger, A., Moyano, P., Rioseco, V., 2003. NaCl soaking treatment for improving the quality of french-fried potatoes. Food Res. Int. 36, 161–166.

Churchill, S.W., Chu, H.H.S., 1975. Correlating equations for laminar and turbulent free convection from a horizontal cylinder. Int. J. Heat Mass Transf. 18, 1049–1053.

Costa, R.M., Oliveira, F. a R., 1999. Modelling the kinetics of water loss during potato frying with a compartmental dynamic model. J. Food Eng. 41, 177–185.

Costa, R.M., Oliveira, F.A.R., Boutcheva, G., 2001. Structural changes and shrinkage of potato during frying. Int. J. Food Sci. Technol. 36, 11–23.

Costa, R.M., Oliveira, F.A.R., Delaney, O., Gekas, V., 1999. Analysis of the heat transfer coefficient during potato frying. J. Food Eng. 39, 293–299.

Dincer, I., 1995. Development of new correlations for forced convection heat transfer during cooling of products. Int. J. Energy Res. 19, 791–801.

Duckham, S.C., Dodson, A.T., Bakker, J., Ames, J.M., 2002. Effect of cultivar and storage time on the volatile flavor components of baked potato. J. Agric. Food Chem. 50, 5640–5648.

Dueik, V., Moreno, M.C., Bouchon, P., 2012. Microstructural approach to understand oil absorption during vacuum and atmospheric frying. J. Food Eng. 111, 528–536.

Duru, P., Nicolas, M., Hinch, J., Guazzelli, É., 2002. Constitutive laws in liquid-fluidized beds. J. Fluid Mech. 452, 371–404.

en.wikipedia.org [WWW Document], 2015.

Ergun, S., 1949. Fluid Flow through Randomly Packed Columns and Fluidized Beds. Ind. Eng. Chem. 41, 1179–1184.

Farid, M., 2001. A unified approach to the heat and mass transfer in melting , solidification, frying and different drying processes. Chem. Eng. Sci. 56, 5419–5427.

Farid, M., Kizilel, R., 2009. A new approach to the analysis of heat and mass transfer in drying and frying of food products. Chem. Eng. Process. Process Intensif. 48, 217–223.

Farkas, B.E., Hubbard, L.J., 2000. Analysis of convective heat transfer during immersion frying. Dry. Technol. 18, 1269–1285.

Farkas, B.E., Singh, R.P., Rumsey, T.R., 1996. Modeling heat and mass transfer in immersion frying. I, model development. J. Food Eng. 29, 211–226.

Fazzari, R.J., Hebel, R.J., Skorina, F.K., 1997. High speed mass flow food sorting apparatus for optically inspecting and sorting bulk food products. US5887073 A.

Forster, H.K., Zuber, N., 1955. Dynamics of Vapor Bubbles and Boiling Heat Transfer. AIChE Annu. Meet. 1, 531–535.

Gamble, M.H., Rice, P., Selman, J.D., 1987. Relationship between oil uptake and moisture loss during frying of potato slices from c. v. Record U.K. tubers. Int. J. Food Sci. Technol. 22, 233–241.

Gekas, V., Öste, R., Lamberg, I., 1993. Diffusion in Heated Potato Tissues. J. Food Sci. 58, 827–831.

Halder, A., Dhall, A., Datta, A.K., 2007. An improved, easily implementable, porous media based model for deep-fat frying - Part I: Model development and input parameters. Food Bioprod. Process. 85, 209–219.

Halder, A., Dhall, A., Datta, A.K., 2006. Modeling of Frying and Related Processes Involving Strong Evaporation : A Porous Media Approach. Proceedings of the COMSOL Users Conference 2006 Boston.

Hewitt, G.F., 2002. Single phase fluid flow, in: Heat Exchanger Design Handbook. New York : Begell House.

Ho, Q.T., Carmeliet, J., Datta, A.K., Defraeye, T., Delele, M. a., Herremans, E., Opara, L., Ramon, H., Tijskens, E., van der Sman, R., Van Liedekerke, P., Verboven, P., Nicolaï, B.M., 2013. Multiscale modeling in food engineering. J. Food Eng. 114, 279–291.

Huffaker, B., 2003. North American Potato Market News.

Ingram, a, Hausard, M., Fan, X., Parker, D.J., Seville, J.P.K., Finn, N., Evans, M., 2007. Portable Positron Emission Particle Tracking (PEPT) for Industrial Use. 2007 ECI Conf. 12th Int. Conf. Fluid. - New Horizons Fluid. Eng. 497–504.

Jiang, B., Liu, Y.T., Bhandari, B., Zhou, W.B., 2008. Impact of caramelization on the glass transition temperature of several caramelized sugars. Part 1: Chemical analyses. J. Agric. Food Chem. 56, 5148–5152.

Kalogianni, E.P., Papastergiadis, E., 2014. Crust pore characteristics and their development during frying of French-fries. J. Food Eng. 120, 175–182.

Kalogianni, E.P., Smith, P.G., 2013. Effect of frying variables on French fry properties. Int. J. Food Sci. Technol. 48, 758–770.

Kodam, M., Bharadwaj, R., Curtis, J., Hancock, B., Wassgren, C., 2009. Force model considerations for glued-sphere discrete element method simulations. Chem. Eng. Sci. 64, 3466–3475.

Krokida, M.K., Oreopoulou, V., Maroulis, Z.B., 2001. Effect of pre-drying on quality of french fries. J. Food Eng. 49.

Krokida, M.K., Oreopoulou, V., Maroulis, Z.B., 2000a. Water loss and oil uptake as a function of frying time. J. Food Eng. 44, 39–46.

Krokida, M.K., Oreopoulou, V., Maroulis, Z.B., 2000b. Effect of frying conditions on shrinkage and porosity of fried potatoes. J. Food Eng. 43, 147–154.

Krozel, J.W., Palazoglu, A.N., Powell, R.L., 2000. Experimental observation of dip-coating phenomena and the prospect of using motion control to minimize fluid retention. Chem. Eng. Sci. 55, 3639–3650.

Langston, P. a, Al-Awamleh, M. a, Fraige, F.Y., Asmar, B.N., 2004. Distinct element modelling of non-spherical frictionless particle flow. Chem. Eng. Sci. 59, 425–435.

Le Meste, M., Champion, D., Roudaut, G., Blond, G., Simato, D., 2002. Glass Transition and Food Technology: A Critical Appraisal. J. Food Sci. 67, 2444–2458.

Li, L., Ma, W., 2011. Experimental Study on the Effective Particle Diameter of a Packed Bed with Non-Spherical Particles. Transp. Porous Media 89, 35–48.

Lima, I., Singh, R.P., 2001. Mechanical Properties of a Fried Crust. J. of Text. Stud. 32, 31–40.

Lioumbas, J.S., Karapantsios, T.D., 2015. Bubble dynamics and substrate thermalization during boiling in water saturated porous medium. Exp. Therm. Fluid Sci. 67, 75–80.

Lioumbas, J.S., Karapantsios, T.D., 2012. Effect of Potato Orientation on Evaporation Front Propagation and Crust Thickness Evolution during Deep-Fat Frying. J. Food Sci. 77, E297–E305.

Lioumbas, J.S., Kostoglou, M., Karapantsios, T.D., 2012a. On the capacity of a crust–core model to describe potato deep-fat frying. Food Res. Int. 46, 185–193.

Lioumbas, J.S., Kostoglou, M., Karapantsios, T.D., 2012b. Surface water evaporation and energy components analysis during potato deep fat frying. Food Res. Int. 48, 307–315.

Makki, S.S., Plummer, C., 2005. Globalization of the Frozen Potato Industry. Agric. Econ. 2.

Miranda, M.L., Aguilera, J.M., 2006. Structure and texture properties of fried potato products. Food Rev. Int. 22, 173–201.

Moreira, R.G., Castell-Perez, M.E., Barrufet, M., 1999. Deep Fat Frying: Fundamentals and Applications. Springer US.

Moyano, P.C., Pedreschi, F., 2006. Kinetics of oil uptake during frying of potato slices:: Effect of pre-treatments. LWT - Food Sci. Technol. 39, 285–291.

Ni, H., Datta, A.K., 1999. Moisture, Oil and Energy Transport During Deep-Fat Frying of Food Materials. Food Bioprod. Process. 77, 194–204.

Nitz, M., Taranto, O.P., 2007. Drying of beans in a pulsed fluid bed dryer: Drying kinetics, fluid-dynamic study and comparisons with conventional fluidization. J. Food Eng. 80, 249–256.

Ozahi, E., Gundogdu, M.Y., Carpinlioglu, M.Ö., 2008. A Modification on Ergun's Correlation for Use in Cylindrical Packed Beds With Non-spherical Particles. Adv. Powder Technol. 19, 369–381.

Perry, R.H., Green, D.W., Maloney, J.O., 1997. Perry's Chemical Engineers' Handbook Seventh Edition. McGraw- Hill.

Pinthus, E.J., Weinberg, P., Saguy, I.S., 1995. Oil Uptake in Deep Fat Frying as Affected by Porosity. J. Food Sci. 60, 767–769.

Pravisani, C.I., Calvelo, a., 1986. Minimum Cooking Time for Potato Strip Frying. J. Food Sci. 51, 614–617.

Rossell, J.B., 2001. Introduction, in: Rossell, J.B. (Ed.), Frying. Elsevier, pp. 1–3.

Sandhu, J., Bansal, H., Takhar, P.S., 2013. Experimental measurement of physical pressure in foods during frying. J. Food Eng. 115, 272–277.

Schutyser, M. a. I., Briels, W.J., Rinzema, a., Boom, R.M., 2003. Numerical simulation and PEPT measurements of a 3D conical helical-blade mixer: A high potential solids mixer for solid-state fermentation. Biotechnol. Bioeng. 84, 29–39.

Schutyser, M.A.I., Padding, J.T., Weber, F.J., Briels, W.J., Rinzema, A., Boom, R., 2001. Discrete particle simulations predicting mixing behavior of solid substrate particles in a rotating drum fermenter. Biotechnol. Bioeng. 75, 666–675.

Senadeera, W., Bhandari, B.R., Young, G., Wijesinghe, B., 2000. Methods for Effective Fluidization of Particulate Food Materials. Dry. Technol. 18, 1537–1557.

Somsen, D., Capelle, A., Tramper, J., 2004. Manufacturing of par-fried French-fries - Part 3: a blueprint to predict the maximum production yield. J. Food Eng. 61, 209–219.

Somsen, D., Capelle, A., Tramper, J., 2004. Manufacturing of par-fried French-fries. Part 2: Modelling yield efficiency of peeling. J. Food Eng. 61, 199–207.

Srinivasakannan, C., Balasubramanian, N., 2008. An Analysis on Modeling of Fluidized Bed Drying of Granular Material. Adv. Powder Technol. 19, 73–82.

Stier, R.F., 2004. Frying as a science - An introduction. Eur. J. Lipid Sci. Technol. 106, 715–721.

Suárez, R.B., Campañone, L. a., García, M. a., Zaritzky, N.E., 2008. Comparison of the deep frying process in coated and uncoated dough systems. J. Food Eng. 84, 383–393.

Teruel, M.D.R., Gordon, M., Linares, M.B., Garrido, M.D., Ahromrit, A., Niranjan, K., 2015. A Comparative Study of the Characteristics of French Fries Produced by Deep Fat Frying and Air Frying. J. Food Sci. 80, E349–E358.

Thanatuksorn, P., Kajiwara, K., Suzuki, T., 2007. Characterization of deep-fat frying in a wheat flour–water mixture model using a state diagram. J. Sci. Food Agric. 87, 2648–2656.

Truong Van, D., Biermann, C.J., Marlett, J. a, 1986. Simple sugars, oligosaccharides and starch concentrations in raw and cooked sweet potato. J. Agric. Food Chem. 34, 421–425.

Van der Sman, R.G.M., Meinders, M.B.J., 2011. Prediction of the state diagram of starch water mixtures using the Flory-Huggins free volume theory. Soft Matter 7, 429–442.

Van Koerten, K.N., Schutyser, M. a. I., Somsen, D., Boom, R.M., 2015a. A pore inactivation model for describing oil uptake of French fries during pre-frying. J. Food Eng. 146, 92–98.

Van Koerten, K.N., Schutyser, M. a. I., Somsen, D., Boom, R.M., 2015b. Crust morphology and crispness development during deep-fat frying of potato. Food Res. Int. doi: 10.1016/j.foodres.2015.09.022

Van Koerten, K.N., Schutyser, M.A.I., Somsen, D., Boom, R.M., 2015c. Cross-flow deep fat frying and its effect on fry quality distribution and mobility. J. Food Sci. Technol. doi: 10.1007/s13197-015-2070-2

Van Vliet, T., Visser, J.E., Luyten, H., 2007. On the mechanism by which oil uptake decreases crispy/crunchy behaviour of fried products. Food Res. Int. 40, 1122–1128.

Vauvre, J.M., Kesteloot, R., Patsioura, A., Vitrac, O., 2014. Microscopic oil uptake mechanisms in fried products 741–755.

Vitrac, O., Trystram, G., Raoult-Wack, A.-L., 2000. Deep-fat frying of food: heat and mass transfer, transformations and reactions inside the frying material. Eur. J. Lipid Sci. Technol. 102, 529–538.

Wang, T., 2010. Simulation of bubble column reactors using CFD coupled with a population balance model. Front. Chem. Sci. Eng. 5, 162–172.

Warning, A., Dhall, A., Mitrea, D., Datta, A.K., 2012. Porous media based model for deep-fat vacuum frying potato chips. J. Food Eng. 110, 428–440.

www.kudu.com.sa [WWW Document], 2015.

www.minghongfood.com [WWW Document], 2015.

www.myfries.ca [WWW Document], 2015.

www.pasundan.nl [WWW Document], 2015.

www.smulweb.nl [WWW Document], 2015.

Ziaiifar, A.M., Achir, N., Courtois, F., Trezzani, I., Trystram, G., 2008. Review of mechanisms, conditions, and factors involved in the oil uptake phenomenon during the deep-fat frying process. Int. J. Food Sci. Technol. 43, 1410–1423.

Ziaiifar, A.M., Courtois, F., Trystram, G., 2010. Porosity Development and Its Effect on Oil Uptake During Frying Process. J. Food Process Eng. 33, 191–212.

Summary

Deep frying is one of the most used methods in the food processing industry. Though practically any food can be fried, French fries are probably the most well-known deep fried products. The popularity of French fries stems from their unique taste and texture, a crispy outside with a mealy soft interior, but also because of the ease and speed of preparation. However, despite being a practical and easy method, the fundamental phenomena that occur during frying are very complex. This thesis aimed at gaining a deeper understanding of the frying of French fries. This was done at the product level, with regards to heat transfer, moisture loss, oil uptake and crust formation, and at the process level, which encompasses the oil movement in a frying unit and the consequent oil-fry interactions.

Firstly a numerical model was developed to describe the water evaporation during frying (**Chapter 2**). Though various models exist for describing moisture loss, they all use constant values for the heat transfer coefficient. However, the heat transfer coefficient actually varies greatly due to the varying degrees of turbulence, induced by the vapour bubbles escaping from the fry surface. Therefore, the model in this thesis incorporated an evaporation rate dependent heat transfer coefficient. Other than the varying heat transfer coefficient, the model was heat transfer dependent, with a sharp moving evaporation boundary and Darcy flow describing the flow of water vapour through the crust. The model was successfully validated against experimental results for moisture loss and temperature profiles in the fry.

For oil uptake during frying, a pore inactivation model from membrane technology was adopted (**Chapter 3**). In membranes, pores will inactivate when the transmembrane pressure becomes too low. In fries, this can be translated as pores in the crust inactivating when the evaporation rate becomes too low. As pores stop expelling water vapour, oil can migrate into the fry. The model also took into account the lengthening of the pores with increasing crust thickness, allowing for more oil uptake in inactivated pores. The model fitted well with experimental data for oil uptake during frying. Also, the pore inactivation model better described oil uptake during the initial stages of frying, where the evaporation rate is still relatively high, compared to the linear relation between oil uptake and moisture content, which is usually assumed in literature.

Both the influences of frying temperature and moisture content on crust structure and consequent textural properties were studied (**Chapter 4**). The crust structure was visualized

and quantified using X-ray tomography (XRT), which uses multiple 2D X-ray pictures of a rotated sample to reconstruct a 3D density map. Textural properties, like hardness and crispness, were quantified using force deformation curves from a texture analyser. Moisture loss was shown to greatly increase porosity and pore size in fries. More crispy behaviour was also shown for higher moisture loss, though not significantly at moisture contents close to the initial moisture content. Though increased frying temperatures also showed an increased porosity and pore size, there was no significantly observed increase in crispness. This is most likely because the texture analysis was not sensitive enough to discern any increased crispness for porosities below a certain degree. Strikingly, for frying temperature around 195 °C, a decrease in crispness was observed. These samples visually also showed more plastic behavior. The most likely cause for this is degradation of sucrose, which happens around 186 °C, and consequent caramelization of glucose, thus increasing the glass transition temperature.

At the process level, oil flow and fry quality distribution were investigated using a pilot scale cross-flow fryer (**Chapter 5**). Oil circulation velocities were varied to observe the initial fluidization behavior of the fry bed through an observation window. This fluidization behavior was well described by the Ergun equation, modified for non-spherical particles. The distribution in moisture content of the fries was used as an indicator for quality distribution. Though increased oil circulation initially increased the homogeneity of the moisture content, upon fluidization the homogeneity actually decreased. Image analysis of fries before and after frying showed local packing of fries around their fluidization point. This was due to the non-spherical shape of the fries, making them more sensitive to channelling.

The results obtained in this thesis were finally discussed, together with the possibility to also model the process scale of the frying process (**Chapter 6**). The possibility of modelling the oil flow through a packed bed of fries, and the free-convective heat transfer during frying, using a CFD software package (STARCCM+) was shown. Additionally, the possibility of linking oil flows computed using CFD to the general models developed in this thesis was discussed. Modelling the momentum transfer of the expelled vapour bubbles to the oil, but also the movement of the fries themselves is still a faraway goal. However, a multiphase model that can describe both the entire frying setup as the consequent individual fry parameters would be invaluable.

Samenvatting

Frituren is een veelgebruikt proces in de levensmiddelen industrie, waarbij bevroren voorgefrituurde Franse friet een van de meest bekende producten is. Franse friet is vooral populair dankzij de unieke smaak en textuur, een knapperige buitenkant met een zachte kern, maar ook door de gemakkelijke bereidingswijze. Hoewel frituren zelf vrij eenvoudig is, zijn de onderliggende fysische verschijnselen complex. Het doel van het onderzoek in dit proefschrift was dan ook om beter inzicht te verkrijgen in het frituurproces, zowel op product- als op processchaal. Op productschaal zijn warmte overdracht, waterverdamping, olieopname en korstvorming onderzocht. Op processchaal zijn de oliestromingen in een speciaal ontworpen frituurapparaat en de daaruit volgende olie-friet interacties bestudeerd.

Als eerste is er een numeriek model ontwikkeld dat waterverdamping tijdens het frituurproces beschrijft (Hoofdstuk 2). Hoewel er verschillende modellen bestaan die het vochtverlies beschrijven gebruiken ze allemaal een constante warmteoverdrachtscoëfficiënt. Echter, in de praktijk varieert de warmteoverdrachtscoëfficiënt wel degelijk tijdens het frituren. Dit is het gevolg van de mate waarin waterdampbellen ontsnappen aan het frietoppervlak en deze varieert. Daarom maakt het model in dit proefschrift gebruik van een warmteoverdrachtscoëfficiënt die functie is van de verdampingssnelheid. Naast de variërende warmteoverdrachtscoëfficiënt maakt het model gebruik van een scherp verdampingsfront en wordt de stroming van waterdamp door de korst beschreven met de wet van Darcy. Het model is gevalideerd met experimentele metingen van vochtverlies en temperatuurverloop tijdens frituren van enkele frietjes.

Een porie-inactivatie model uit de membraantechnologie is toegepast om olieopname tijdens het frituurproces te beschrijven (Hoofdstuk 3). Tijdens membraan emulsificatie kunnen poriën non-actief worden als de trans-membraandruk te laag wordt. In friet kan dit vertaald worden naar poriën in de korst die non-actief worden als de waterverdampingssnelheid te laag wordt. Zodra de vorming van dampbellen uit een porie stopt, kan olie de korst binnendringen. Het model hield ook rekening met verlenging van de poriën door groei van de korst, waardoor non-actieve poriën tijdens het proces steeds meer olie kunnen opnemen. Het model kwam overeen met experimentele data voor olieopname tijdens het frituren van enkele frietjes. Daarnaast was de olieopname voor een korter tijdsinterval beter te beschrijven met het porie-inactivatie model dan met de veelgebruikte lineaire relatie tussen olieopname en vochtgehalte.

Zowel het effect van temperatuur als van vochtgehalte op de korststructuur en de resulterende textuureigenschappen zijn bestudeerd (Hoofdstuk 4). De korststructuur is gevisualiseerd en gekwantificeerd met behulp van X-ray tomografie (XRT), wat gebruik maakt van meerdere 2D röntgenfoto's van een roterend object om een 3D dichtheidsgrafiek te construeren. Textuureigenschappen, zoals hardheid en knapperigheid, zijn gekwantificeerd met kracht-deformatie grafieken via trekbank experimenten. Water verlies resulteerde in een sterke stijging van de porositeit en poriegrootte in friet. Ook werd een toename in de knapperigheid geconstateerd met toenemend waterverlies, hoewel in mindere mate dan de porositeit. Hogere frituurtemperaturen resulteerden ook in een verhoogde porositeit en poriegrootte, maar niet in een significante toename van de knapperigheid. Dit komt hoogstwaarschijnlijk doordat metingen met de trekbank niet accuraat genoeg zijn om verschillen in knapperigheid te meten bij een lagere porositeit. Opvallend genoeg werd voor frituurtemperaturen rond de 195 °C een afname in knapperigheid waargenomen. Deze monsters vertoonden ook visueel meer plastisch gedrag. De meest waarschijnlijke verklaring hiervoor is de degradatie van sucrose (dit gebeurd rond 186 °C) en de karamellisatie van de gevormde glucose met als gevolg een verhoging van de glastemperatuur.

Voor de processchaal zijn oliestroming en friet kwaliteitsverdeling onderzocht met behulp van een dwarsstroom frituuropstelling (Hoofdstuk 5). De oliecirculatiesnelheid werd gevarieerd om het initiële fluidizatiegedrag van het frietbed te bestuderen door een kijkvenster. Dit fluidizatiegedrag bleek goed te worden beschreven met de Ergun vergelijking, aangepast voor niet-sferische deeltjes. De verdeling van eindvochtgehalte van verschillende frietjes werd gebruikt als een indicatie voor de kwaliteitsverdeling. Hoewel verhoogde oliecirculatiesnelheden de homogeniteit van het eindvochtgehalte in eerste instantie verbeterde, werd de verdeling van het eindvochtgehalte juist minder homogeen voorbij het fluidizatiepunt. Uit beeldanalyse van het frietbed voor en na frituren bleek dat er clustering optrad rond het fluidizatiepunt van de friet. Dit werd veroorzaakt door de niet-sferische vorm van de friet waardoor ze minder weerstand ondervinden in een gepakte toestand.

Tot slot zijn de resultaten verkregen in dit proefschrift bediscussieerd samen met de mogelijkheid om de processchaal van het frituurproces ook te modelleren (Hoofdstuk 6). De mogelijkheid om oliestroming door een gepakt bed van friet en de convectieve warmteoverdracht tijdens het frituren te modelleren werd aangetoond met behulp van een CFD-software pakket (STARCCM+). Daarnaast is de mogelijkheid om de oliestromingen, berekend met CFD, te koppelen aan de algemene modellen ontwikkeld in dit proefschrift

behandeld. Het modelleren van momentum overdracht van dampbellen naar de oliefase en de verplaatsing van individuele frietjes is nog toekomstmuziek. Concluderend zou een multiscale model, dat zowel de olie-friet interacties als de daaruit volgende individuele friet parameters kan beschrijven, van grote waarde zijn om het frituurproces in al zijn details te ontwerpen.

Acknowledgements

Finally, the section most people read. I would like to thank all the people who made the making of this thesis possible. Also, I want to acknowledge GO *Gebundelde innovatiekracht* and EFRO for the financial support for this thesis.

Maarten, thank you for all your support, guidance and advice. I enjoyed working with you and I learned so much from it. Our weekly meetings kept me in check and without you I would never have finished this booklet. Remko, thanks for your endless supply of ideas and positivity. You could sell ice to an eskimo, and it was great working with you. Many thanks also to Derk, your more practical view on things and knowledge greatly contributed to this thesis, I enjoyed our collaboration very much.

Next, I would like to thank everybody at the Food Process Engineering department. It was great to work together with everyone, and it was great fun at all the conferences, trips and outings. Martin, thanks for dealing with all the nitty-gritty of the paperwork and finances, you made signing stuff fun. Thanks to Jos, Maurice and Jarno for not only dealing with the harder questions and problems but also the dumb ones. Joyce and Marjan, thank you for always arranging everything. I would also like to thank Pieter for all his help with IT and CFD simulations, Ruud for his great advise on modelling, and Remco for all his help with the XRT. Many thanks to all my students, Marijn, Annelieke, Liu, Sasja, Hua, Amber, Dane and Xingying for all their hard work and effort, it was great working with all of you.

I would also like to thank everybody who made my time at Wageningen that much more fun. Tim, thank you for your guidance during my Master thesis, I learned a lot from you and had a great time. Also, your advice to follow a PhD turned out great, thank you. Thanks to Fransisco and Laura for showing me how to supervise courses and the laughs. Other Tim, also thanks for making my Bachelor and Master time hilarious, and full of prosperity. Karolina, thanks for making not only bioinformatics more enjoyable but also my PhD time and Poland.

Tot slot wil ik al mijn vrienden en familie bedanken voor alle steun en hulp. En Gaby, bedankt voor al het liefs, geks en goeds, en het lekkere eten;) hou van jou.

About the author

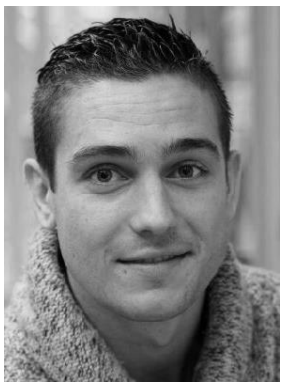

Kevin van Koerten was born on March 4, 1988 in Ermelo, The Netherlands. He finished his secondary education (VWO) in 2006 at Christelijk College Groevenbeek in Ermelo. That same year he started with the study Biotechnology at Wageningen University. He finished his BSc in 2009 and wrote his thesis on "Stability of enzymes entrapped in polymeric micelles" at the department of Bioprocess Engineering. Subsequently, Kevin chose the MSc specialization "Process Technology". He finished his MSc thesis, title "Exergy analysis of dairy processes", at the department of Food Process Engineering. He followed an internship at Aviko B.V. in Steenderen, as an introduction to a PhD project.

In 2011, Kevin obtained his MSc degree and started his PhD at the department of Food Process Engineering. He studied the pre-frying of French fries as a collaboration project together with Aviko, aiming to gain deeper understanding of the science behind frying using a modelling approach. The results from these four years of research are described in this thesis. Since November 2015, Kevin works at NIZO Food Research as a Process Scientist focussing on modelling and optimizing different aspects of food production processes.

Publications

Van Koerten, K.N., Somsen, D., Boom, R.M., Schutyser, M. A. I., (2015). Modelling water evaporation during frying with an evaporation dependent heat transfer coefficient. *Submitted for publication*.

van Koerten, K. N., Schutyser, M. A. I., Somsen, D., & Boom, R. M. (2015). A pore inactivation model for describing oil uptake of French fries during pre-frying. *Journal of Food Engineering*, 146, 92-98.

van Koerten, K. N., Schutyser, M. A. I., Somsen, D., & Boom, R. M. (2015). Crust morphology and crispness development during deep-fat frying of potato. *Food Research International*, 78, 336-342.

van Koerten, K. N., Schutyser, M. A. I., Somsen, D., & Boom, R. M. (2015). Cross-flow deep fat frying and its effect on fry quality distribution and mobility. *Journal of Food Science and Technology*, available online since 4 November 2015, doi: 10.1007/s13197-015-2070-2

Overview of completed training activities

Discipline specific activities

CFD for Chemical Engineers, The Netherlands	2011
Reaction kinetics in food science, The Netherlands	2012
Advanced Food Analysis, The Netherlands	2013
Advanced Thermodynamics, The Netherlands	2014
NPS11, Papendal, The Netherlands (poster)	2011
IDS,Xiamen, China (poster)	2012
ECCE9, The Hague, The Netherlands (presentation)	
Eurodrying, Paris, France (presentation)	2013
Effost, Uppsala, Sweden (poster)	2014

General courses

PhD VLAG week, The Netherlands	2012
Project & Time management, The Netherlands	2011
Scientific writing, The Netherlands	2012
Competence assessment, The Netherlands	2012
Teaching and supervising Thesis students, The Netherlands	2012

Optionals

PhD Project Proposal	2011
PhD excursion FPE, Finland & Baltic States	2012
PhD excursion FPE, Chili & Brazil	2013
Dry Food Processing meetings	2011-2015

The research described in this thesis was financially supported by GO *Gebundelde innovatiekracht* and EFRO, an initiative by the European Union.

Cover design by Megan van Koerten

Thesis printed by Proefschriftmaken.nl || Uitgeverij BOXPress